On the adaptive multi-stage detector for cancellation of multiuser interference in CDMA wireless communication systems

Nadir Sezgin
New Jersey Institute of Technology

ABSTRACT

ON THE ADAPTIVE MULTI-STAGE DETECTOR FOR CANCELLATION OF MULTIUSER INTERFERENCE IN CDMA WIRELESS COMMUNICATION SYSTEMS

by
Nadir Sezgin

The classical multiple access techniques such as Frequency Division Multiple Access (FDMA) and Time Division Multiple Access (TDMA) schemes are band limited in terms of their capacity to be used for mobile radio communication. Recent developments in the area of digital signal processing, makes Code Division Multiple Access (CDMA) as a possible solution to the demand of capacity for the mobile radio communication. The capacity of CDMA is limited by multiuser interference, that is the interference from the other users.

The goal of this dissertation is to improve the multiuser CDMA detector with high Bit Error Rate (BER) performance, low complexity, near-far resistance as well as flexibility to be applied to a wide range of communication channels. We developed an adaptive multi-stage CDMA detector to cancel the multiuser interference. The first-stage of the detector, called decorrelating detector, decorrelates the correlated signals obtained at the match filter bank. The second-stage, called canceller, cancels the multiuser interference exist in the desired signals, using the decorrelated user signals obtained at the decorrelating detector output. The key future of this multi-stage detector is being purely adaptive. The combination of adaptive decorrelating detector and adaptive canceller allows the multi-stage detector achieve near-optimum BER performance and at the same time remain computationally effective. To increse achievable BER performance an adaptive soft limiter is used at the canceller stage. The underlying structure of this multi-stage detector

(i.e. being purely adaptive) allows it to be applied to different channel characteristics. However, throughout this dissertation we use Additive White Gaussian Noise (AWGN) channel for simplicity. To address some of the potential problems that may arise in practice, the adaptive decorrelating detector is tested using computer simulation and in-depth analysis of the problem. If necessary, an alternative solution that do not change the main characteristics of the detector (such as adaptivity and simplicity) is provided. Overall, we conclude that our adaptive detector with its high BER performance and adaptation ability to different channel characteristics, can be considered as an alternative solution to the problem of multiuser interference cancellation in CDMA communication.

ON THE ADAPTIVE MULTI-STAGE DETECTOR FOR CANCELLATION OF MULTIUSER INTERFERENCE IN CDMA WIRELESS COMMUNICATION SYSTEMS

by
Nadir Sezgin

A Dissertation
Submitted to the Faculty of
New Jersey Institute of Technology
in Partial Fulfillment of the Requirements for the Degree of
Doctor of Philosophy

Department of Electrical and Computer Engineering

January 1996

APPROVAL PAGE

ON THE ADAPTIVE MULTI-STAGE DETECTOR FOR CANCELLATION OF MULTIUSER INTERFERENCE IN CDMA WIRELESS COMMUNICATION SYSTEMS

Nadir Sezgin

Dr. Yeheskel Bar-Ness, Dissertation Advisor — Date
Distinguished Professor of Electrical and Computer Engineering, NJIT

Dr. Alex Haimovich, Committee Member — Date
Associate Professor of Electrical and Computer Engineering, NJIT

Dr. Zoran Siveski, Committee Member — Date
Assistant Professor of Electrical and Computer Engineering, NJIT

Dr. Eliza Michalopoulou, Committee Member — Date
Assistant Professor of Mathematics, NJIT

Dr. Branimir Vojcic, Committee Member — Date
Associate Professor of Electrical Engineering and Computer Science,
The George Washington University

BIOGRAPHICAL SKETCH

Author: Nadir Sezgin

Degree: Doctor of Philosophy

Date: January 1996

Undergraduate and Graduate Education:

- Doctor of Philosophy in Electrical Engineering,
  New Jersey Institute of Technology, Newark, NJ, 1996
- Master of Science in Electrical Engineering,
  New Jersey Institute of Technology, Newark, NJ, 1992
- Bachelor of Science in Electrical Engineering,
  Middle East Technical University, Ankara, Turkey, 1990

Major: Electrical Engineering

ACKNOWLEDGMENT

The author wishes to express his gratitude to Dr. Bar-Ness for his supervision throughout this research.

Special thanks to Dr. Haimovich, Dr. Siveski, Dr. Michalopoulou and Dr. Vojcic for serving as members of the Committee.

Finally the author appreciates the help and support of all the members of Center for Communication and Signal Processing Research.

TABLE OF CONTENTS

TABLE OF CONTENTS
(Continued)

LIST OF FIGURES

LIST OF FIGURES
(Continued)

CHAPTER 1

INTRODUCTION

There has been a substantial increase in demand for mobile wireless communication in recent years. This trend is evident especially in the popularity of mobile phones. The transmission media that exist for wireless communication is unfortunately limited by the band-width of radio channel. As the number of the subscribers for the wireless communication grows, the multiple access schemes with a higher capacity become more crucial.

Three main multiple access schemes are customarily in use. These are Frequency Division Multiple Access (FDMA), Time Division Multiple Access (TDMA) and Code Division Multiple Access (CDMA). With FDMA and TDMA the radio channel is partitioned into the independent single-user subchannels. These are called "static channel sharing multiple access methods" [33], that is the allocated channel for a specific user cannot be used for any other user for the duration of communication. Therefore these strategies are bandwidth limited in terms of their capacity to provide multiuser access for the wireless communication. This results in a very inefficient channel sharing especially for the voice communication. Because, during a typical conversation, a person talks only one third of the time. On the other hand, CDMA is a dynamic channel sharing technique, all the available spectrum is used by for every user. A distinct signature sequence is assigned to each user, and the received signal is correlated with this signature sequence in order to detect the data. As a result of the cross correlation between the user signature sequences the CDMA capacity is limited by the interference from the other users. Any reduction of interference from the other users linearly contributes to the capacity [16]. In this prospect, CDMA is believed to be a good candidate for the multiple access wireless radio communication.

The near-far problem is known as the inability of recovering a weak signal in the presence of strong interfering signals. The closed or open loop power control has been suggested as a solution to this problem. By controlling mobile radio's transmitting power it is possible to assure all the received signals, desired or interfering, have equal power. However, power control requires significant reduction in signal energies of strong users in order for the weak user to achieve a reliable communication. Therefore power control becomes self defeating since it decreases the anti-jamming capability of the system as well as reduction in the multiple access ranges. For this reason the design of near-far resistant detectors can be considered as a primary goal in CDMA communication [33].

The characteristics of the mobile radio communication channel is another important issue for the successful design and development of the CDMA detectors. Even though some of the analytical models such as Rayleigh, Rician, Lognormal [28] have been developed to characterize the channel, the mobile communication channel, especially the indoor mobile communication channel is highly non-linear, time variant as well as location dependent [17]. Therefore the CDMA detector that adapts itself to the channel characteristics with a minimum overhead data is an important research task of our work.

As a solution to the near-far problem in CDMA, an adaptive detector that can be used at the base station for mobile radio communication, is proposed. This detector contains two stages. The first stage; the decorrelating detector, decorrelates the multiuser signals from each other in an adaptive manner and generate tentative estimates of users' data. The second stage; the canceller, exploit the tentative decision at the output of the decorrelating detector to cancel multiuser interferences that interfere with the desired signal of each user.

Since the capacity of the CDMA system is limited by the multiuser interference the developed detector increases the system capacity. The adaptive stages of the detectors are tested under different scenarios and compared to the their non-adaptive or pre-existing adaptive counterparts. For the ease of analysis AWGN channel with multiuser interference is assumed throughout the dissertation.

1.1 Outline of Dissertation

We briefly described the limitations of FDMA and TDMA for the increasing demand in wireless communications in this chapter. We also stated the most important problems of CDMA, as a limit to its capacity. In this dissertation, an adaptive multi-stage detector which is proposed as a solution to reduce the multiuser interference and hence increase the multi access capability of the system is discussed. Some issues related to its BER performance improvement are presented. Particular attention is paid to the asynchronous uplink channel. In Chapter 2, the Direct Sequence (DS)[1] CDMA system is first described as a background to understand multi-stage detection schemes. The basic concept of multi-stage detection schemes is then explained. The first-stage (decorrelating detector) and second-stage (canceller) detectors are examined briefly.

Chapter 3 presents the adaptive bootstrap decorrelating detector as the first-stage detector for the one-shot asynchronous CDMA communication system, when the delay estimation of the user codes is not precise. A detailed analysis of this one-shot asynchronous CDMA system, the steady state weights for this Bootstrap separator, and the corresponding BER performance of the system are given.

In Chapter 4 an adaptive setting of the threshold of soft limiter at the output of the first stage detector, rather than hard limiter is proposed. Optimum adaptive weights and soft limiter thresholds with respect to minimizing multiuser interference at the detector output are found. In order to make calculations tractable, BER

[1]Throughout this dissertation DS-CDMA is used as the CDMA communication protocol. For the convenience of the reader the use of the word "DS" is avoided, since it is clear from the context.

performance of two-user synchronous CDMA system is obtained and compared to the BER performances for the systems, previously proposed, with hard limiter or heuristic soft limiter.

Chapter 5 deals with the problem of singularity, that may arise in the one-shot asynchronous CDMA communication system. It has been shown that under certain relative delays between user codes, the "partial cross correlation matrix" (PCCM)[2] becomes singular. We show that with such circumstances, the adaptive weights of the bootstrap decorrelating detector proposed in Chapter 3 do not converge. Two different adaptive schemes are proposed as a solution to this problem. In the first scheme, we eliminate the rows of the PCCM which cause reduced rank and decorrelate only the independent outputs. For finding this rows we use adaptive algorithm that minimizes the decorrelator output powers, and show that, in fact, these rows correspond to zero output power. In the second scheme, for controlling the bootstrap weights, we propose a soft limiter instead of hard limiter. We show that with a wide range of the threshold, this modified bootstrap decorrelating detector weights converge regardless of the PCCM singularity. A detailed derivation of steady state weights is provided for both approaches. The BER performances of the proposed schemes are also obtained by simulation and compared to the performance of the "non-adaptive decorrelating detector" which is based on generalized inverse under the same scenario.

Finally, Chapter 6 concludes the main results of the dissertation.

1.2 Contributions

The design of near-far resistant CDMA detectors for the reduction of multiuser interference has been one of the active research areas in Center for Communication and Signal Processing Research (Communication Lab) at NJIT [4-11], [23-26], [35] in

[2]Definition of PCCM will be given later.

recent years. This dissertation extends some of the previously done research in this area, as well as brings some new developments to the problem of interference cancellation and multiuser detection in general. The focus of this work is on the use of adaptive schemes with a reasonable complexity for the reduction of the multiuser interference in CDMA systems. The work presented in Chapters 3, 4 and 5 is new. Chapter 3 is mainly contributed by Prof. Bar-Ness, Chapter 4 is the joint contribution of the author and Prof. Bar-Ness. Chapter 5 is mainly contributed by the author.

CHAPTER 2

BACKGROUND FOR MULTI-STAGE CDMA DETECTION

In this chapter, we first describe a general CDMA transmission system for asynchronous communication. Then, the limitations of the conventional matched filter-bank detector used in multiuser CDMA detection are stated for both synchronous and asynchronous communication. In Section 2.2 the notion of near-far resistant decorrelating detection is introduced as a solution to the multiuser detection of CDMA signals. This is also used as a first stage for the multi-stage detection. However, with this detector, increase in the spectral density of the AWGN noise results in a degraded BER performance. Instead, in a two-stage detector, the output of the decorrelating detector is used to generate a tentative decision which is employed by the canceller stage to reduce the multiuser interference present in the matched filter-bank output. The interference canceller stage is explained in Section 2.3. One may use the outputs of the second stage as tentative decisions to be used for another canceller as a third stage. This can be extended to as many stages as possible in order to obtain a better cancellation of multiuser interference. However, to illustrate the concept, we restrict ourselves to two stages (decorrelator-canceller) only.

Adaptive and non-adaptive counter parts are presented for both first and second stages of the detector. The material presented in this chapter is not new, however it serves as a background for the thorough understanding of the work presented in the following chapters.

2.1 Baseband CDMA Transmitter

A baseband transmitter model of a basic CDMA system for K asynchronous users is depicted in Figure 2.1.

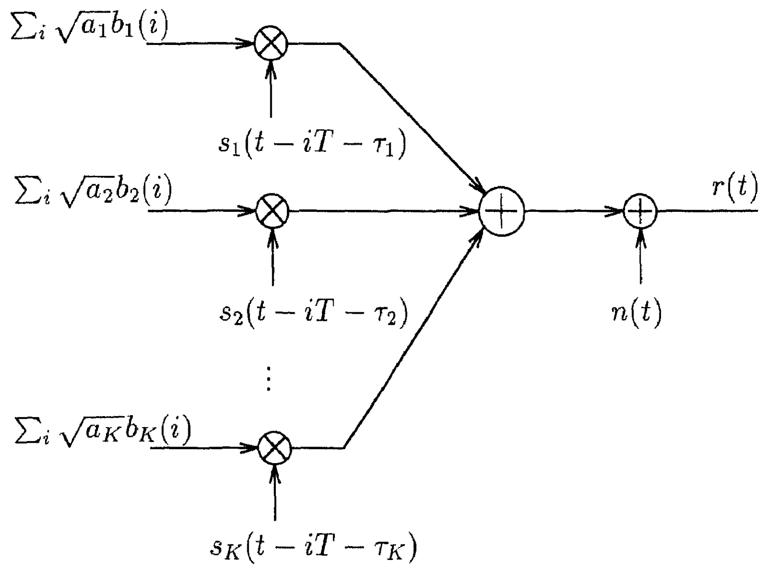

Figure 2.1 Baseband equivalent CDMA transmitter model

Each user is assumed to transmit a sequence of statistically independent data bits $b_k(i)$ with a bit energy a_k and a unique signature sequence s_k delayed by τ_k at a bit interval T. The received equivalent baseband signal is

$$r(t) = \sum_{k=1}^{K} \sum_{i} b_k(i) \sqrt{a_k(i)} s_k(t - iT - \tau_k) + n(t), \tag{2.1}$$

where $n(t)$ is a zero mean AWGN with a two-sided power spectral density of $N_0/2$.

2.1.1 Matched Filtered Detection for Synchronous CDMA

The CDMA communication is synchronous, if all the users transmit their ith bits at the same time. That is, the signature delays τ_ks in Eq. (2.1) are the same for all users. Without loss of generality, we take $\tau_k = 0, \quad k = 1, \ldots, K$. We also assume that the signature sequences are periodic with a bit interval T. Therefore, for the synchronous CDMA communication the received equivalent baseband signal can be written as

$$r(t) = \sum_{k=1}^{K} \sum_{i} b_k(i)\sqrt{a_k(i)}s_k(t) + n(t). \tag{2.2}$$

The matched filter-bank for K-user synchronous CDMA is depicted in Figure 2.2.

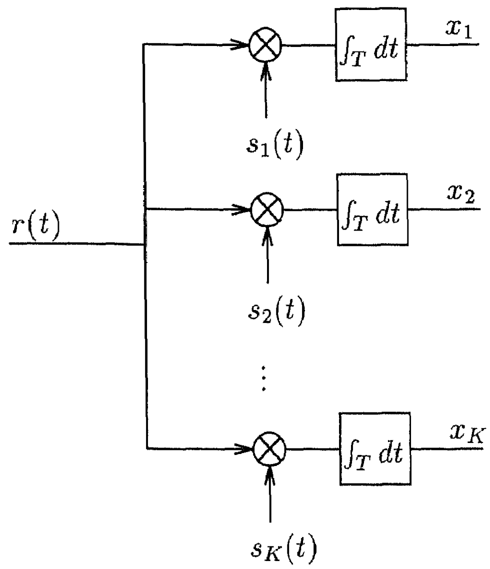

Figure 2.2 Matched filter bank for synchronous CDMA.

Each matched filter output x_k is obtained by correlating the received signal by the signature sequence of the kth user. The matched filter-bank output can be written in a vector form as

$$\boldsymbol{x} = \boldsymbol{PAb} + \boldsymbol{n} \tag{2.3}$$

where $\boldsymbol{P}$ is the $K \times K$ cross correlation matrix:

$$\boldsymbol{P} = \begin{bmatrix} 1 & \rho_{12} & \cdots & \rho_{1K} \\ \rho_{12} & 1 & \cdots & \rho_{2K} \\ \vdots & \vdots & \ddots & \vdots \\ \rho_{1K} & \rho_{2K} & \cdots & 1 \end{bmatrix}, \tag{2.4}$$

so that

$$\rho_{kl} = \int_0^T s_k(t)s_l(t)dt, \quad k, l = 1, \ldots, K; \tag{2.5}$$

$\boldsymbol{A} = \mathrm{diag}(\sqrt{a_1}, \cdots, \sqrt{a_K})$, $\boldsymbol{b}(i) = [b_1(i), \cdots, b_K(i)]^T$, and $\boldsymbol{n}(i)$ is a zero-mean Gaussian noise vector with covariance vector $\boldsymbol{P}N_0/2$.

One may apply hard limiter to the matched filter-bank output vector $\boldsymbol{x}$ for the multiuser detection. This detection scheme is also known as conventional single user detection which is optimum in terms of BER performance for the interference-free AWGN channels. However, in the case of multiuser interference, the conventional single user detector performance degrades quickly as the level of interference increases. The assumption that multiuser interference can be modeled as a white Gaussian process does not hold in practical situations [33]. Therefore, the multiuser signals obtained at the output of the matched filter-bank are further decorrelated before the decision is made. This procedure is called decorrelating detection and is briefly explained in Section 2.2.

2.1.2 One-Shot Matched Filtering for Asynchronous CDMA

The received equivalent low pass signal for the asynchronous communication in Eq. (2.1) can be written in "one-shot of ith bit" of any user[1] (without loss of generality we take user-1 and $i = 0$),

$$\begin{aligned} r(t) &= \sqrt{a_1}s_1(t)b_1(0) + \sum_{k=2}^{K}\left[\sqrt{a_k\epsilon_k}\frac{1}{\sqrt{\epsilon_k}}s_k^L(t)b_k(-1)\right. \\ &\quad \left. +\sqrt{a_k(1-\epsilon_k)}\frac{1}{\sqrt{1-\epsilon_k}}s_k^R(t)b_k(0)\right] + n(t), \end{aligned} \tag{2.6}$$

where $0 < \tau_2 < \tau_3 \ldots \tau_K < T$ is considered known,

$$\begin{aligned} s_k^L(t) &= \begin{cases} s_k(t+T-\tau_k) & \text{if } 0 \le t \le \tau_k \\ 0 & \text{if } \tau_k < t \le T \end{cases} \\ s_k^R(t) &= \begin{cases} 0 & \text{if } 0 \le t \le \tau_k \\ s_k(t-\tau_k) & \text{if } \tau_k < t \le T \end{cases} \\ \epsilon_k &= \int_0^{\tau_k} s_k^2(t+T-\tau_k)dt. \end{aligned} \tag{2.7}$$

The received signal, $r(t)$, is applied to a bank of filters matched to $s_1(t),\ \ s_k^L(t)/\sqrt{\epsilon_k},\ \ s_k^R(t)/\sqrt{1-\epsilon_k}$, $k = 2, \ldots, K$ as shown in Figure 2.3.

---

[1]This means in synchronous with the bits of that user.

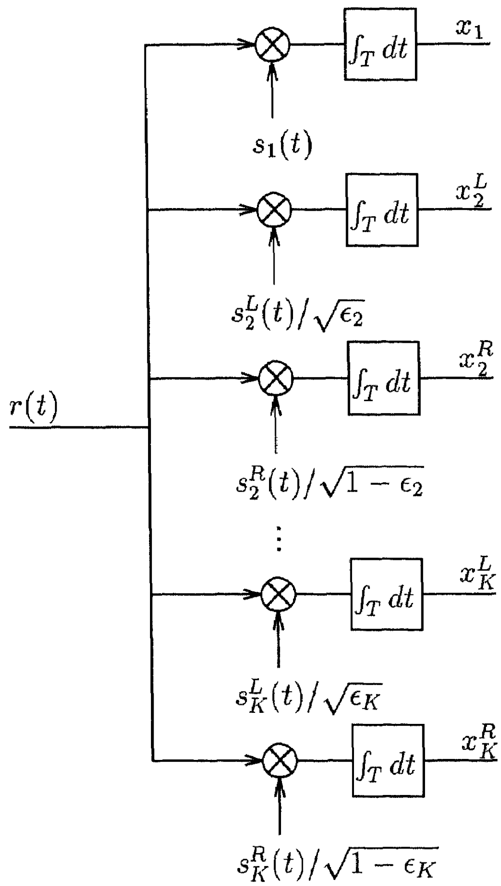

Figure 2.3 Matched filter bank for one-shot asynchronous CDMA.

The output of the matched filter bank in matrix notation is given by

$$\boldsymbol{x} = \boldsymbol{PAb} + \boldsymbol{n}, \tag{2.8}$$

where $\boldsymbol{P}$ is the $(2K-1)\times(2K-1)$ cross correlation matrix:

$$\boldsymbol{P} = \begin{bmatrix} 1 & \rho_{12}^L & \rho_{12}^R & \cdots & \rho_{1K}^L & \rho_{1K}^R \\ \rho_{21}^L & 1 & 0 & & \rho_{2K}^{LL} & \rho_{2K}^{LR} \\ \rho_{21}^R & 0 & 1 & & \rho_{2K}^{RL} & \rho_{2K}^{RR} \\ \vdots & & & \ddots & & \vdots \\ \rho_{K1}^L & \rho_{K2}^{LL} & \rho_{K2}^{LR} & & 1 & 0 \\ \rho_{K1}^R & \rho_{K2}^{RL} & \rho_{K2}^{RR} & \cdots & 0 & 1 \end{bmatrix}, \tag{2.9}$$

$\boldsymbol{A} = \mathrm{diag}\left(\sqrt{a_1}, \sqrt{a_2\epsilon_2}, \sqrt{a_2(1-\epsilon_2)}, \ldots, \sqrt{a_K\epsilon_K}, \sqrt{a_K(1-\epsilon_K)}\right)$, and $\boldsymbol{b} = [b_1(0), b_2(-1), b_2(0), \ldots, b_K(-1), b_K(0)]^T$. The $\boldsymbol{n}$ is a zero-mean Gaussian noise vector with covariance matrix $\boldsymbol{P}N_0/2$, $\boldsymbol{x}(0) = [x_1(0), x_2^L(0), x_2^R(0), \ldots, x_K^L(0), x_K^R(0)]^T$, which corresponds to the output of the filters matched to $s_1(t), s_k^L(t)$, where $s_k^R(t)$, $k = 2, 3, \ldots, K$ respectively, and

$$\begin{aligned}
\rho_{1k}^L &= \frac{1}{\sqrt{\epsilon_k}} \int_0^T s_1(t) s_k^L(t) dt \\
\rho_{1k}^R &= \frac{1}{\sqrt{1-\epsilon_k}} \int_0^T s_1(t) s_k^R(t) dt, \\
\rho_{kl}^{LL} &= \frac{1}{\sqrt{\epsilon_k \epsilon_l}} \int_0^T s_k^L(t) s_l^L(t) dt \\
\rho_{kl}^{RR} &= \frac{1}{\sqrt{(1-\epsilon_k)(1-\epsilon_l)}} \int_0^T s_k^R(t) s_l^R(t) dt \\
\rho_{kl}^{LR} &= \frac{1}{\sqrt{\epsilon_k (1-\epsilon_l)}} \int_0^T s_k^L(t) s_l^R(t) dt \\
\rho_{lm}^{RL} &= \frac{1}{\sqrt{(1-\epsilon_k)\epsilon_l}} \int_0^T s_k^R(t) s_l^L(t) dt, \quad k, l = 2, 3, \ldots, K. \qquad (2.10)
\end{aligned}$$

Clearly, $\rho_{kk}^{LL} = \rho_{kk}^{RR} = 1$, $\rho_{kk}^{RL} = \rho_{kk}^{LR} = 0$, $\rho_{kl}^{LR} = 0$ for $\tau_k < \tau_l$, $\rho_{kl}^{RL} = 0$ for $\tau_k > \tau_l$ and $\boldsymbol{n}(0) = [n_1(0), n_2^L(0), n_2^R(0), \ldots, n_K^L(0), n_K^R(0)]^T$ with

$$\begin{aligned}
n_1(0) &= \int_0^T n(t) s_1(t) dt, \\
n_k^L(0) &= \frac{1}{\sqrt{\epsilon_k}} \int_0^T n(t) s_k^L dt, \\
n_k^R(0) &= \frac{1}{\sqrt{1-\epsilon_k}} \int_0^T n(t) s_k^R(t) dt, \quad k = 2, 3, \ldots, K. \qquad (2.11)
\end{aligned}$$

2.2 Multi-Stage Detection

Upon realizing the inefficiency of using the matched filter detector for multiuser detection in CDMA, Verdú developed multiuser detectors that are optimum in terms of their BER performance for both synchronous and asynchronous CDMA systems [34]. The problem with these detectors is their exponential complexity with respect to the number of users, which may render them impractical.

Multi-stage detection is a suboptimum solution to the CDMA multiuser detection problem. Its complexity is linearly proportional to the the number of users. The main idea of the multiuser detection is to obtain a tentative estimate of the multiuser bits, then use these bits to reconstruct the multiuser interference and finally subtract the constructed interference from the matched filter-bank output signal. The better the tentative estimate of the original bits are, the better the multiuser interference cancellation is.

The tentative decision of the user bits can be obtained using a decorrelating detector as the first-stage. Then the output of the decorrelating detector is used to reconstruct and cancel the interference in the second-stage. This stage is referred to as the canceller stage. One may use the output of the canceller stage as the tentative decision and apply it to another canceller in the third-stage. This can be repeated for as many stages as we want, hence the name multi-stage.

We restrict ourselves to two-stage detectors only –the decorrelating detector as the first-stage and the canceller as the second-stage. Both of these stages are briefly explained in the following subsections.

2.2.1 Decorrelating Detector

This detector decorrelates the correlated matched filter-bank output signal vector. We present two types of decorrelating detectors commonly in use, one is non-adaptive and the other is adaptive[2].

2.2.1.1 Non-adaptive Decorrelating Detector This decorrelating detector uses the inverse of the cross correlation matrix $\boldsymbol{P}$ to transform the output the matched filter-bank. That is the output signal vector of the decorrelating detector can be written as

$$\begin{aligned} \boldsymbol{z} &= \boldsymbol{P}^{-1}\boldsymbol{x} \\ &= \boldsymbol{A}\boldsymbol{b} + \boldsymbol{\xi}, \end{aligned} \tag{2.12}$$

[2]The term "decorrelator" for the adaptive version is only used loosely, since it only decorrelate each output with a nonlinear function of the other outputs.

where $\boldsymbol{\xi} = \boldsymbol{P}^{-1}\boldsymbol{n}$.

The kth output signal is

$$z_k = \sqrt{a_k} b_k + \xi_k, \quad k = 1, \ldots, K. \tag{2.13}$$

Note that there is no multiuser interference in the output signal of the decorrelating detector. However, the AWGN variance is increased such that

$$\sigma^2_{\xi_k} = P^{-1}_{kk} N_0/2, \tag{2.14}$$

where P^{-1}_{kk} is the kkth element of $\boldsymbol{P}^{-1}$.

The tentative multiuser bit estimates are obtained by passing the decorrelating detector output signals through a hard limiter. Therefore from Eq. (2.13)

$$\hat{b}_k = \mathrm{sgn}(z_k), \quad k = 1, \ldots, K, \tag{2.15}$$

and in vector form,

$$\hat{\boldsymbol{b}} = \mathrm{sgn}(\boldsymbol{z}). \tag{2.16}$$

2.2.1.2 Adaptive Decorrelating Detector This decorrelating detector, also known as the "Bootstrap Separator," was first introduced by Bar-Ness [1,2] in his work for cancelling cross polarization interference. It was thereafter used in number of applications [3], [13,14], [21]. Its particular advantage as a decorrelating detector in the context of this work is given in [5]. It exploits the fact that the transmitted multiuser signals are uncorrelated with each other, and use this fact for the weight iteration algorithm to decorrelate the signals obtained at the matched filter-bank. It does not need any other information or reference bits for the convergence of the weights.

The bootstrap decorrelating detector is an adaptive linear transformation applied to the output of the matched filter-bank. The block diagram of the bootstrap detector for K CDMA users is depicted in Figure 2.4.

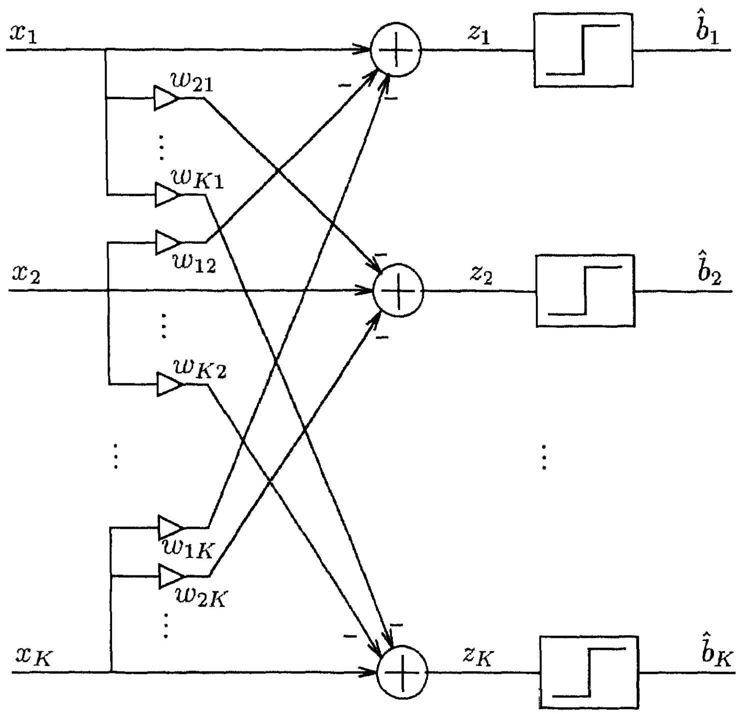

Figure 2.4 Adaptive bootstrap separator for K CDMA signals.

The matched filter-bank output vector $\boldsymbol{x}$ is linearly transformed by the bootstrap separator such that

$$\boldsymbol{z} = \boldsymbol{V}\boldsymbol{x}, \tag{2.17}$$

where $\boldsymbol{V}$ is a matrix defined as $\boldsymbol{V} = \boldsymbol{I} - \boldsymbol{W}$. The $\boldsymbol{I}$ is the $K \times K$ identity matrix and $\boldsymbol{W}$ is the adaptive weight matrix

$$\boldsymbol{W} = \begin{bmatrix} 0 & w_{12} & \cdots & w_{1K} \\ w_{21} & 0 & \cdots & w_{2K} \\ \vdots & & \ddots & \vdots \\ w_{K1} & w_{K2} & \cdots & 0 \end{bmatrix}. \tag{2.18}$$

The kth output of the bootstrap decorrelating detector is

$$z_k = x_k - \boldsymbol{w}_k^T \boldsymbol{x}_k, \quad k = 1, \ldots, K, \tag{2.19}$$

where $\boldsymbol{w}_k$ is the kth row vector of weight matrix $\boldsymbol{W}$, without its kth element and $\boldsymbol{x}_k$ is the matched filter-bank output vector $\boldsymbol{x}$ without its kth element x_k.

The adaptive weights for kth user are updated such that, the cross correlations between the kth output and signum function of all other users are minimized. That is

$$w_{kl} \leftarrow w_{kl} - \mu E\{z_k \mathrm{sgn}(z_l)\}, \quad k,l = 1,\ldots,K, \quad k \neq l, \tag{2.20}$$

where sgn($\cdot$) is used as a discrimination function in order to discriminate the bootstrap decorrelating detector outputs.

The decorrelating detector bit estimate vector can be written as

$$\hat{\boldsymbol{b}} = \mathrm{sgn}(\boldsymbol{z}). \tag{2.21}$$

2.2.2 Multiuser Interference Canceller

The tentative multiuser bit estimates obtained at the decorrelating detector output are used to estimate the multiuser interference present at the matched filter-bank output signals. The estimation is done in a non-adaptive or adaptive manner.

2.2.2.1 Non-adaptive Canceller The cross correlation matrix $\boldsymbol{P}$ is used to reconstruct the multiuser interference at the canceller. Then the reconstructed multiuser interference is subtracted from the actual multiuser interference present in the matched filter-bank output signal vector [31,32]. This is done as follows:

$$\boldsymbol{y} = \boldsymbol{x} + (\boldsymbol{I} - \boldsymbol{P})\boldsymbol{A}\hat{\boldsymbol{b}}, \tag{2.22}$$

where $\boldsymbol{I}$ is the $K \times K$ identity matrix.

Note that, in order to reconstruct the interference, the canceller needs to know the signal energy of every user, beside the knowledge of the cross correlation matrix $\boldsymbol{P}$.

Finally, the multiuser bit estimate at the canceller output is obtained by passing the canceller output signal vector through a hard limiter. That is,

$$\hat{\hat{\boldsymbol{b}}} = \mathrm{sgn}(\boldsymbol{y}). \tag{2.23}$$

2.2.2.2 Adaptive Canceller This adaptive multiuser interference canceller, is based on the idea of minimizing the signal energy of the kth detector output y_k with respect to the other users' tentative estimate bits obtained at the decorrelating detector. The adaptive canceller is depicted in Figure 2.5.

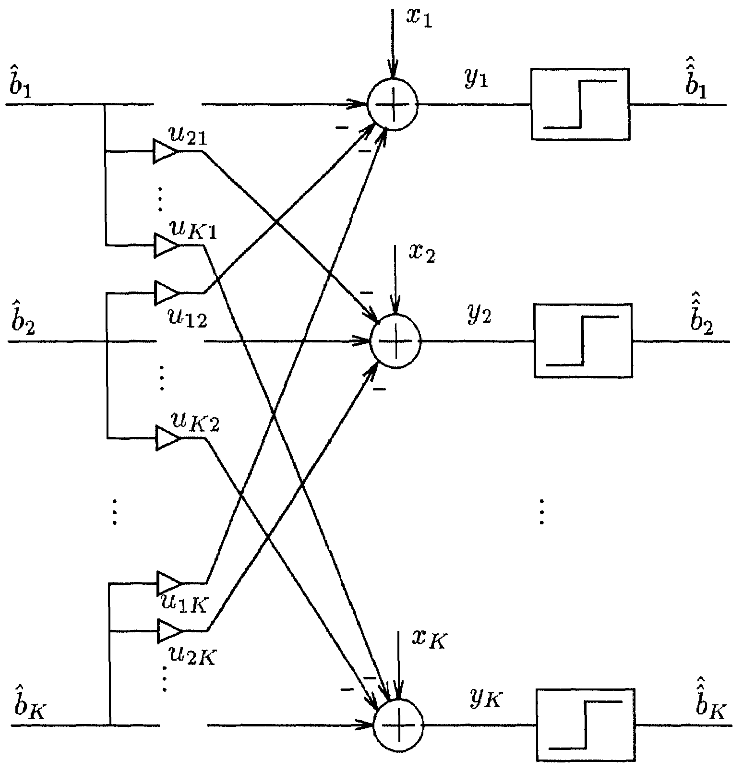

Figure 2.5 Adaptive multiuser interference canceller for K CDMA signals.

The adaptive weight matrix of the canceller can be written as

$$\boldsymbol{U} = \begin{bmatrix} 0 & u_{12} & \cdots & u_{1K} \\ u_{21} & 0 & \cdots & u_{2K} \\ \vdots & \vdots & \ddots & \vdots \\ u_{K1} & u_{K2} & \cdots & 0 \end{bmatrix}. \tag{2.24}$$

The kth output signal of the canceller is

$$y_k = x_k - \boldsymbol{u}_k^T \hat{\boldsymbol{b}}_k, \tag{2.25}$$

where $\boldsymbol{u}_k$ is kth row vector of the weight matrix $\boldsymbol{U}$ without its kth element and $\hat{\boldsymbol{b}}_k$ is obtained from the decorrelating detector output bit estimate vector $\hat{\boldsymbol{b}}$ by deleting its kth element $\hat{b}_k$.

The minimization of power of the kth output signal y_k with respect to the other users' estimate bits takes place in an iterative manner such that

$$\begin{aligned} u_{kl} &\leftarrow u_{kl} - \mu \frac{\partial E\{y_k^2\}}{\partial u_{kl}} \\ u_{kl} &\leftarrow u_{kl} - 2\mu E\{y_k \hat{b}_l\}, \quad k, l = 1, \ldots, K, \quad k \neq l. \end{aligned} \tag{2.26}$$

Finally, the kth user bit estimate obtained at the canceller output can be written as

$$\hat{\hat{b}}_k = \mathrm{sgn}(y_k) \tag{2.27}$$

2.3 Summary

This chapter serves as a background to the CDMA communication system and multi-stage detection scheme. We have briefly explained synchronous and asynchronous CDMA communication systems. For the ease of the analysis, the baseband equivalent model is used. It is demonstrated that with respect to the chosen one-shot user, except for system dimension, the asynchronous CDMA system is essentially equivalent to the synchronous CDMA system.

We also explained, in this chapter, the principles of multi-stage detection. The first two stages of the multi-stage CDMA detector, that is, the decorrelating detector and the canceller were presented in detail. These are the essential components of the multi-stage detector. For these stages, both adaptive and non-adaptive schemes were introduced.

CHAPTER 3

BOOTSTRAP SEPARATOR FOR ASYNCHRONOUS CDMA COMMUNICATION WITH CODE-DELAY ESTIMATION ERROR

In asynchronous CDMA communication the delay estimation of the user codes depends on the accuracy of the synchronization scheme used. In many practical situations, however, perfect delay estimation is not possible. Therefore, the decorrelating detector used as the first stage for the multi-stage detector has to be robust to the code delay estimation errors.

In this chapter the BER performances of the adaptive and non-adaptive decorrelating detectors are compared for an asynchronous CDMA communication system with a code delay estimation error. In Section 3.1, the one-shot matched filter-bank output signal vector with a code delay estimation error is formulated. In Section 3.2 the BER performances of non-adaptive and adaptive decorrelating detectors are found numerically for two asynchronous CDMA users whose code delay estimates are erroneous. Finally, in Section 3.3 simulation results for these two users are demonstrated and observations from these results are stated.

3.1 One-Shot Matched Filter with Code Delay Estimation Error

For the asynchronous CDMA system, the equivalent low pass received signal to the one-shot matched filter-bank input is given in Eq. (2.6) and reproduced here for convenience

$$\begin{aligned} r(t) &= \sqrt{a_1} s_1(t) b_1(0) + \sum_{k=2}^{K} \left[\sqrt{a_k \epsilon_k} \frac{1}{\sqrt{\epsilon_k}} s_k^L(t) b_k(-1) \right. \\ &\quad \left. + \sqrt{a_k(1-\epsilon_k)} \frac{1}{\sqrt{1-\epsilon_k}} s_k^R(t) b_k(0) \right] + n(t), \end{aligned} \tag{3.1}$$

For the sake of simplicity we will restrict ourselves to two asynchronous CDMA users only. Extension to a higher number of users is relatively simple.

Representing the signal of Eq. (3.1) in one-shot of the ith bit of user one, and without loss of generality, letting $i = 0$, we write,

$$\begin{aligned} r(t) &= \sqrt{a_1} s_1(t) b_1(0) + \sqrt{a_2 \epsilon_2} \frac{1}{\sqrt{\epsilon_2}} s_2^L(t) b_2(-1) \\ &\quad + \sqrt{a_2(1-\epsilon_2)} \frac{1}{\sqrt{1-\epsilon_2}} s_2^R(t) b_2(0) + n(t), \end{aligned} \tag{3.2}$$

where $0 \le \tau_2 \le T$ is considered to be estimated with an error, and;

$$\begin{aligned} s_2^L(t) &= \begin{cases} s_2(t+T-\tau_2) & \text{if } 0 \le t \le \tau_2 \\ 0 & \text{if } \tau_2 < t \le T \end{cases} \\ s_2^R(t) &= \begin{cases} 0 & \text{if } 0 \le t \le \tau_2 \\ s_2(t-\tau_2) & \text{if } \tau_2 < t \le T \end{cases} \\ \epsilon_2 &= \int_0^{\tau_2} s_2^2(t+T-\tau_2)dt. \end{aligned} \tag{3.3}$$

As shown in Figure 3.1, $r(t)$ is applied to the one-shot matched filter-bank with a code delay estimation error.

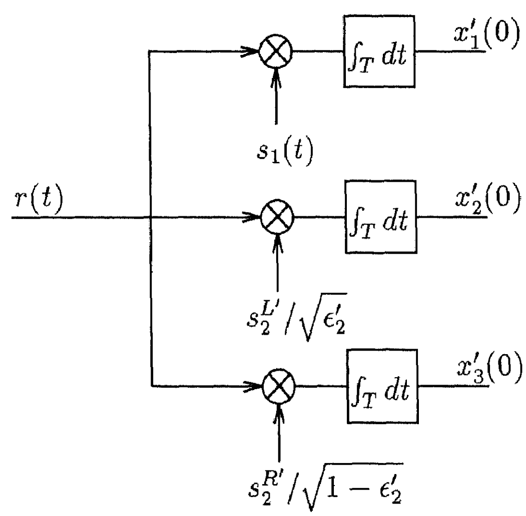

Figure 3.1 One-shot matched filter-bank for 2 asynchronous CDMA users with code-delay estimation error.

That is, the signature function of Eq. (3.3) is extended to τ_2' instead of τ_2 and normalized by ϵ_2' instead of ϵ_2. That is,

$$s_2^{L'}(t) = \begin{cases} s_2(t+T-\tau_2') & \text{if } 0 \le t \le \tau_2 \\ 0 & \text{if } \tau_2' < t \le T \end{cases}$$

$$
\begin{aligned}
s_2^{R'}(t) &= \begin{cases} 0 & \text{if } 0 \le t \le \tau_2' \\ s_2(t-\tau_2') & \text{if } \tau_2' < t \le T \end{cases} \\
\epsilon_2' &= \int_0^{\tau_2'} s_2^2(t+T-\tau_2')dt. \qquad (3.4)
\end{aligned}
$$

The output of the first filter is

$$
\begin{aligned}
x_1'(0) &= \int_0^T r(t)s_1(t)dt \\
&= \sqrt{a_1}b_1(0) + \sqrt{a_2\epsilon_2}\rho_{12}^L b_2(-1) \\
&\quad + \sqrt{a_2(1-\epsilon_2)}\rho_{12}^R b_2(0) + n_1'(0), \qquad (3.5)
\end{aligned}
$$

where $n_1'(0) = \int_0^T n(t)s_1(t)dt$ is a zero-mean Gaussian noise with variance $N_0/2$, and

$$
\begin{aligned}
\rho_{12}^L &= \frac{1}{\sqrt{\epsilon_2}}\int_0^T s_1(t)s_2^L(t)dt \\
\rho_{12}^R &= \frac{1}{\sqrt{1-\epsilon_2}}\int_0^T s_1(t)s_2^R(t)dt. \qquad (3.6)
\end{aligned}
$$

The output of the second filter is given by

$$
\begin{aligned}
x_2'(0) &= \frac{1}{\sqrt{\epsilon_2'}}\int_0^T r(t)s_2^{L'}(t)dt \\
&= \sqrt{a_1}\rho_{21}^{L'}b_1(0) + \sqrt{a_2\epsilon_2}\rho_{22}^{L'L}b_2(-1) \\
&\quad + \sqrt{a_2(1-\epsilon_2)}\rho_{22}^{L'R}b_2(0) + n_2'(0), \qquad (3.7)
\end{aligned}
$$

where

$$
\begin{aligned}
\rho_{21}^{L'} &= \frac{1}{\sqrt{\epsilon_2'}}\int_0^T s_1(t)s_2^{L'}(t)dt \\
\rho_{22}^{L'L} &= \frac{1}{\sqrt{\epsilon_2'\epsilon_2}}\int_0^T s_2^{L'}(t)s_2^L(t)dt \\
\rho_{22}^{L'R} &= \frac{1}{\sqrt{\epsilon_2'(1-\epsilon_2)}}\int_0^T s_2^{L'}(t)s_2^R(t)dt \qquad (3.8)
\end{aligned}
$$

and

$$
n_2'(0) = \frac{1}{\sqrt{\epsilon_2'}}\int_0^T s_2^{L'}n(t)dt\ . \qquad (3.9)
$$

The output of the third filter is given by

$$\begin{aligned} x_3'(0) &= \frac{1}{\sqrt{1-\epsilon_2'}}\int_0^T r(t)s_2^{R'}(t)dt \\ &= \sqrt{a_1}\rho_{21}^{R'}b_1(0) + \sqrt{a_2\epsilon_2}\rho_{22}^{R'L}b_2(-1) \\ &\quad + \sqrt{a_2(1-\epsilon_2)}\rho_{22}^{R'R}b_2(0) + n_3'(0), \end{aligned} \tag{3.10}$$

where

$$\begin{aligned} \rho_{21}^{R'} &= \frac{1}{\sqrt{1-\epsilon_2'}}\int_0^T s_2^{R'}(t)s_1(t)dt \\ \rho_{22}^{R'L} &= \frac{1}{\sqrt{(1-\epsilon_2')\epsilon_2}}\int_0^T s_2^{R'}(t)s_2^{L}(t)dt \\ \rho_{22}^{R'R} &= \frac{1}{\sqrt{(1-\epsilon_2')(1-\epsilon_2)}}\int_0^T s_2^{R'}(t)s_2^{R}(t)dt \end{aligned} \tag{3.11}$$

and

$$n_3'(0) = \frac{1}{\sqrt{1-\epsilon_2'}}\int_0^T n(t)s_2^{R'}dt\ . \tag{3.12}$$

Combining Eqs. (3.5), (3.7) and (3.10) in a matrix form,

$$\boldsymbol{x}'(0) = \boldsymbol{P}'\boldsymbol{A}\boldsymbol{b}(0) + \boldsymbol{n}'(0), \tag{3.13}$$

where

$$\boldsymbol{P}' = \begin{bmatrix} 1 & \rho_{12}^{L} & \rho_{12}^{R} \\ \rho_{21}^{L'} & \rho_{22}^{L'L} & \rho_{22}^{L'R} \\ \rho_{21}^{R'} & \rho_{22}^{R'L} & \rho_{22}^{R'R} \end{bmatrix}, \tag{3.14}$$

$$\begin{aligned} \boldsymbol{A} &= \operatorname{diag}\left(\sqrt{a_1}, \sqrt{\epsilon_2 a_2}, \sqrt{(1-\epsilon_2)a_2}\right) \\ &= \operatorname{diag}(\alpha_1, \alpha_2, \alpha_3), \end{aligned} \tag{3.15}$$

$\boldsymbol{b}(0) = [b_1(0), b_2(-1), b_3(0)]^T$ and $\boldsymbol{n}'(0)$ is a zero-mean Gaussian noise vector with the covariance matrix,

$$\boldsymbol{C}' = \begin{bmatrix} 1 & \rho_{21}^{L'} & \rho_{21}^{R'} \\ \rho_{21}^{L'} & 1 & 0 \\ \rho_{21}^{R'} & 0 & 1 \end{bmatrix} \frac{N_0}{2}. \tag{3.16}$$

3.2 Decorrelating Detector

In this section both non-adaptive and adaptive decorrelating detectors are examined when the user code delay estimations are not precise. Their BER performances are also formulated in the following sub-sections.

3.2.1 Non-Adaptive Decorrelating Detector

The non-adaptive decorrelating detector was explained in Section 2.2. It decorrelates the signal vector obtained at the matched filter-bank output by multiplying it with the inverse of the cross correlation matrix. The cross correlation matrix is obtained from the user codes and their delay estimations. For two asynchronous CDMA users when the delay estimation of the second user code is erroneous, the receiver will assume that the cross correlation matrix is

$$\boldsymbol{P} = \begin{bmatrix} 1 & \rho_{21}^{L'} & \rho_{21}^{R'} \\ \rho_{21}^{L'} & 1 & 0 \\ \rho_{21}^{R'} & 0 & 1 \end{bmatrix} \tag{3.17}$$

and use it to obtain the output of the decorrelating detector. That is

$$\begin{aligned} \boldsymbol{z}(0) &= \boldsymbol{P}^{-1}\boldsymbol{x}'(0) \\ &= \boldsymbol{J}\boldsymbol{A}\boldsymbol{b}(0) + \boldsymbol{\xi}(0), \end{aligned} \tag{3.18}$$

where $\boldsymbol{J} = \boldsymbol{P}^{-1}\boldsymbol{P}'$ and $\boldsymbol{\xi}(0) = \boldsymbol{P}^{-1}\boldsymbol{n}'(0)$. Comparing Eqs. (3.16) and (3.17) we note that $E\{\boldsymbol{n}'(0)\boldsymbol{n}'^T(0)\} = \boldsymbol{P}N_0/2$. Therefore $\boldsymbol{\xi}(0)$ is a Gaussian noise vector with covariance matrix $\boldsymbol{P}^{-1}N_0/2$.

Note that $\boldsymbol{J}$ is not a diagonal matrix. Therefore, the use of the inverse of $\boldsymbol{P}$ as a linear transformation on the matched filter-bank output vector cannot decorrelate the matched filter-bank output vector. That is, the non-adaptive decorrelating detector is no longer near-far resistant. This results in a substantial BER performance degradation for the non-adaptive decorrelating detector. The BER for the kth user can be calculated as

$$\mathrm{BER}_k = \frac{1}{2^2} \sum_{\boldsymbol{b}_k \in \{\cdot\}} Q\left(\frac{J_{kk}\sqrt{\alpha_k} + \boldsymbol{j}_k^T \boldsymbol{b}_k}{\sigma_{\xi_k}}\right), \quad k = 1, 2, 3, \tag{3.19}$$

where J_{kk} is the kth diagonal element of $\boldsymbol{J}$, α_k is the kth diagonal element of $\boldsymbol{A}$, $\boldsymbol{j}_k$ is the kth row vector of $\boldsymbol{J}$ without its kth element, $\boldsymbol{b}_k$ is the bit vector $\boldsymbol{b}$ without its kth element and $\sigma_{\xi_k}^2$ is the variance of ξ_k. The set $\{\cdot\}$ contains all the possible combinations of bit vector $\boldsymbol{b}_k$.

The BER performance of the first user is calculated for 2 asynchronous CDMA users. It is assumed that the actual second user code delay is 0.4 and estimated to be 0.35 at the matched filter-bank. The corresponding cross correlation matrices at the matched filter-bank and at the decorrelating detector are

$$\boldsymbol{P}' = \begin{bmatrix} 1 & 0.3162 & 0.7746 \\ 0.3101 & 0.9354 & 0 \\ 0.9297 & 0.0981 & 0.9608 \end{bmatrix}, \tag{3.20}$$

and

$$\boldsymbol{P} = \begin{bmatrix} 1 & 0.3101 & 0.9297 \\ 0.3101 & 1 & 0 \\ 0.9297 & 0 & 1 \end{bmatrix}, \tag{3.21}$$

respectively.

Figures 3.2 and 3.3 depict the BER performance of user-1 using Eq. (3.19). The first figure shows the BER performance of the user-1 as a function of SNR_1 when SNR_2 is 4 dB above and below SNR_1. The second figure shows the BER performance of user-1 as a function of $\mathrm{SNR}_2 - \mathrm{SNR}_1$ when SNR_1 is fixed at 6 dB, 8 dB and 10 dB. Note that in all cases the performance is very poor.

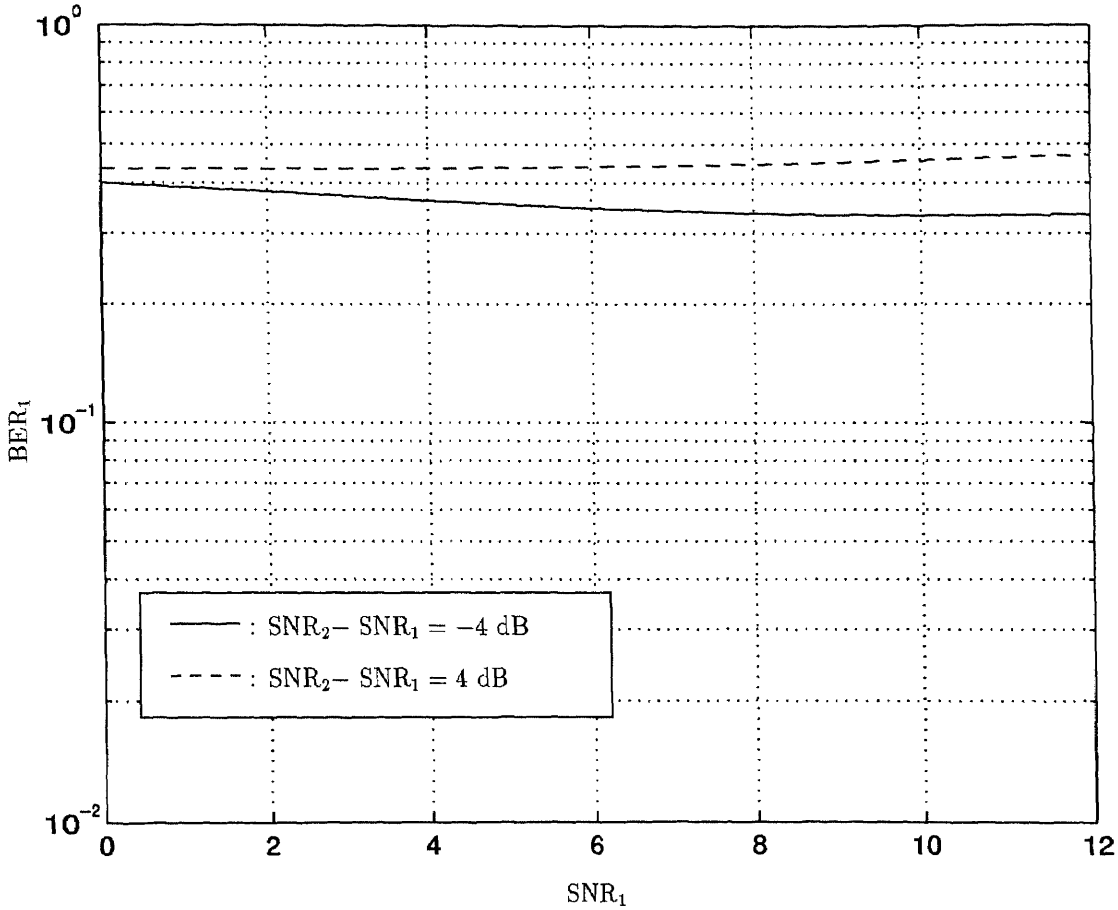

Figure 3.2 Numerical BER performance of the non-adaptive decorrelating detector for fixed interference and variable SNR_1.

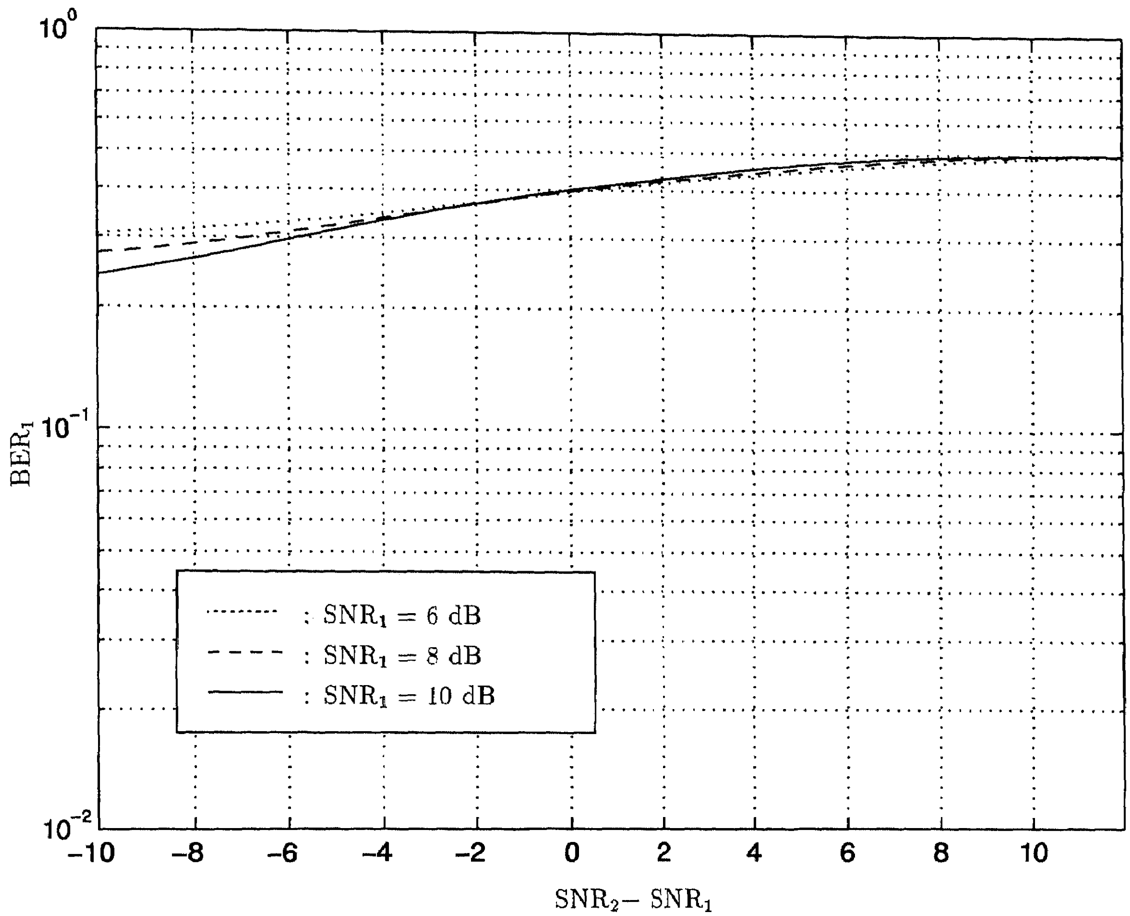

Figure 3.3 Numerical BER performance of the non-adaptive decorrelating detector for variable interference and fixed SNR_1.

3.2.2 Bootstrap Decorrelating Detector

Since the code delay estimations used at the one-shot matched filter-bank are erroneous, the cross correlation matrix obtained at the matched filter-bank is also erroneous. Using the inverse of the cross correlation matrix that corresponds to erroneous delays, to transform output of the one-shot matched filter-bank, results in BER performance degradation. Instead we propose to use the bootstrap adaptive decorrelating detector for this purpose. The bootstrap decorrelating detector for two asynchronous users is depicted in Figure 3.4.

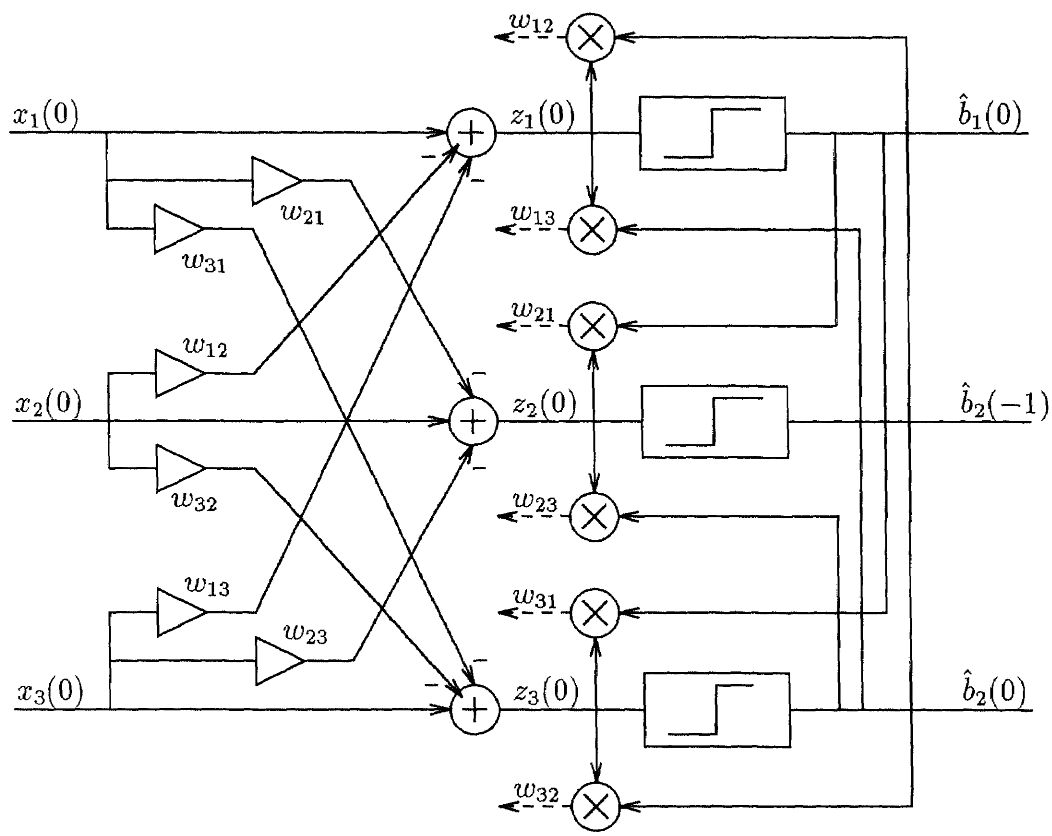

Figure 3.4 Adaptive bootstrap decorrelating detector for two asynchronous CDMA users.

From Eq. (2.17) the bootstrap decorrelating detector output can be written as

$$\boldsymbol{z}(0) = \boldsymbol{x}(0) - \boldsymbol{W}\boldsymbol{x}(0), \tag{3.22}$$

where

$$\boldsymbol{W} = \begin{bmatrix} 0 & w_{12} & w_{13} \\ w_{21} & 0 & w_{23} \\ w_{31} & w_{32} & 0 \end{bmatrix}. \tag{3.23}$$

3.2.2.1 Steady State Weights The kth output of the decorrelator can be expressed as,

$$z_k = x_k - \boldsymbol{w}_k^T \boldsymbol{x}_k \tag{3.24}$$

where $\boldsymbol{w}_k^T$ is the kth row vector of $\boldsymbol{W}$ with the element w_{kk} deleted and $\boldsymbol{x}_k$ is the vector obtained from $\boldsymbol{x}$ by deleting x_k.

For controlling the weights, we use the steepest descent algorithm which simultaneously reduces the absolute value of the correlation between the outputs of the decorrelator and the decision on all other outputs. That is, the weight w_{kl} is controlled by the recursion

$$w_{kl} \leftarrow w_{kl} - \mu E\{z_k \mathrm{sgn}(z_l)\}, \quad k, l = 1, \ldots, K, \quad k \neq l. \tag{3.25}$$

The above recursion reaches steady-state in the mean when $E\{z_k \mathrm{sgn}(z_l)\} = 0$. Note that w_{12}, for example, is used to cancel the residue of $b_2(-1)$ at the output of z_1. It will settle down only when that residue (being correlated with $\hat{b}_2(-1)$) is zero. But any reduction of $b_2(-1)$ at z_1 will improve $b_1(0)$ (smaller error), being more effective in reducing the residue of $b_1(0)$ at z_2 and z_3 through the weights w_{21} and w_{31}. Therefore, the process of residue cancellation is enhanced successively which justify, using the name "bootstrap" in previous applications.

Eq. (3.25) can be written in vectoral form as

$$\boldsymbol{w}_k \leftarrow \boldsymbol{w}_k - \mu E\{z_k \mathrm{sgn}(\boldsymbol{z}_k)\}, \tag{3.26}$$

where again $\boldsymbol{z}_k$ is obtained from $\boldsymbol{z}$ by deleting z_k. The steady state is reached if $E\{z_k \text{sgn}(\boldsymbol{z}_k)\} = \boldsymbol{0}$ for $k = 1, 2, 3$.

In the following derivations the cross correlation matrix is assumed to be non-singular. Let $\text{sgn}(\boldsymbol{z}_k) = \hat{\boldsymbol{b}}_k$. If we assume the SNR's are large enough so that the main contribution to the decorrelating detector output error is the multiuser interference, then $E\{z_k \hat{\boldsymbol{b}}_k\}$ can be approximated by

$$\begin{aligned} E\{z_k \hat{\boldsymbol{b}}_k\} &\approx [\boldsymbol{I} - 2Pr(\hat{\boldsymbol{b}}_k \text{ is erroneous})] E\{z_k \boldsymbol{b}_k\} \\ &\approx E\{z_k \boldsymbol{b}_k\}. \end{aligned} \tag{3.27}$$

Equating $E\{z_k \hat{\boldsymbol{b}}_k\}$ to zero and using the above approximation we get

$$E\{z_k \hat{\boldsymbol{b}}_k\} \approx E\{(\rho_{kk}\sqrt{a}_k b_k + \boldsymbol{\rho}_k^T \boldsymbol{A}_k \boldsymbol{b}_k + n_k - \boldsymbol{w}_k^T \boldsymbol{x}_k)\boldsymbol{b}_k\} = \boldsymbol{0}, \tag{3.28}$$

where ρ_{kk} is the kth term of the diagonal of $\boldsymbol{P}$, the $\sqrt{a}_k$ is the kth diagonal term of $\boldsymbol{A}$, the $\boldsymbol{\rho}_k$ is the kth row vector of $\boldsymbol{P}$ without its kth element and the $\boldsymbol{A}_k$ is a matrix obtained from $\boldsymbol{A}$ by deleting its kth row and column.

From the above equation

$$E\{\rho_{kk}\sqrt{a}_k b_k \boldsymbol{b}_k\} + E\{(\boldsymbol{\rho}_k^T \boldsymbol{A}_k \boldsymbol{b}_k)\boldsymbol{b}_k\} + E\{n_k \boldsymbol{b}_k\} - E\{(\boldsymbol{w}_k^T \boldsymbol{x}_k)\boldsymbol{b}_k\} = \boldsymbol{0}. \tag{3.29}$$

It is easy to show that $E\{b_k \boldsymbol{b}_k\} = \boldsymbol{0}$, $E\{(\boldsymbol{\rho}_k^T \boldsymbol{A}_k \boldsymbol{b}_k)\boldsymbol{b}_k\} = \boldsymbol{A}_k \boldsymbol{\rho}_k$, and $E\{n_k \boldsymbol{b}_k\} = \boldsymbol{0}$, so that

$$E\{(\boldsymbol{w}_k^T \boldsymbol{x}_k)\boldsymbol{b}_k\} = \boldsymbol{A}_k \boldsymbol{\rho}_k. \tag{3.30}$$

From (2.8)

$$\begin{aligned} \boldsymbol{x}_k &= \begin{bmatrix} \boldsymbol{P}_k & \boldsymbol{p}_k \end{bmatrix} \begin{bmatrix} \boldsymbol{A}_k & \boldsymbol{0} \\ \boldsymbol{0} & \sqrt{a}_k \end{bmatrix} \begin{bmatrix} \boldsymbol{b}_k \\ b_k \end{bmatrix} + \boldsymbol{n}_k \\ &= \boldsymbol{P}_k \boldsymbol{A}_k \boldsymbol{b}_k + \boldsymbol{p}_k \sqrt{a}_k b_k + \boldsymbol{n}_k. \end{aligned} \tag{3.31}$$

where $\boldsymbol{P}_k$ is obtained from $\boldsymbol{P}$ by deleting its kth row and column and the $\boldsymbol{p}_k$ is the kth column vector of $\boldsymbol{P}$ without its kth element. Therefore,

$$E\{(\boldsymbol{w}_k^T \boldsymbol{x}_k)\boldsymbol{b}_k\} = \boldsymbol{A}_k \boldsymbol{P}_k^T \boldsymbol{w}_k. \tag{3.32}$$

The steady state weights can be found from Eqs. (3.30) and (3.32) as

$$\boldsymbol{w}_k^T = \boldsymbol{\rho}_k^T \boldsymbol{P}_k^{-1}. \tag{3.33}$$

3.2.2.2 BER Performance The decorrelating decorrelator's steady state output for kth user, $k = 1, 2, 3$, can be written from Eq. (3.24) together with Eq. (3.33),

$$\begin{aligned} z_k &= \rho_{kk}\sqrt{a}_k b_k + \boldsymbol{\rho}_k^T \boldsymbol{A}_k \boldsymbol{b}_k + n_k - \boldsymbol{\rho}_k^T \boldsymbol{P}_k^{-1}(\boldsymbol{P}_k \boldsymbol{A}_k \boldsymbol{b}_k + \boldsymbol{p}_k \sqrt{a}_k b_k + \boldsymbol{n}_k) \\ &= (\rho_{kk} - \boldsymbol{\rho}_k^T \boldsymbol{P}_k^{-1} \boldsymbol{p}_k)\sqrt{a}_k b_k + n_k - \boldsymbol{\rho}_k^T \boldsymbol{P}_k^{-1} \boldsymbol{n}_k. \end{aligned} \tag{3.34}$$

Note that the decorrelating detector perfectly cancels the interfering signal energy. On the other hand, the desired user bit energy is modified by $(1 - \boldsymbol{\rho}_k^T \boldsymbol{P}_k^{-1} \boldsymbol{p}_k)$, and the noise variance is given by

$$\begin{aligned} \sigma_{\xi_k}^2 &= E\{(n_k - \boldsymbol{\rho}_k^T \boldsymbol{P}_k^{-1} \boldsymbol{n}_k)^2\} \\ &= (1 + \boldsymbol{\rho}_k^T \boldsymbol{P}_k^{-1} \boldsymbol{C}_k \boldsymbol{P}_k^{-T} \boldsymbol{\rho}) N_0/2 \end{aligned} \tag{3.35}$$

where $\boldsymbol{C}_k$ is obtained from the covariance matrix $\boldsymbol{C}$ by deleting its kth row and column.

From the above equation, the BER for the kth user can be calculated as

$$\mathrm{BER}_k = Q\left(\frac{(1 - \boldsymbol{\rho}_k^T \boldsymbol{P}_k^{-1} \boldsymbol{p}_k)\sqrt{a}_k}{\sigma_{\xi_k}}\right) \tag{3.36}$$

where $Q(x) = \frac{1}{\sqrt{2\pi}} \int_x^\infty e^{-y^2/2} dy$.

3.3 Simulation Results

A two user one-shot asynchronous CDMA system is simulated with the actual delay of the second user signature sequence with respect to the first user ϵ_2 being 0.4 and the estimated delay ϵ_2' being 0.35. The resulting cross correlation matrix at the matched filter-bank with the delay estimation error is assumed to be

$$\boldsymbol{P} = \begin{bmatrix} 1 & 0.3162 & 0.7746 \\ 0.3101 & 0.9354 & 0 \\ 0.9297 & 0.0981 & 0.9608 \end{bmatrix}. \tag{3.37}$$

The matched filter-bank output vector is then applied to the non-adaptive decorrelating detector as well as to the bootstrap separator. The BER performance of the desired user (user 1) is depicted in Figure 3.5 and Figure 3.6 for various desired and interfering signal energies.

It is observed that the non-adaptive decorrelating detector is very sensitive to the signature sequence delay estimation errors, whereas the bootstrap separator is not so sensitive to the delay estimation errors.

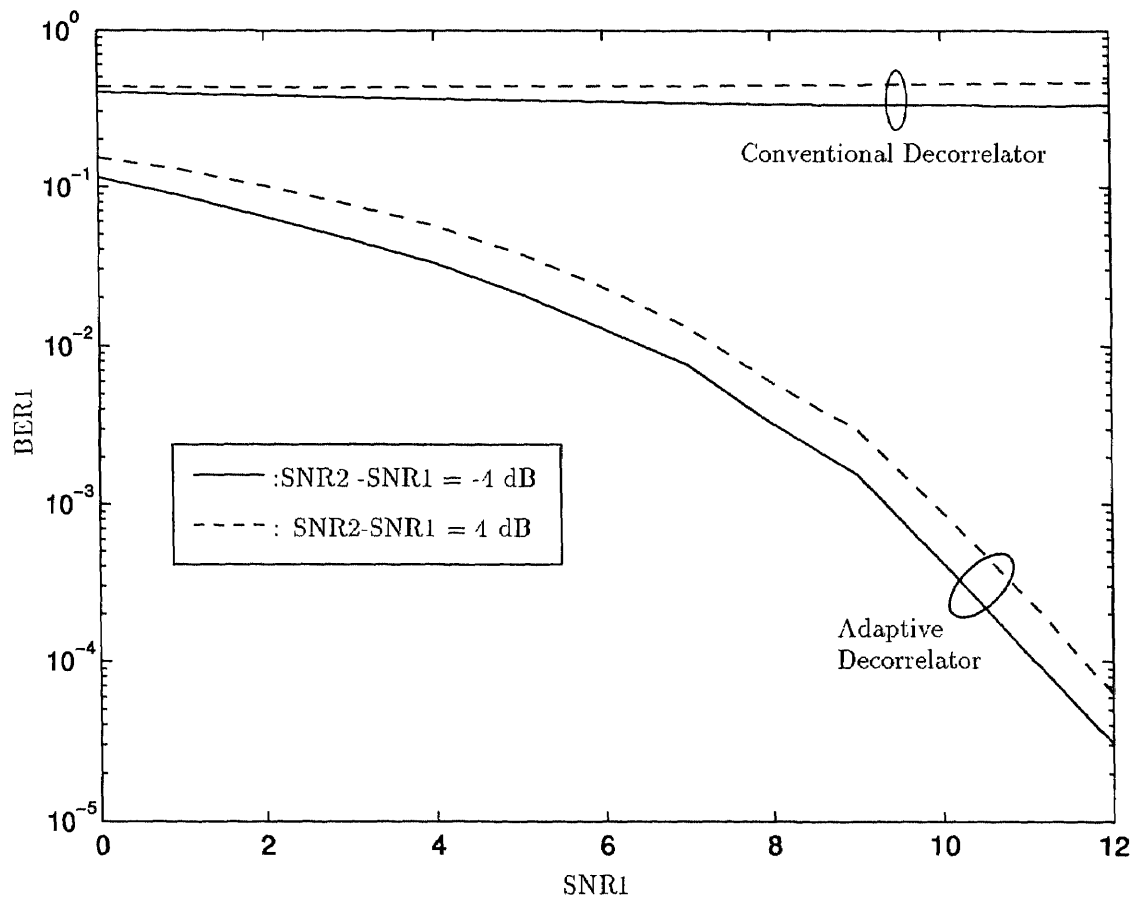

Figure 3.5 Simulated BER performance comparison of the adaptive and non-adaptive decorrelating detectors for fixed interference and variable SNR_1.

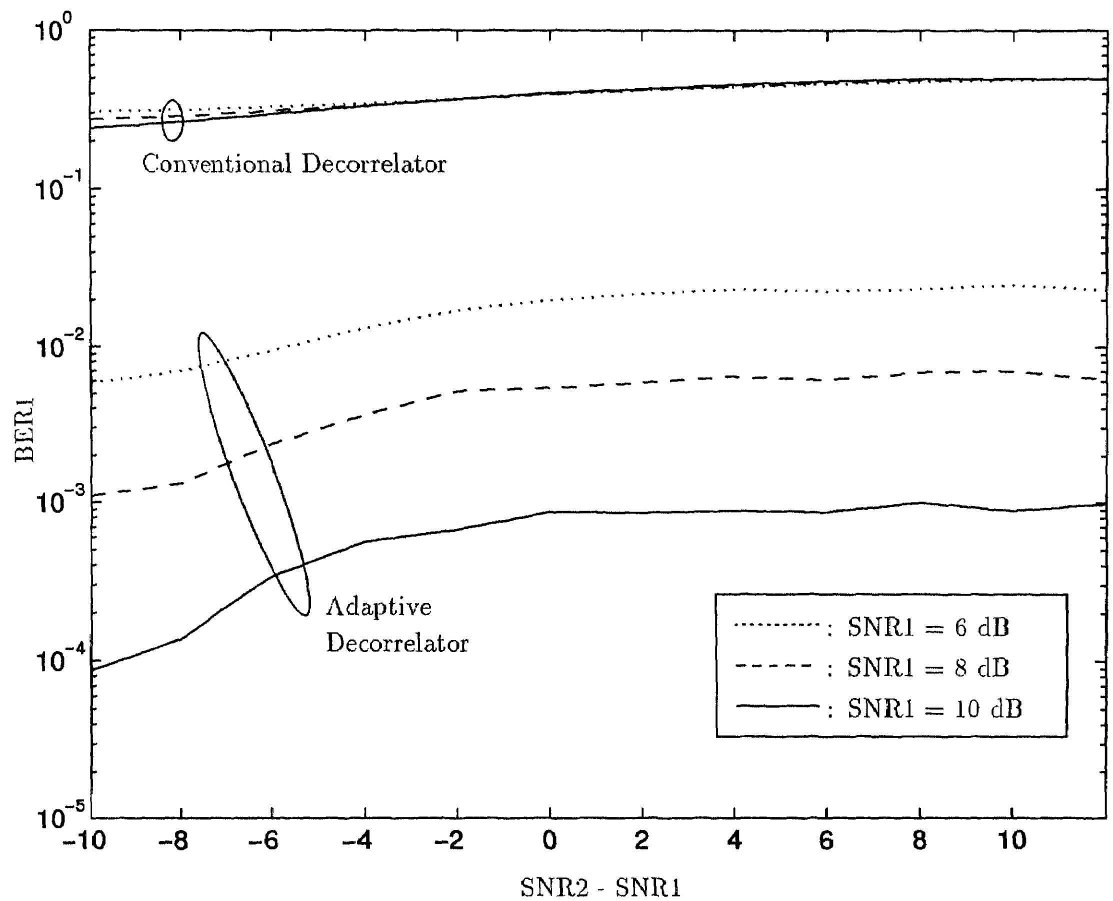

Figure 3.6 Simulated BER performance comparison of the adaptive and non-adaptive decorrelating detectors for variable interference and fixed SNR_1.

3.4 Summary

In this chapter we have compared the robustness of adaptive and non-adaptive decorrelating detectors against the code delay estimation error. The delay estimation error is a problem of asynchronous (up-link) CDMA communication. Therefore, we used the one-shot detection scheme.

The effect of the code delay estimation error on the matched filter-bank was derived in detail. Both the adaptive and non-adaptive decorrelating detector BER performances are obtained for comparison. Because of the code delay estimation error, it is observed that the non-adaptive decorrelating detector is no longer near-far resistant and its BER performance depreciates significantly. On the other hand, the adaptive decorrelating detector (the bootstrap separator) is robust against the delay estimation error and has a superior BER performance compared to the non-adaptive decorrelating detector.

CHAPTER 4

ADAPTIVE TENTATIVE SOFT LIMITER FOR ADAPTIVE MULTI-STAGE CDMA DETECTOR

When the interfering signal bit energies are low, the tentative bit estimates for these signals, obtained at the decorrelating detector output, are not accurate. It is observed that if the hard limiters are eliminated and these signals are used directly instead of their bit estimates a better BER performance is obtained for the canceller in the low interference region. This is depicted in Figure 4.1 for two synchronous CDMA users. Wherein two-stage detector without hard limiters perform better than one with the hard limiters when $\mathrm{SNR}_2 - \mathrm{SNR}_1 < -1$ dB. This is the main motivation for using soft limiter [11]. For setting up the thresholds of these limiters [11] suggests a "heuristic formula" which requires signal measurements at the output of the decorrelating detector.

In this chapter, we adopt the idea of setting the soft limiter thresholds adaptively. Thus the major drawback of the heuristic threshold method, the need for signal measurement and evaluating the threshold values, are avoided. In the following section the system model used is described. Then, in Section 4.2, the detector's adaptive optimal parameters, that is, steady-state canceller weights and steady state threshold values, are evaluated. Also in this section the iteration algorithms for both canceller weights and threshold settings are described. In Section 4.3, a two-user case is demonstrated as an example. In this section also the BER performance of the two-user system is analytically evaluated and conclusions are drawn from numerical calculations.

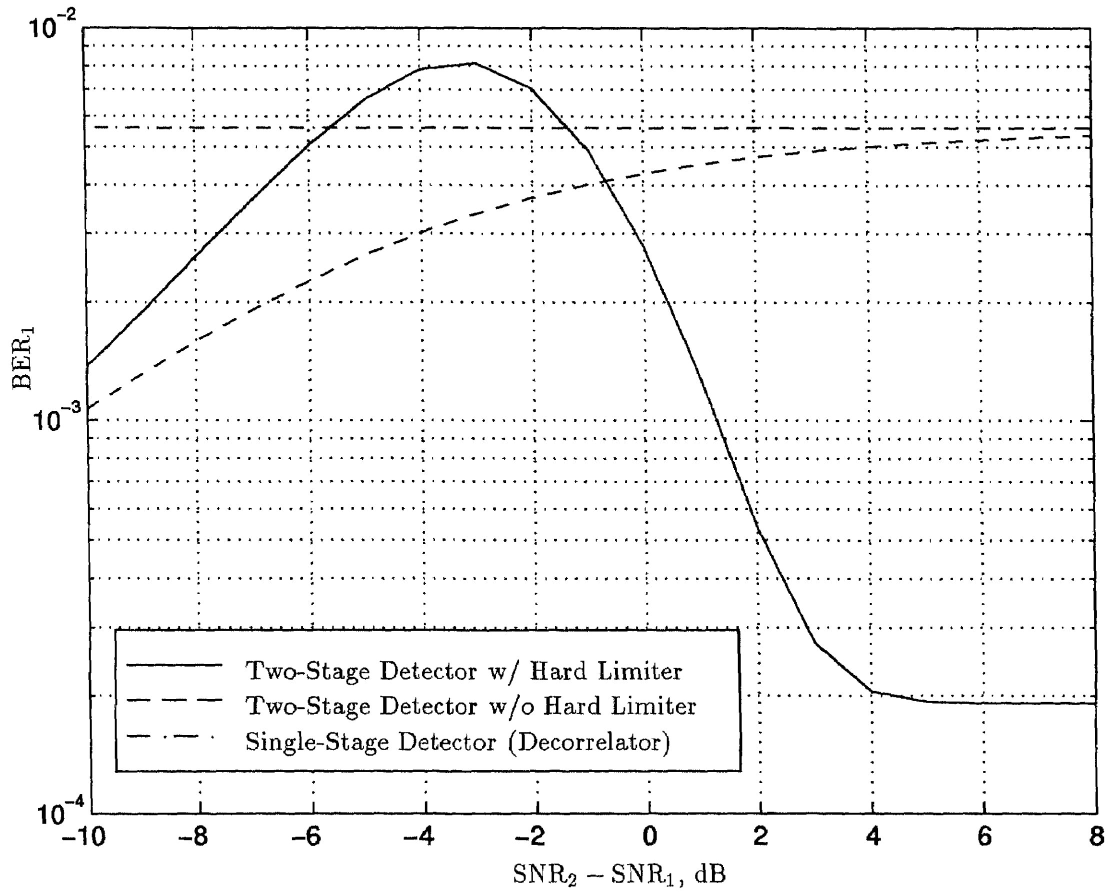

Figure 4.1 BER performance comparison of a two-stage detector, with hard limiter and without hard limiter. $SNR_1 = 8$ dB and $\rho = 0.7$.

4.1 System Model

Both synchronous and one-shot asynchronous CDMA communication systems are briefly explained in Chapter 2. These communication systems are essentially equivalent except for system dimensions. That is for K users the synchronous CDMA system has K dimensions, whereas the asynchronous CDMA system has $2K-1$ dimensions. Without loss of generality we consider synchronous CDMA communication.

The soft limiter for cancelling the lth user interfering signal from the kth user signal is given by

$$f(z_l) = \begin{cases} z_l/t_{kl} & \text{if } |z_l| < t_{kl} \\ \mathrm{sgn}(z_l) & \text{otherwise,} \end{cases} \qquad l = 1, \ldots, K, \quad l \neq k, \tag{4.1}$$

where t_{kl} is the threshold value.

Let $\lambda_{kl} = 1/t_{kl}$. Then the above equation can be written as

$$f(\eta_{kl}) = \begin{cases} 1 & \text{if } \eta_{kl} > 1 \\ \eta_{kl} & \text{if } -1 \leq \eta_{kl} < 1 \\ -1 & \text{if } \eta_{kl} < -1. \end{cases} \tag{4.2}$$

where $\eta_{kl} = z_l \lambda_{kl}$. Therefore this function can be implemented with a gain whose value is λ_{kl} followed by a soft limiter with unity slope, as depicted in Figure 4.2.

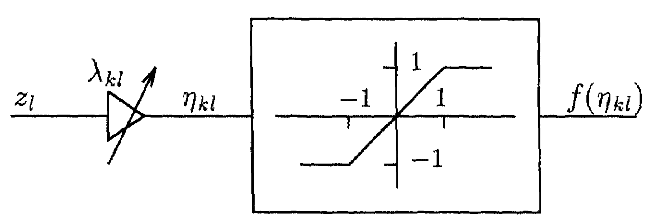

Figure 4.2 Soft limiter with adaptively controlled threshold.

With the soft limiter implementation of Figure 4.2, Figure 4.3 depicts a block diagram of the proposed two-stage (decorrelator-canceller) adaptive detector.

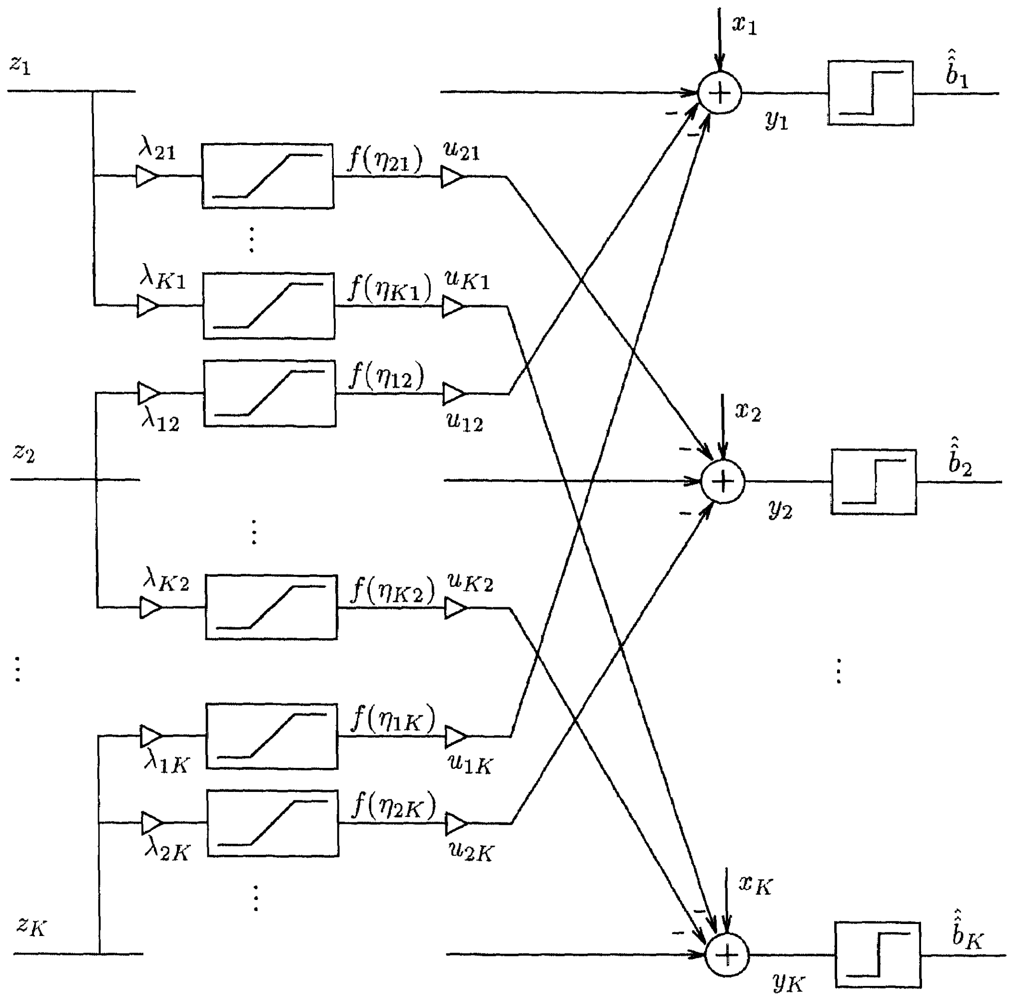

Figure 4.3 Two-stage (decorrelator/canceller) detector with adaptive soft limiter.

4.2 Optimal Parameters

From Figure 4.3 the adaptive decorrelating detector thresholds for a K-user CDMA system can be represented in a matrix form as

$$\boldsymbol{\Lambda} = \begin{bmatrix} 0 & \lambda_{12} & \cdots & \lambda_{1K} \\ \lambda_{21} & 0 & \cdots & \lambda_{2K} \\ \vdots & \vdots & \ddots & \vdots \\ \lambda_{K1} & \lambda_{K2} & \cdots & 0 \end{bmatrix}. \tag{4.3}$$

As shown in Eq. (2.24), the adaptive canceller weights for the K-user CDMA system is represented in a matrix form as

$$\boldsymbol{U} = \begin{bmatrix} 0 & u_{12} & \cdots & u_{1K} \\ u_{21} & 0 & \cdots & u_{2K} \\ \vdots & \vdots & \ddots & \vdots \\ u_{K1} & u_{K2} & \cdots & 0 \end{bmatrix}. \tag{4.4}$$

In this section, the algorithm for adjusting the adaptive parameters given in Eqs (4.3) and (4.4), that is, for the weights and the thresholds, is first stated. Then the optimal (steady state) values of these parameters are found for the K-user CDMA system.

4.2.1 Adaptive Control Algorithm

In order to control the adaptive weights and the threshold values, a steepest descent algorithm, which minimizes the desired user's energy with respect to the interfering users, is used.

The adaptive weights for the kth user in terms of the adaptive threshold values are updated iteratively at the bit intervals as follows:

$$\begin{aligned} u_{kl}(\lambda_{kl}) &\leftarrow u_{kl}(\lambda_{kl}) - \mu \frac{\partial E\{y_k^2\}}{\partial u_{kl}(\lambda_{kl})} \\ u_{kl}(\lambda_{kl}) &\leftarrow u_{kl}(\lambda_{kl}) + 2\mu E\{y_k f(\eta_{kl})\}, \quad l = 1, \ldots, K, \quad l \neq k, \end{aligned} \tag{4.5}$$

where μ is the step size of the convergence. Then the adaptive thresholds are updated at the same bit intervals as follows:

$$\begin{aligned} \lambda_{kl} &\leftarrow \lambda_{kl} - \mu \frac{\partial E\{y_k^2\}}{\partial \lambda_{kl}} \\ \lambda_{kl} &\leftarrow \lambda_{kl} + 2\mu E\{y_k u_{kl} z_l \frac{df(\eta_{kl})}{d\eta_{kl}}\} \\ \lambda_{kl} &\leftarrow \lambda_{kl} + \begin{cases} 2\mu E\{y_k u_{kl} z_l\} & \text{if } |\eta_{kl}| < 1 \\ 0 & \text{otherwise,} \end{cases} \quad l = 1, \ldots, K, \quad l \neq k, \end{aligned} \tag{4.6}$$

where we used the fact that

$$\frac{df(\eta_{kl})}{d\lambda_{kl}} = z_l \frac{df(\eta_{kl})}{d\eta_{kl}}, \tag{4.7}$$

and

$$\frac{df(\eta_{kl})}{d\eta_{kl}} = \begin{cases} 1 & \text{if } |\eta_{kl}| < 1 \\ 0 & \text{otherwise,} \end{cases} \tag{4.8}$$

since the $f(\eta_{kl})$ is a soft limiter with unity slope (see Figure 4.2).

Note that the weights u_{kl} are a function of the thresholds λ_{kl}. Hence, the notation $u_{kl}(\lambda_{kl})$ is used in Eq. (4.5) for the weights.

4.2.2 Optimal Weights

From Eq. (4.5), when the algorithm for the adaptive weights converges, we have

$$\begin{aligned} \frac{\partial E\{y_k^2\}}{\partial \boldsymbol{u}_k(\boldsymbol{\lambda}_k)} &= \frac{\partial}{\partial \boldsymbol{u}_k(\boldsymbol{\lambda}_k)} E\{(x_k - \boldsymbol{u}_k^T(\boldsymbol{\lambda}_k) f(\boldsymbol{\eta}_k))^2\} \\ &= -2E\{(x_k - \boldsymbol{u}_k^T(\boldsymbol{\lambda}_k) f(\boldsymbol{\eta}_k)) f(\boldsymbol{\eta}_k)\} \\ &= \mathbf{0} \end{aligned} \tag{4.9}$$

where $\boldsymbol{u}_k(\boldsymbol{\lambda}_k)$ is the kth row vector of $\boldsymbol{U}$ without its kth element.

From the above equation, the steady-state values of the adaptive weights in terms of the thresholds for the kth CDMA user are

$$\begin{aligned} \boldsymbol{u}_{k,\text{opt}}(\boldsymbol{\lambda}_k) &= E\{f(\boldsymbol{\eta}_k) f^T(\boldsymbol{\eta}_k)\}^{-1} E\{x_k f(\boldsymbol{\eta}_k)\} \\ &= E\{f(\boldsymbol{\eta}_k) f^T(\boldsymbol{\eta}_k)\}^{-1} \boldsymbol{A}_k E\{f(\boldsymbol{\eta}_k) \boldsymbol{b}_k^T\} \boldsymbol{\rho}_k \end{aligned} \tag{4.10}$$

where $\boldsymbol{A}_k$ is matrix $\boldsymbol{A}$ without its kth row and column and $\boldsymbol{\rho}_k$ is the kth row of matrix $\boldsymbol{P}$ without its kth element.

In the above equation, $E\{f(\boldsymbol{\eta}_k) f^T(\boldsymbol{\eta}_k)\}$ is a $(K-1) \times (K-1)$ matrix with diagonal elements $E\{f(\eta_{kl})^2\}, \quad l = 1, \ldots, K, \quad l \neq k$, derived in Appendix A, and off diagonal elements $E\{f(\eta_{kl}) f(\eta_{kj})\}, \quad l, j = 1, \ldots, K, \quad l, j \neq k, \quad l \neq j$. From Eq. (A.5), the diagonal elements are

$$\begin{aligned} E\{f^2(\eta_{kl})\} &= \frac{\sigma_{\eta_{kl}}^2}{\sqrt{2\pi}} \left[(2\alpha_0 - \alpha_2) e^{-\alpha_2^2/2} - (2\alpha_0 + \alpha_1) e^{-\alpha_1^2/2}\right] \\ &\quad + \sigma_{\eta_{kl}}^2 (1 + \alpha_0^2) \left[1 - Q(\alpha_1) - Q(\alpha_2)\right] + Q(\alpha_1) + Q(\alpha_2), \end{aligned} \tag{4.11}$$

where $\alpha_0 = \lambda_{kl}\sqrt{a_l}/\sigma_{\eta_{kl}}$, $\alpha_1 = (1-\lambda_{kl}\sqrt{a_l})/\sigma_{\eta_{kl}}$, and $\alpha_2 = (1+\lambda_{kl}\sqrt{a_l})/\sigma_{\eta_{kl}}$. The off diagonal elements can be calculated as

$$E\{f(\eta_{kl})f(\eta_{kj})\} = \frac{1}{4}\sum_{b_l,b_j}\sum_{s=1}^{9}\int\int_{D_s} f(\eta_{kl})f(\eta_{kj})p(\eta_{kl},\eta_{kj})d\eta_{kl}d\eta_{kj}, \tag{4.12}$$

where b_l and b_j are the lth and jth user bits respectively. Function $p(\eta_{kl},\eta_{kj})$ is the joint Gaussian density function of the random variables η_{kl} and η_{kj}. Both random variables η_{kl} and η_{kj} span the intervals $(-\infty,-1]$, $[-1,1]$ and $[1,\infty)$. Therefore in the above equation the integration is performed over 9 different regions. Region D_s is the appropriate region of integration.

The term $E\{f(\boldsymbol{\eta}_k)\boldsymbol{b}_k^T\}$ in Eq. (4.10) is a diagonal matrix with the diagonal elements $E\{b_l f(\eta_{kl})\}$, $l = 1,\ldots,K$, $l \neq k$, derived in Appendix A. From Eq. (A.2)

$$E\{b_l f(\eta_{kl})\} = \frac{\sigma_{\eta_{kl}}}{\sqrt{2\pi}}(e^{-\alpha_2^2/2} - e^{-\alpha_1^2/2}) + \lambda_{kl}\sqrt{a_l}\,[1 - Q(\alpha_1) - Q(\alpha_2)] + Q(\alpha_1) - Q(\alpha_2), \tag{4.13}$$

where α_1 and α_2 are defined in Eq. (4.11).

4.2.3 Optimal Thresholds

From Eq. (4.6), when the algorithm for the adaptive thresholds converges, we have

$$\begin{aligned}\frac{\partial E\{y_k^2\}}{\partial \boldsymbol{\lambda}_k} &= \frac{\partial}{\partial \boldsymbol{\lambda}_k}E\{(x_k - \boldsymbol{u}_k^T f(\boldsymbol{\eta}_k))^2\} \\ &= -2\tilde{\boldsymbol{U}}_k E\{(x_k - \boldsymbol{u}_k^T f(\boldsymbol{\eta}_k))\frac{df(\boldsymbol{\eta}_k)}{d\boldsymbol{\lambda}_k}\} \\ &= \mathbf{0},\end{aligned} \tag{4.14}$$

where $\partial E\{y_k^2\}/\partial\boldsymbol{\lambda}_k$ is a vector with elements $\partial E\{y_k^2\}/\partial\lambda_{kl}$, $l = 1,\ldots,K$, $l \neq k$. The $\tilde{\boldsymbol{U}}_k$ is a diagonal matrix with elements u_{kl}, $l = 1,\ldots,K$, $l \neq k$ and $df(\boldsymbol{\eta}_k)/d\boldsymbol{\lambda}_k$ is a vector with elements $df(\eta_{kl})/d\lambda_{kl}$, $l = 1,\ldots,K$, $l \neq k$.

Assuming all the weights for the kth user, u_{kl}, are non-zero. From the above equation we have

$$E\{(x_k - \boldsymbol{u}_k^T f(\boldsymbol{\eta}_k))\frac{df(\boldsymbol{\eta}_k)}{d\boldsymbol{\lambda}_k}\} = \mathbf{0}. \tag{4.15}$$

From Eq. (4.15) the adaptive weights in terms of the optimal threshold values for the kth user, can be calculated as

$$\begin{aligned} \boldsymbol{u}_k(\boldsymbol{\lambda}_{k,\mathrm{opt}}) &= E\{\frac{df(\boldsymbol{\eta}_k)}{d\boldsymbol{\lambda}_k} f^T(\boldsymbol{\eta}_k)\}^{-1} E\{x_k \frac{df(\boldsymbol{\eta}_k)}{d\boldsymbol{\lambda}_k}\} \\ &= E\{\frac{df(\boldsymbol{\eta}_k)}{d\boldsymbol{\lambda}_k} f^T(\boldsymbol{\eta}_k)\}^{-1} \boldsymbol{A}_k E\{\frac{df(\boldsymbol{\eta}_k)}{d\boldsymbol{\lambda}_k} \boldsymbol{b}_k^T\} \rho_k. \end{aligned} \tag{4.16}$$

In the above equation, $E\{[df(\boldsymbol{\eta}_k)/d\boldsymbol{\lambda}_k]\boldsymbol{b}^T\}$ is a diagonal matrix with the diagonal elements $E\{b_l df(\eta_{kl})/d\lambda_{kl}\}$, $l = 1, \ldots, K$, $l \neq k$, derived in Appendix A. From Eq. (A.7)

$$E\left\{b_l \frac{df(\eta_{kl})}{d\lambda_{kl}}\right\} = \frac{1}{\lambda_{kl}} \left\{\frac{\sigma_{\eta_{kl}}}{\sqrt{2\pi}}(e^{-\alpha_2^2/2} - e^{-\alpha_1^2/2}) + \lambda_{kl}\sqrt{a_l}\,[1 - Q(\alpha_2) - Q(\alpha_2)]\right\} \tag{4.17}$$

where α_1 and α_2 are defined in (4.11).

The term $E\{[df(\boldsymbol{\eta}_k)/d\boldsymbol{\lambda}_k]f^T(\boldsymbol{\eta}_k)\}$ in Eq. (4.16) is a $(K-1) \times (K-1)$ matrix with the diagonal elements $E\{f(\eta_{kl})df(\eta_{kl})/d\lambda_{kl}\}$, $l = 1, \ldots, K$, $l \neq k$, derived in Appendix A, Eq. (A.10):

$$\begin{aligned} E\left\{f(\eta_{kl})\frac{df(\eta_{kl})}{d\lambda_{kl}}\right\} &= \frac{\sigma_{\eta_{kl}}^2}{\lambda_{kl}\sqrt{2\pi}}\left[(2\alpha_0 - \alpha_2)e^{-\alpha_2^2/2} - (2\alpha_0 + \alpha_1)e^{-\alpha_1^2/2}\right] \\ &\quad + \frac{\sigma_{\eta_{kl}}^2}{\lambda_{kl}}(1 + \alpha_0^2)\,[1 - Q(\alpha_1) - Q(\alpha_2)] \end{aligned} \tag{4.18}$$

and off diagonal elements $E\{f(\eta_{kl})df(\eta_{kj})/d\lambda_{kj}\}$, $l, j = 1, \ldots, K$, $l, j \neq k$, $l \neq j$. The off diagonal elements can be calculated as

$$E\{f(\eta_{kl})df(\eta_{kj})/d\lambda_{kj}\} = \frac{1}{4}\sum_{b_l, b_j}\sum_{s=1}^{3}\int\int_{D_s} f(\eta_{kl})\frac{df(\eta_{kj})}{d\lambda_{kj}} p(\eta_{kl}, \eta_{kj})d\eta_{kl}d\eta_{kj}. \tag{4.19}$$

4.3 Two-User Case

The block diagram of the proposed scheme for two-user CDMA is depicted in Figure 4.4.

The evaluation of Eqs. (4.12) and (4.19) requires numerical integration over the specified regions using joint Gaussian density function. Nevertheless, using two-users

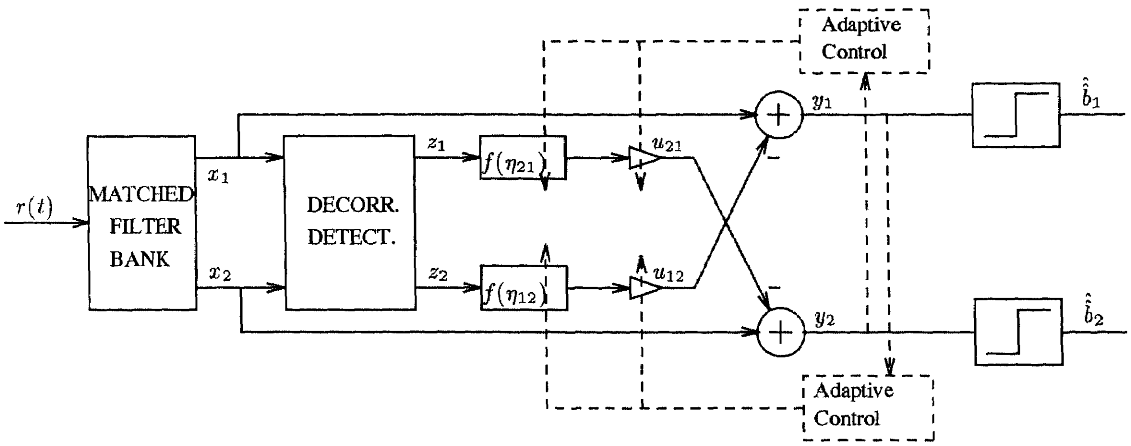

Figure 4.4 Two-stage (decorrelator/canceller) detector with adaptive soft limiter for two-user CDMA.

eliminates the need for using numerical integration. Therefore, in this section, the optimal canceller weights and the optimal soft-limiter thresholds are evaluated for a two-user synchronous CDMA system in order to obtain the BER performance of the system as well as to compare the performance of the system to the performances of the previously implemented systems.

4.3.1 Optimal Canceller Weights

To find the optimal weight for the canceller stage, we write

$$y_1 = x_1 - u_{12} f(\lambda_{12} z_2). \tag{4.20}$$

Equating the derivative of $E\{y_1^2\}$ with respect to u_{12} to zero we find

$$u_{12,\text{opt}}(\lambda_{12}) = \frac{E\{x_1 f(\lambda_{12} z_2)\}}{E\{f^2(\lambda_{12} z_2)\}}. \tag{4.21}$$

Note that Eq. (4.21) describes the optimal weight in terms of the threshold $1/\lambda_{12}$ and other system parameters. Using (4.10), (4.11) and (4.13) we get

$$u_{12,\text{opt}}(\lambda_{12}) = \frac{\rho\sqrt{a_2}\{G_1(\alpha_1,\alpha_2) + \lambda_{12}\sqrt{a_2}G_3(\alpha_1,\alpha_2) + Q(\alpha_1) - Q(\alpha_2)\}}{G_2(\alpha_0,\alpha_1,\alpha_2) + \sigma^2_{\eta_{12}}(1+\alpha_0^2)G_3(\alpha_1,\alpha_2) + Q(\alpha_1) + Q(\alpha_2)}, \tag{4.22}$$

where

$$\begin{aligned}
G_1(\alpha_1,\alpha_2) &= \frac{\sigma_{\eta_{12}}}{\sqrt{2\pi}}\left(e^{-\alpha_2^2/2}-e^{-\alpha_1^2/2}\right),\\
G_2(\alpha_0,\alpha_1,\alpha_2) &= \frac{\sigma_{\eta_{12}}^2}{\sqrt{2\pi}}\left((2\alpha_0-\alpha_2)e^{-\alpha_2^2/2}-(2\alpha_0+\alpha_1)e^{\alpha_1^2/2}\right),\\
G_3(\alpha_1,\alpha_2) &= 1-Q(\alpha_1)-Q(\alpha_2),\\
\alpha_0 &= \lambda_{12}\sqrt{a_2}/\sigma_{\eta_{12}},\\
\alpha_1 &= (1-\lambda_{12}\sqrt{a_2})/\sigma_{\eta_{12}},\\
\alpha_2 &= (1+\lambda_{12}\sqrt{a_2})/\sigma_{\eta_{12}},
\end{aligned} \tag{4.23}$$

and $Q(\alpha)=\frac{1}{\sqrt{2\pi}}\int_\alpha^\infty e^{-x^2/2}dx$.

The hard limiter case can be obtained from Eq. (4.22) by letting λ_{12} go to infinity. The first terms in the numerator and denominator clearly go to zero. The second term can be shown to go to zero by applying L'Hospital's Rule.

Thus, we are left with

$$\begin{aligned}
\lim_{\lambda_{12}\to\infty} u_{12,\mathrm{opt}}(\lambda_{12}) &= \rho\sqrt{a_2}\lim_{\lambda_{12}\to\infty}\frac{Q(\alpha_1)-Q(\alpha_2)}{Q(\alpha_1)+Q(\alpha_2)}\\
&= \rho\sqrt{a_2}[1-2Q(\sqrt{\frac{a_2(1-\rho^2)}{\sigma^2}})],
\end{aligned} \tag{4.24}$$

which is the same result obtained in [24].

4.3.2 Optimal Threshold Level

To find the optimal threshold, by using Eq. (4.14) we get

$$\frac{\partial E\{y_1^2\}}{\partial\lambda_{12}} = 2u_{12}^2E\left\{f(\lambda_{12}z_2)\frac{df(\lambda_{12}z_2)}{d\lambda_{12}}\right\} - 2u_{12}E\left\{x_1\frac{df(\lambda_{12}z_2)}{d\lambda_{12}}\right\} = 0. \tag{4.25}$$

For $u_{12}\neq 0$

$$u_{12}(\lambda_{12,\mathrm{opt}}) = \frac{E\{x_1 df(\lambda_{12}z_2)/d\lambda_{12}\}}{E\{f(\lambda_{12}z_2)df(\lambda_{12}z_2)/d\lambda_{12}\}}. \tag{4.26}$$

Note that the above equation implicitly describes $\lambda_{12,\mathrm{opt}}$ as a function of the weight u_{12}.

Using Eqs. (4.16), (4.17) and (4.18) we get

$$u_{12}(\lambda_{12,\mathrm{opt}}) = \frac{\rho\sqrt{a_2}[G_1(\alpha_1,\alpha_2)+\lambda_{12}\sqrt{a_2}G_3(\alpha_1,\alpha_2)]}{G_2(\alpha_0,\alpha_1,\alpha_2)+\sigma^2_{\eta_{12}}(1+\alpha_0^2)G_3(\alpha_1,\alpha_2)}, \tag{4.27}$$

where α_0, α_1 and α_2 are defined in Eq. (4.23). Clearly, for the definition of α_0, α_1 and α_2 in the above equation we use $\lambda_{12,\mathrm{opt}}$.

If we define the terms in the numerator of Eq. (4.27) as A and those in the denominator as B, then Eqs. (4.22) and (4.27) can be written as

$$u_{12,\mathrm{opt}}(\lambda_{12}) = \frac{A+\rho\sqrt{a_2}[Q(\alpha_1)-Q(\alpha_2)]}{B+Q(\alpha_1)+Q(\alpha_2)} \tag{4.28}$$

and

$$u_{12}(\lambda_{12,\mathrm{opt}}) = \frac{A}{B}, \tag{4.29}$$

respectively.

To obtain the optimal weight and optimal threshold $u_{12,\mathrm{opt}}$ and $\lambda_{12,\mathrm{opt}}$, we equate Eq. (4.28) to Eq. (4.29) and get

$$\begin{aligned} u_{12,\mathrm{opt}}(\lambda_{12,\mathrm{opt}}) &= \frac{\rho\sqrt{a_2}[Q(\alpha_1)-Q(\alpha_2)]}{Q(\alpha_1)+Q(\alpha_2)} = \frac{A}{B} \\ &= \frac{\rho\sqrt{a_2}[G_1(\alpha_1,\alpha_2)+\lambda_{12}\sqrt{a_2}G_3(\alpha_1,\alpha_2)]}{G_2(\alpha_0,\alpha_1,\alpha_2)+\sigma^2_{\eta_{12}}(1+\alpha_0^2)G_3(\alpha_1,\alpha_2)}. \end{aligned} \tag{4.30}$$

Solving Eq. (4.30) give us the optimal threshold setting $\lambda_{12,\mathrm{opt}}$. With this value,

$$u_{12,\mathrm{opt}}(\lambda_{12,\mathrm{opt}}) = \frac{\rho\sqrt{a_2}[Q(\alpha_{1,\mathrm{opt}})-Q(\alpha_{2,\mathrm{opt}})]}{Q(\alpha_{1,\mathrm{opt}})+Q(\alpha_{2,\mathrm{opt}})}, \tag{4.31}$$

where

$$\begin{aligned} \alpha_{1,\mathrm{opt}} &= (1-\lambda_{12,\mathrm{opt}}\sqrt{a_2})/\sigma_{\eta_{12}}, \\ \alpha_{2,\mathrm{opt}} &= (1+\lambda_{12,\mathrm{opt}}\sqrt{a_2})/\sigma_{\eta_{12}}, \end{aligned} \tag{4.32}$$

and $\sigma_{\eta_{12}} = \lambda_{12}\sigma/\sqrt{1-\rho^2}$.

From Eq. (4.29), after some algebraic manipulation we can get the value of the optimal threshold $t_{12} = 1/\lambda_{12}$:

$$t_{12,\mathrm{opt}} = \frac{\sigma}{\sqrt{1-\rho^2}}(Q(\alpha_1)-Q(\alpha_2))$$

$$\cdot \frac{(1+\mathrm{SNR}_{2,\rho})G_3(\alpha_1,\alpha_2) - \frac{1}{\sqrt{2\pi}}\sqrt{\mathrm{SNR}_{2,\rho}}G_1(\alpha_1,\alpha_2)}{\sqrt{\frac{2}{\pi}}G_4(\alpha_1,\alpha_2) + \sqrt{\mathrm{SNR}_{2,\rho}}(Q(\alpha_1)+Q(\alpha_2))G_3(\alpha_1,\alpha_2)}, \tag{4.33}$$

where $G_4(\alpha_1,\alpha_2) = Q(\alpha_1)e^{-\alpha_2^2/2} - Q(\alpha_2)e^{-\alpha_1^2/2}$ and $\mathrm{SNR}_{2,\rho} = a_2(1-\rho^2)/\sigma$. This equation gives implicitly the dependence of the optimal threshold t_{opt} on SNR_2 and ρ.

4.3.3 BER Performance and Numerical Results

For any setting of λ_{12}, the optimal weight $u_{12,\mathrm{opt}}(\lambda_{12})$ is given by Eq. (4.22). With this weight

$$\begin{aligned} P_{e_1} &= \frac{1}{2}\Big\{1 + [Q(\frac{\delta_1+\sqrt{a_1}}{\sigma}) - Q(\frac{\delta_1-\sqrt{a_1}}{\sigma})]Q(\alpha_1) \\ &+[Q(\frac{\delta_2+\sqrt{a_1}}{\sigma}) - Q(\frac{\delta_2-\sqrt{a_1}}{\sigma})]Q(\alpha_2)\Big\} \\ &+\frac{1}{4}\Big\{\frac{1}{\sqrt{2\pi}\sigma_{\eta_{12}}}\int_{-1}^{1}[Q(\frac{\gamma_1+\sqrt{a_1}}{\sigma}) - Q(\frac{\gamma_1-\sqrt{a_1}}{\sigma})]\exp(-\frac{(\eta_{12}-\lambda_{12}\sqrt{a_2})^2}{2\sigma_{\eta_{12}}^2})d\eta_{12} \\ &+\frac{1}{\sqrt{2\pi}\sigma_{\eta_{12}}}\int_{-1}^{1}[Q(\frac{\gamma_2+\sqrt{a_1}}{\sigma}) - Q(\frac{\gamma_2-\sqrt{a_1}}{\sigma})]\exp(-\frac{(\eta_{12}+\lambda_{12}\sqrt{a_2})^2}{2\sigma_{\eta_{12}}^2})d\eta_{12}\Big\}, \end{aligned} \tag{4.34}$$

where

$$\begin{aligned} \delta_1 = \rho\sqrt{a_2}(c-1), &\quad \delta_2 = \rho\sqrt{a_2}(c+1), \\ \gamma_1 = \rho\sqrt{a_2}(c\eta_{12}-1), &\quad \gamma_2 = \rho\sqrt{a_2}(c\eta_{12}+1), \end{aligned} \tag{4.35}$$

and $c = u_{12}(t_{12})/\rho\sqrt{a_2}$. Note that for $t_{12} = t_{12,\mathrm{opt}}$, using Eq. (4.30) we get

$$c = \frac{Q(\alpha_{1,\mathrm{opt}}) - Q(\alpha_{2,\mathrm{opt}})}{Q(\alpha_{1,\mathrm{opt}}) + Q(\alpha_{2,\mathrm{opt}})}. \tag{4.36}$$

From Eq. (4.33) it is clear that the optimum threshold setting t_{12} is independent of SNR_1. The solution of Eq. (4.33) numerically as a function of ρ is given in Figure 4.5, with SNR_2 as a parameter. In Figure 4.6, we depict $t_{12,\mathrm{opt}}$ as a function of SNR_2 for $\rho = 0.7$. In Figure 4.7 we compare the value of the output energy obtained with the hard limiter and with a threshold calculated according to the heuristic value of [11]. The corresponding probability of error for these cases is given in Figure 4.8. For comparison, we add to this curve the probability of error at the output of the decorrelator. Figure 4.9 depicts the same, except for $\rho = 0.3$.

Note, particularly in Figure 4.8, that the error probability with the heuristic setting is better in some regions than with the optimum setting of the threshold. This is due to the fact that the optimization was performed with respect to minimum energy, not error probability. In Figure 4.9 the performance is almost the same. Nevertheless, the advantage of the adaptive threshold setting is in disposing the need for signal measurement.

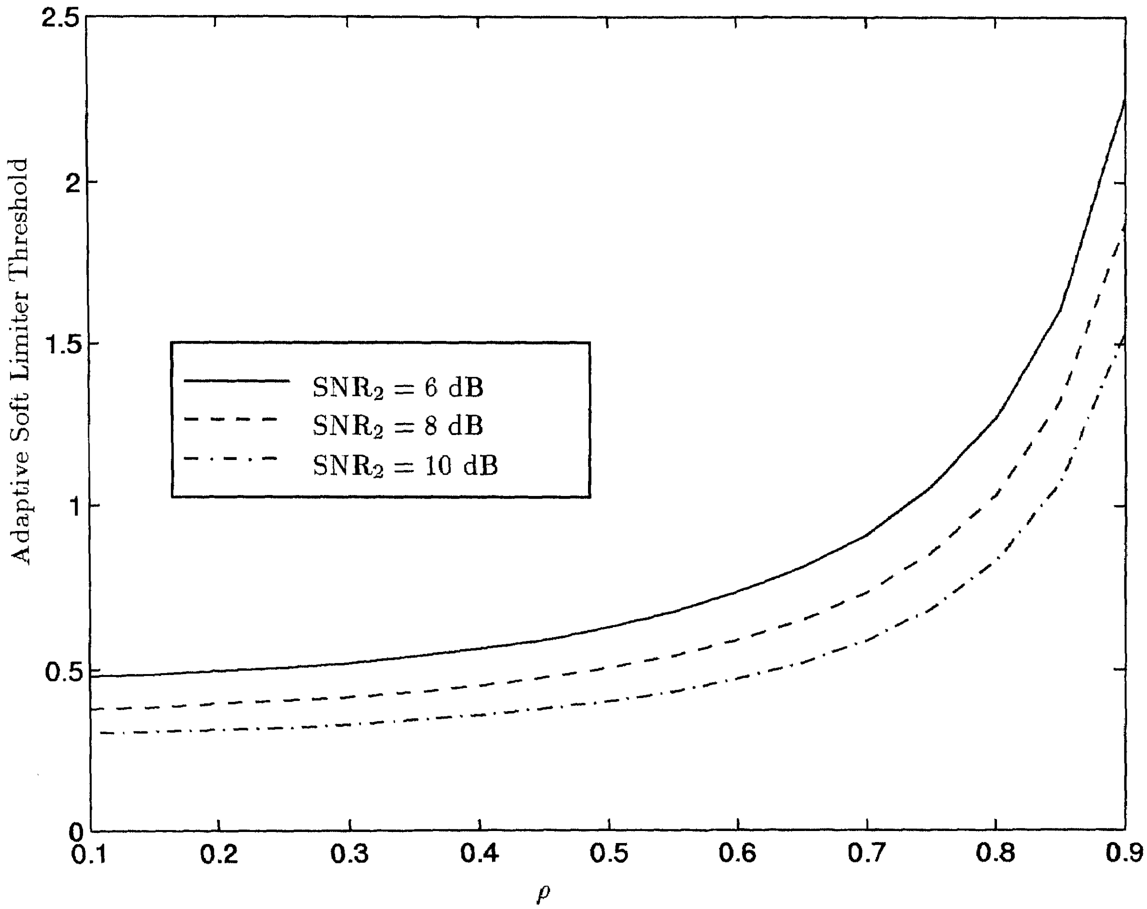

Figure 4.5 Optimal threshold as a function of the correlation coefficient ρ for $\mathrm{SNR}_1 = 8$ dB.

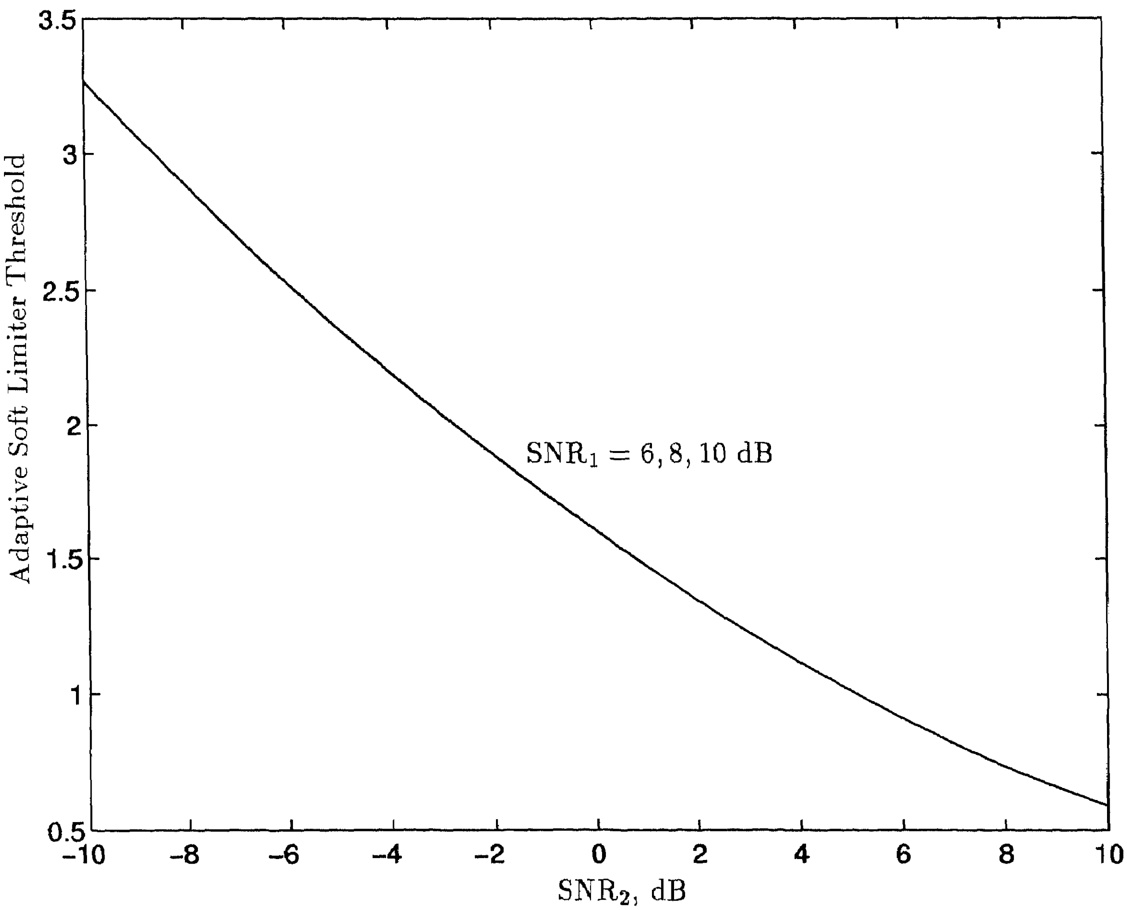

Figure 4.6 Optimal threshold as a function of SNR_2 for $\rho = 0.7$.

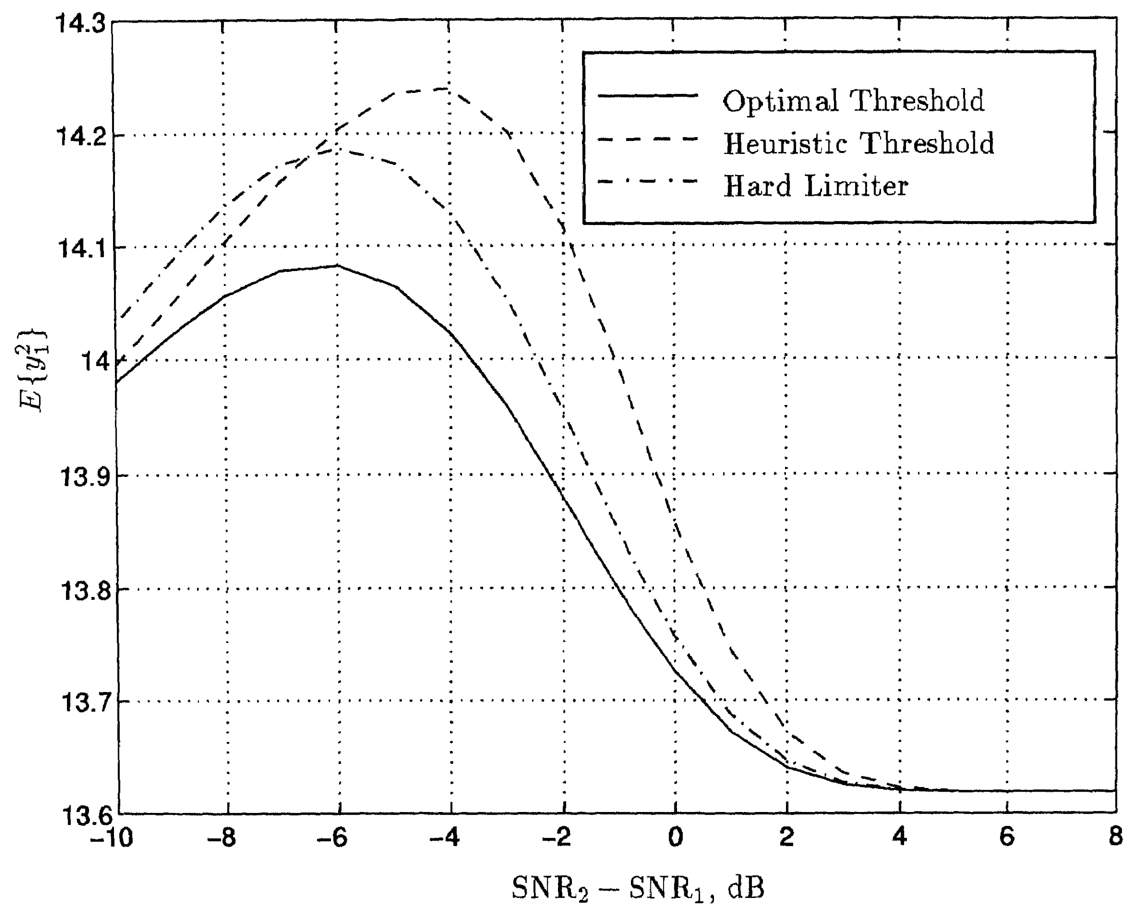

Figure 4.7 Output energy of desired user, $E\{y_1^2\}$, with hard limiter, heuristic threshold and optimal threshold. $\mathrm{SNR}_1 = 8$ dB, $\rho = 0.7$.

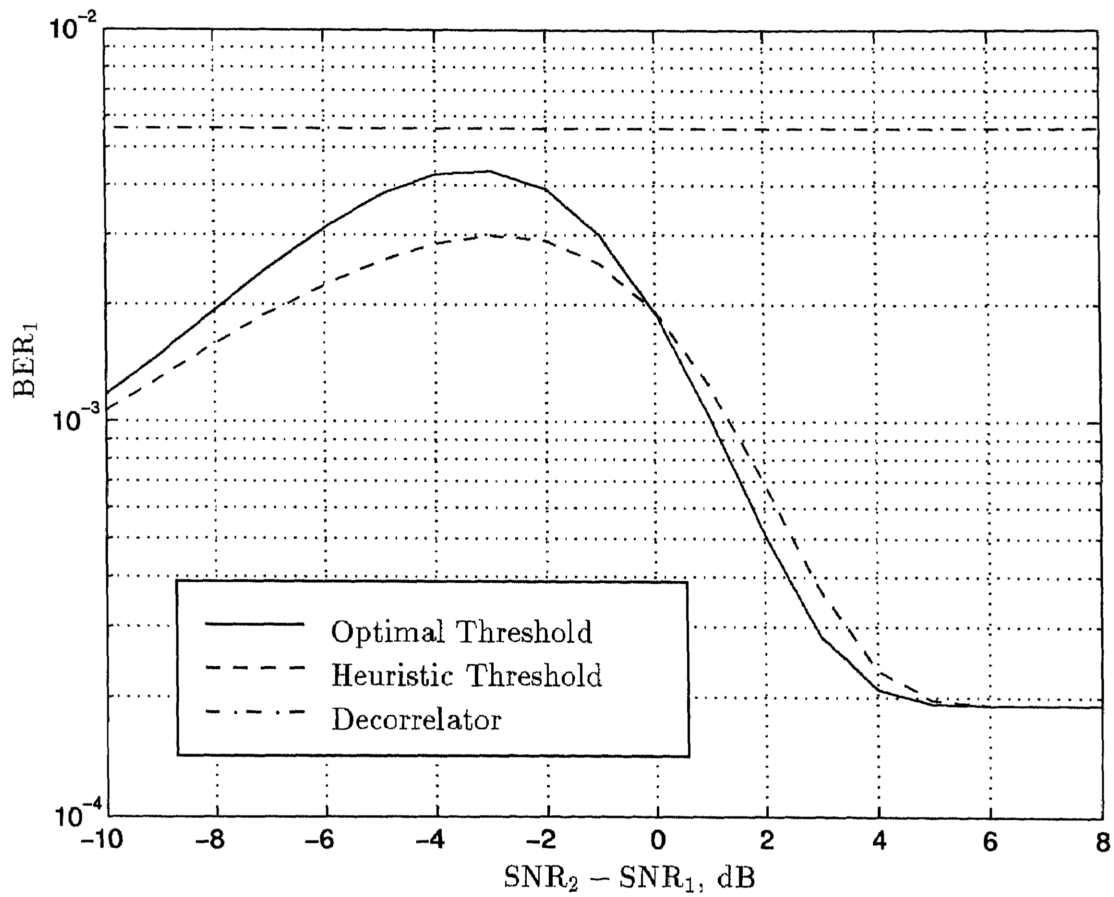

Figure 4.8 BER performance of desired user for decorrelator, heuristic threshold and optimal threshold detector. $\mathrm{SNR}_1 = 8$ dB, $\rho = 0.7$.

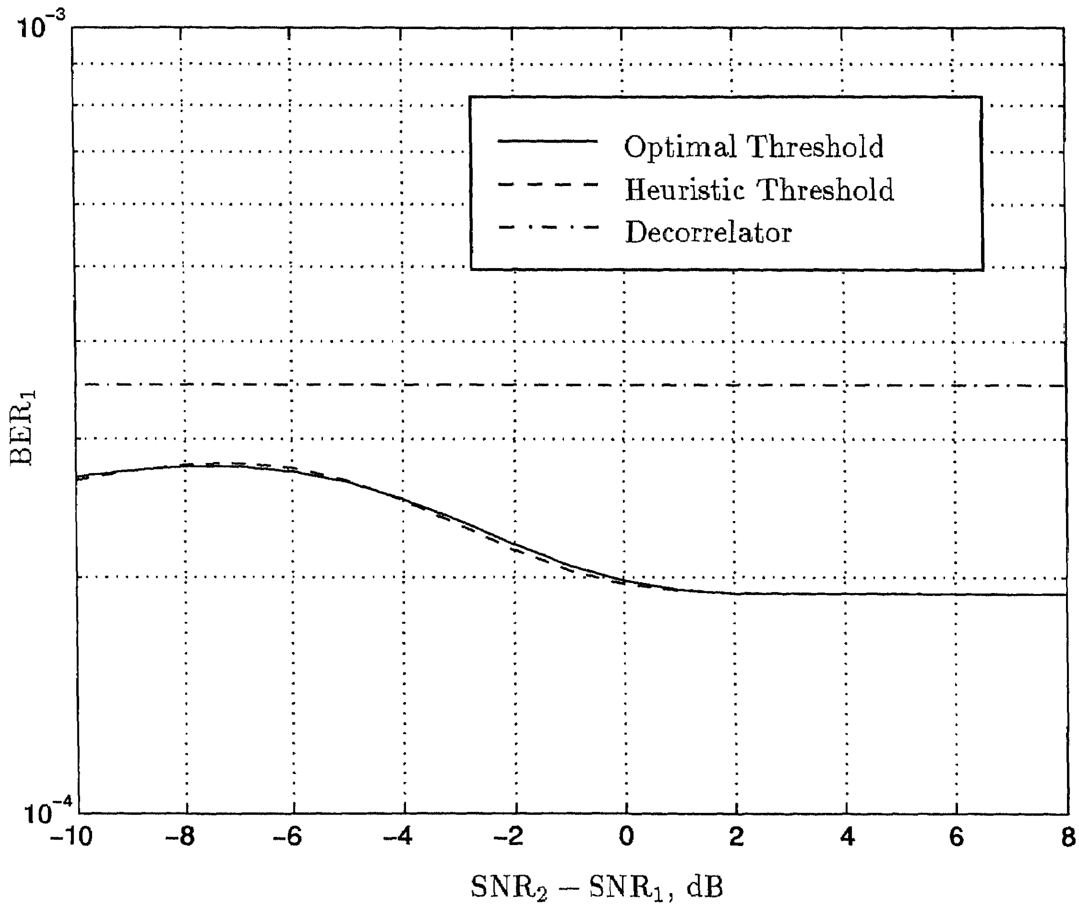

Figure 4.9 BER performance of desired user for decorrelator, heuristic threshold and optimal threshold detector. $SNR_1 = 8$ dB, $\rho = 0.3$.

4.4 Summary

In this chapter, the idea of using a soft limiter for the tentative decision at the decorrelating detector output is extended such that the threshold of the soft limiter is set in an adaptive manner. This scheme, being adaptive in nature, does not need any measurement of the signal energies. The threshold is set using the energy minimization algorithm.

Optimum (steady-state) canceller weights and optimum threshold values are derived for K users. For the ease of analysis, a two-user case is evaluated and its BER performance is compared to the two-user hard-limiter and the two-user soft-limiter with a heuristic threshold. It is demonstrated that the adaptive soft-limiter performs better than the hard-limiter and is almost as good as the heuristic soft-limiter. Note that the adaptive soft-limiter does not need any signal measurement and do not rely on a heuristic calculation. Therefore it is preferable to use the adaptive soft limiter at the decorrelating detector output.

CHAPTER 5

BOOTSTRAP SEPARATOR FOR ASYNCHRONOUS CDMA COMMUNICATION WITH SINGULAR CROSS-CORRELATION MATRIX

The detection of K asynchronous CDMA user data by using the one-shot detection scheme was explained in Chapter 2. At the one-shot matched filter-bank the first user signature sequence is matched in full and the remaining $K-1$ user signature sequences are matched partially generating two outputs for each partial user. Therefore the resulting partial cross correlation matrix (PCCM) has $(2K-1) \times (2K-1)$ dimensions and can be singular. When PCCM is singular then the bootstrap algorithm does not converge and hence cannot be used.

In this chapter, first we prove the non-convergence of the bootstrap algorithm analytically when the cross correlation matrix is non singular. Then, two different solutions are proposed to avoid the non-convergence problem for the bootstrap algorithm.

5.1 The Convergence Problem of Bootstrap Decorrelator

First we remark on the fact that the singularity of PCCM $\boldsymbol{P}$ has been demonstrated with actual Gold code sequences. Singularity occurred for certain set of relative delays between the codes. In order to examine the convergence property of the bootstrap decorrelator, in the following discussion $\boldsymbol{P}$ is assumed to be singular.

The signal vector $\boldsymbol{x}$ generated at the one-shot matched filter-bank output is applied to the bootstrap decorrelating detector. The bootstrap decorrelator was briefly explained in Section 2.2. After a sufficient number of iterations, when the adaptive weights converge to their steady state values, from Eq. (2.20):

$$E\{z_i \mathrm{sgn}(z_j)\} = 0, \quad i,j = 1,\ldots,2K-1; \quad i \neq j, \tag{5.1}$$

where z_i is the ith output of the bootstrap decorrelator.

Substituting z_i and z_j into the above equation, we get

$$\begin{aligned} E\{z_i \mathrm{sgn}(z_j)\} &= E\{\boldsymbol{v}_i^T \boldsymbol{x} \mathrm{sgn}(\boldsymbol{v}_j^T \boldsymbol{x})\} \\ &= E\{\boldsymbol{v}_i^T \boldsymbol{PAb} \mathrm{sgn}(\boldsymbol{v}_j^T \boldsymbol{PAb} + \xi_j)\} \\ &\quad + E\{\xi_i \mathrm{sgn}(\boldsymbol{v}_j^T \boldsymbol{PAb} + \xi_j\}, \end{aligned} \tag{5.2}$$

where $\xi_i = \boldsymbol{v}_i^T \boldsymbol{n}$ and $\xi_j = \boldsymbol{v}_j^T \boldsymbol{n}$.

The first term in the above equation can be written as

$$\begin{aligned} & E\{\boldsymbol{v}_i^T \boldsymbol{PAb} \mathrm{sgn}(\boldsymbol{v}_j^T \boldsymbol{PAb} + \xi_j)\} \\ &= E_{\boldsymbol{b}}\{\boldsymbol{v}_i^T \boldsymbol{PAb}(Pr\{\boldsymbol{v}_i^T \boldsymbol{PAb} + \xi_j > 0\} - Pr\{\boldsymbol{v}_j^T \boldsymbol{PAb} + \xi_j < 0\})\} \\ &= 2^{-(2K-1)} \sum_{\boldsymbol{b} \in \{\cdot\}} \boldsymbol{v}_i^T \boldsymbol{PAb}(Pr\{\xi_j > -\boldsymbol{v}_j^T \boldsymbol{PAb}\} - Pr\{\xi_j > \boldsymbol{v}_j^T \boldsymbol{PAb}\}) \\ &= 2^{-(2K-1)} \sum_{\boldsymbol{b} \in \{\cdot\}} \boldsymbol{v}_i^T \boldsymbol{PAb}[1 - 2Q(\frac{\boldsymbol{v}_j^T \boldsymbol{PAb}}{\sigma_{\xi_j}})], \end{aligned} \tag{5.3}$$

where the set $\{\cdot\}$ contains all $2^{(2K-1)}$ combinations of bit vector $\boldsymbol{b}$.

The second term in Eq. (5.2) can be calculated as (see Appendix B)

$$E\{\xi_i \mathrm{sgn}(\boldsymbol{v}_j^T \boldsymbol{PAb} + \xi_j)\} = 2^{-(2K-1)} \sum_{\boldsymbol{b} \in \{\cdot\}} \frac{\boldsymbol{v}_i^T \boldsymbol{P} \boldsymbol{v}_j}{\boldsymbol{v}_j \boldsymbol{P} \boldsymbol{v}_j} \frac{2\sigma_{\xi_j}}{\sqrt{2\pi}} \exp(-\frac{[\boldsymbol{v}_j^T \boldsymbol{PAb}]^2}{2\sigma_{\xi_j}^2}). \tag{5.4}$$

Substituting Eqs. (5.3) and Eq. (5.4) into Eq. (5.2) we get

$$\begin{aligned} E\{z_i \mathrm{sgn}(z_j)\} &= \boldsymbol{v}_i^T \boldsymbol{P} \left\{ 2^{-(2K-1)} \sum_{\boldsymbol{b} \in \{\cdot\}} \boldsymbol{Ab}[1 - 2Q(\frac{\boldsymbol{v}_j^T \boldsymbol{PAb}}{\sigma_{\xi_j}})] \right. \\ &\qquad \left. + 2^{-(2K-1)} \sum_{\boldsymbol{b} \in \{\cdot\}} \frac{\boldsymbol{v}_j}{\boldsymbol{v}_j^T \boldsymbol{P} \boldsymbol{v}_j} \frac{2\sigma_{\xi_j}}{\sqrt{2\pi}} \exp(-\frac{[\boldsymbol{v}_j^T \boldsymbol{PAb}]^2}{2\sigma_{\xi_j}^2}) \right\} \\ &= \boldsymbol{v}_i^T \boldsymbol{P} \boldsymbol{r}_j, \end{aligned} \tag{5.5}$$

where $\boldsymbol{r}_j$ is the term inside the curly parentheses. Combining terms for all i and j we get

$$E\{\boldsymbol{z} \mathrm{sgn}(\boldsymbol{z}^T)\} = \boldsymbol{VPR}, \tag{5.6}$$

where $\boldsymbol{R}$ is a matrix whose columns are $\boldsymbol{r}_i$, $i = 1, \ldots, 2K-1$. As a result of Eq. (5.1), for the adaptive weight to converge, the off diagonal terms of Eq. (5.6) necessarily vanish, leaving the diagonal terms $E\{z_i \mathrm{sgn}(z_i)\}$, where from Eq. (5.5)

$$\begin{aligned} E\{z_i \mathrm{sgn}(z_i)\} &= 2^{-(2K-1)} \sum_{\boldsymbol{b} \in \{\cdot\}} \boldsymbol{v}_i^T \boldsymbol{P} \boldsymbol{A} \boldsymbol{b} [1 - 2Q(\frac{\boldsymbol{v}_i^T \boldsymbol{P} \boldsymbol{A} \boldsymbol{b}}{\sigma_{\xi_i}})] \\ &+ 2^{-(2K-1)} \frac{2\sigma_{\xi_i}}{\sqrt{2\pi}} \sum_{\boldsymbol{b} \in \{\cdot\}} \exp(-\frac{[\boldsymbol{v}_i^T \boldsymbol{P} \boldsymbol{A} \boldsymbol{b}]^2}{2\sigma_{\xi_i}^2}). \end{aligned} \tag{5.7}$$

Note that both terms on the right-hand side of the above equation are greater than zero for every bit vector $\boldsymbol{b}$. Therefore,

$$E\{z_i \mathrm{sgn}(z_i)\} > 0 \quad i = 1, \ldots, 2K-1, \tag{5.8}$$

and the diagonal matrix in Eq. (5.6) has full rank. Since $\boldsymbol{P}$ is assumed to be singular, however, then $E\{\boldsymbol{z} \mathrm{sgn}(\boldsymbol{z}^T)\}$ is also singular and the diagonal matrix in Eq. (5.6) cannot be a full rank matrix. The only possibility that satisfies Eq. (5.6) is

$$E\{z_i \mathrm{sgn}(z_j)\} \neq 0, \quad \exists\, i, j; \quad i \neq j. \tag{5.9}$$

Therefore, the bootstrap algorithm does not converge in the presence of a singular cross correlation matrix. On the other hand, if $\boldsymbol{P}$ is non-singular then as a result of Eq. (5.8), when the bootstrap algorithm reaches steady state, the left-hand side has full rank only if $\boldsymbol{R}$ is also full rank. As a result $\boldsymbol{V}$ is unique.

5.2 Proposed Solution I

The contradiction presented in Eq. (5.6) is due to the PCCM $\boldsymbol{P}$ not being full rank. The solution to the convergence problem presented here is based on using a full rank part of the $\boldsymbol{P}$. First, the dependent rows in $\boldsymbol{P}$ are determined by using the adaptive power minimization algorithm. Then the dependent row corresponding to the minimum partial bit energy is eliminated and the full rank condition of the cross correlation matrix is checked again by the adaptive power minimization algorithm. If the cross correlation matrix is full rank then the bootstrap algorithm is used on the remaining independent matched filter-bank outputs for the decorrelation. Otherwise, the previous procedure is repeated until the cross correlation matrix is full rank.

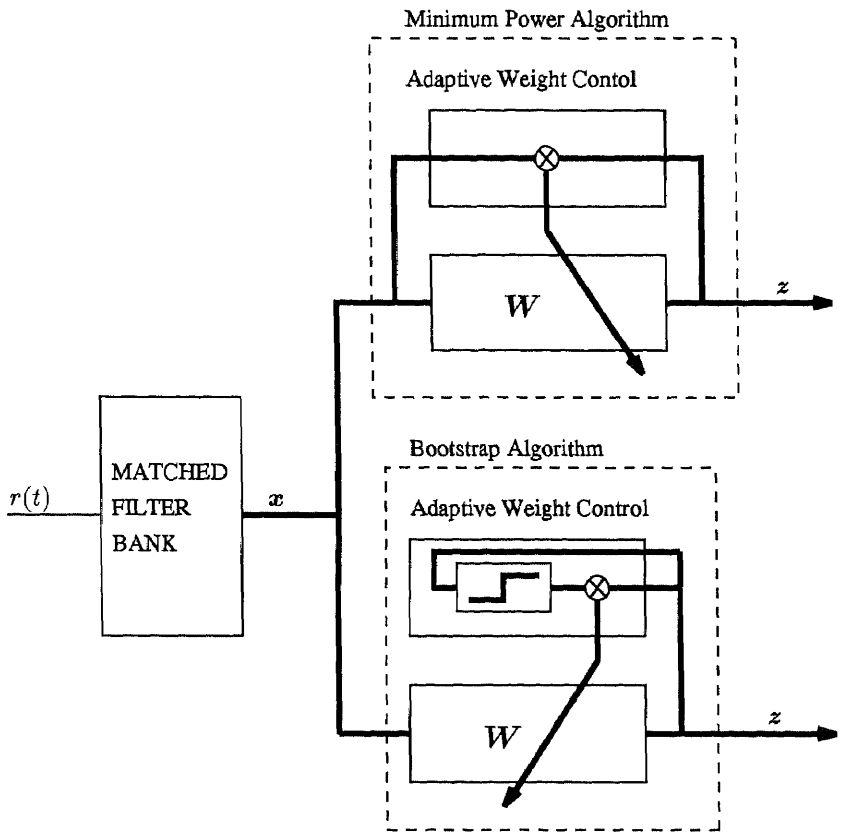

Figure 5.1 Proposed adaptive one-shot decorrelating detector for the dependent user codes.

5.2.1 Determination of Dependent Users

When the PCCM of the one-shot matched filter-bank is singular, some of the row vectors of this matrix depend on each other. In this section, it is proven that one can identify these dependent rows by applying the adaptive power minimization algorithm to the output of the one-shot matched filter-bank.

The one-shot matched filter-bank output signal vector can be written as

$$\boldsymbol{x} = \boldsymbol{PAb} + \boldsymbol{n}. \tag{5.10}$$

The adaptive power minimization algorithm can be viewed as a $(2K-1)\times(2K-1)$ linear transformation applied to the output of the one-shot matched filter-bank in such a way that

$$\boldsymbol{z} = \boldsymbol{V}\boldsymbol{x} \tag{5.11}$$

where

$$\boldsymbol{V} = \boldsymbol{I} - \boldsymbol{W} \tag{5.12}$$

is a $(2K-1)\times(2K-1)$ transformation matrix, $\boldsymbol{I}$ is identity and $\boldsymbol{W}$ is the adaptive weight matrix

$$\boldsymbol{W} = \begin{bmatrix} 0 & w_{12} & \cdots & w_{1,2K-1} \\ w_{21} & 0 & \cdots & w_{2,2K-1} \\ \vdots & \vdots & \ddots & \vdots \\ w_{2K-1,1} & w_{2K-1,2} & \cdots & 0 \end{bmatrix}. \tag{5.13}$$

The adaptive power minimization algorithm has $(2K-1)\times(2K-2)$ adaptive weights updated iteratively at each step. The adaptation rule is given by

$$\begin{aligned} w_{ij} &\leftarrow w_{ij} - \mu\frac{\partial}{\partial w_{ij}}E\{z_i^2\} \\ w_{ij} &\leftarrow w_{ij} - 2\mu E\{z_i x_j\} \quad i,j = 1,\ldots,2K-1; \;\; i \neq j, \end{aligned} \tag{5.14}$$

where μ is the step size of the convergence.

Initially these weights are set to zero and after a sufficient number of iterations they converge to their steady state values. The convergence of the weights is achieved when

$$E\{z_i x_j\} = 0, \;\; \forall i,j; \;\; i \neq j. \tag{5.15}$$

From Eqs. (5.10) and (5.11),

$$\begin{aligned} E\{\boldsymbol{z}\boldsymbol{x}^T\} &= E\{(\boldsymbol{VPAb} + \boldsymbol{Vn})(\boldsymbol{b}^T\boldsymbol{AP}^T + \boldsymbol{n}^T)\} \\ &= \boldsymbol{VPA}^2\boldsymbol{P}^T + \boldsymbol{VP}\sigma^2 \\ &= \boldsymbol{VPQ} \end{aligned} \tag{5.16}$$

where $\boldsymbol{Q} = \boldsymbol{A}^2\boldsymbol{P}^T + \boldsymbol{I}\sigma^2$.

Claim 1: $\boldsymbol{Q}$ is always non-singular.

Proof: Note that $\boldsymbol{A}^2\boldsymbol{P}^T\boldsymbol{A}^2$ is a positive semidefinite matrix. That is, its smallest eigenvalue is zero. On the other hand $\boldsymbol{A}^2\sigma^2$ is positive definite matrix with the smallest eigenvalue greater than zero. Therefore the smallest eigenvalue of $\boldsymbol{A}^2\boldsymbol{P}^T\boldsymbol{A}^2+\boldsymbol{A}^2\sigma^2$ is greater than zero [29]. That is, $\boldsymbol{A}^2\boldsymbol{P}^T\boldsymbol{A}^2+\boldsymbol{A}^2\sigma^2$ is a non-singular matrix. Since

$$\begin{aligned} \boldsymbol{A}^2\boldsymbol{P}^T\boldsymbol{A}^2+\boldsymbol{A}^2\sigma^2 &= (\boldsymbol{A}^2\boldsymbol{P}^T+\boldsymbol{I}\sigma^2)\boldsymbol{A}^2 \\ &= \boldsymbol{Q}\boldsymbol{A}^2 \end{aligned} \tag{5.17}$$

is non-singular then $\boldsymbol{Q}$ is also non-singular. (Q.E.D)

Claim 2: At the steady state, the signal power of the outputs corresponding to the dependent rows of $\boldsymbol{P}$ are zero.

Proof: From Eq. (5.15), if the algorithm converges, then the matrix $E\{\boldsymbol{z}\boldsymbol{x}^T\}$ becomes diagonal whose elements are $E\{z_ix_i\}$. From Eq. (5.16), however, this diagonal matrix must be singular if $\boldsymbol{P}$ is singular. That is,

$$E\{z_ix_i\}=0, \quad \exists i, \quad i=1,\ldots,2K-1. \tag{5.18}$$

Now, when the algorithm converges the ith row of Eq. (5.16) is given by

$$\begin{bmatrix} 0 & \cdots & 0 & E\{z_ix_i\} & 0 & \cdots & 0 \end{bmatrix} = \boldsymbol{v}_i^T\boldsymbol{P}\boldsymbol{Q}, \tag{5.19}$$

where $\boldsymbol{v}_i^T$ is the ith row of the matrix $\boldsymbol{V}$.

If the ith row of $\boldsymbol{P}\boldsymbol{Q}$ does not depend on the other rows, then in the above equation, for $E\{z_ix_i\}$ to be equal to zero, v_{ii} has to be equal to zero, a contradiction since by definition in Eq. (5.12) v_{ii} is equal to 1. Therefore

$$E\{z_ix_i\}\neq 0, \quad \text{if the } i\text{th row of } \boldsymbol{P}\boldsymbol{Q} \text{ does not depend on the other rows.} \tag{5.20}$$

But $v_{ii}=1$, then:

$$\text{for } E\{z_ix_i\}=0, \quad \text{it is necessary that the } i\text{th row of } \boldsymbol{P}\boldsymbol{Q} \text{ depends on the other rows.} \tag{5.21}$$

From Eqs. (5.10) and (5.11),

$$\begin{aligned} E\{z_i^2\} &= E\{(\boldsymbol{v}_i^T\boldsymbol{PAb} + \boldsymbol{v}_i^T\boldsymbol{n})(\boldsymbol{b}^T\boldsymbol{AP}^T\boldsymbol{v}_i + \boldsymbol{n}^T\boldsymbol{v}_i)\} \\ &= \boldsymbol{v}_i^T\boldsymbol{PA}^2\boldsymbol{P}^T\boldsymbol{v}_i + \boldsymbol{v}_i^T\boldsymbol{P}\boldsymbol{v}_i\sigma^2 \\ &= \boldsymbol{v}_i^T\boldsymbol{PQ}\boldsymbol{v}_i. \end{aligned} \tag{5.22}$$

Substituting Eq. (5.19) into the above equation, we get

$$\begin{aligned} E\{z_i^2\} &= \begin{bmatrix} 0 & \cdots & 0 & E\{z_i x_i\} & 0 & \cdots & 0 \end{bmatrix} \boldsymbol{v}_i \\ &= E\{z_i x_i\}, \end{aligned} \tag{5.23}$$

where we again used the fact that $v_{ii} = 1$. Combining the results of Eqs. (5.21) and (5.23), we conclude that if the power of the ith output obtained by using the adaptive power minimization algorithm, $E\{z_i^2\}$ is zero, then the ith row of $\boldsymbol{PQ}$ necessarily depends on the other rows. The situation is the same for $\boldsymbol{P}$ since $\boldsymbol{Q}$ has been shown to be non-singular. (Q.E.D)

5.2.2 Weight Convergence of Bootstrap Separator

Upon identification of the dependent rows, the row that corresponds to the minimum bit energy (that is, the partial user with minimum τ) is eliminated. The elimination is done by not correlating the received signal with the user's partial signature sequence. After eliminating all the dependent rows of the cross correlation matrix $\boldsymbol{P}$, the outputs of the one-shot matched filter-bank with a full rank $\boldsymbol{P}$ are applied to the adaptive bootstrap separator for signal separation.

The modified matrix $\boldsymbol{P}$ is a full rank rectangular matrix. In order to distinguish it from the square and singular $\boldsymbol{P}$, we use $\tilde{\boldsymbol{P}}$. Similarly, we use "tilde" for the other modified parameters such as the one-shot matched filter-bank correlation noise vector $\boldsymbol{n}$, the output signal vector $\boldsymbol{x}$, the adaptive bootstrap separator transformation matrix $\boldsymbol{V}$, the weight matrix $\boldsymbol{W}$ and the output signal vector matrix $\boldsymbol{z}$.

Let $\tilde{\boldsymbol{P}}$ be a $\tilde{K} \times (2K-1)$ matrix where $\tilde{K}$ is the rank of $\boldsymbol{P}$. From Eq. (5.5), when the adaptive weights of the bootstrap separator converge, we have

$$\begin{aligned} E\{\tilde{z}_i \mathrm{sgn}(\tilde{z}_j)\} &= 2^{-(2K-1)} \sum_{\boldsymbol{b}\in\{\cdot\}} \tilde{\boldsymbol{v}}_i^T \tilde{\boldsymbol{P}} \boldsymbol{A}\boldsymbol{b}[1-2Q(\frac{\tilde{\boldsymbol{v}}_j^T \tilde{\boldsymbol{P}}\boldsymbol{A}\boldsymbol{b}}{\sigma_{\tilde{\xi}_j}})] \\ &+ 2^{-(2K-1)} \sum_{\boldsymbol{b}\in\{\cdot\}} \frac{\tilde{\boldsymbol{v}}_i^T \tilde{\boldsymbol{P}}_{\mathbf{n}} \tilde{\boldsymbol{v}}_j}{\tilde{\boldsymbol{v}}_j^T \tilde{\boldsymbol{P}}_{\mathbf{n}} \tilde{\boldsymbol{v}}_j} \frac{2\sigma_{\tilde{\xi}_j}}{\sqrt{2\pi}} \exp(-\frac{[\tilde{\boldsymbol{v}}_j^T \tilde{\boldsymbol{P}}\boldsymbol{A}\boldsymbol{b}]^2}{2\sigma^2_{\tilde{\xi}_j}}), \end{aligned} \tag{5.24}$$

where $\tilde{\boldsymbol{P}}_{\mathbf{n}}$ is the $\tilde{K} \times \tilde{K}$ covariance matrix of $\tilde{\boldsymbol{n}}$, obtained from $\tilde{\boldsymbol{P}}$ by eliminating the columns corresponding to the rows that were eliminated to generate $\tilde{\boldsymbol{P}}$ from $\boldsymbol{P}$. The $\tilde{\boldsymbol{v}}_i$ is the ith row vector of $\tilde{\boldsymbol{V}}$. As in Eq. (5.8), $E\{\tilde{z}_i \mathrm{sgn}(\tilde{z}_i)\} > 0$ for $k = 1, \ldots, \tilde{K}$. Rewriting Eq. (5.24),

$$\begin{aligned} E\{\tilde{z}_i \mathrm{sgn}(\tilde{z}_j)\} &= \tilde{\boldsymbol{v}}_i^T \tilde{\boldsymbol{P}} \left\{ 2^{-(2K-1)} \sum_{\boldsymbol{b}\in\{\cdot\}} \boldsymbol{A}\boldsymbol{b}[1-2Q(\frac{\tilde{\boldsymbol{v}}_j^T \tilde{\boldsymbol{P}}\boldsymbol{A}\boldsymbol{b}}{\sigma_{\tilde{\xi}_j}})] \right. \\ &\left. + 2^{-(2K-1)} \sum_{\boldsymbol{b}\in\{\cdot\}} \frac{\tilde{\boldsymbol{I}}_{\mathbf{n}} \tilde{\boldsymbol{v}}_j}{\tilde{\boldsymbol{v}}_j^T \tilde{\boldsymbol{P}}_{\mathbf{n}} \tilde{\boldsymbol{v}}_j} \frac{2\sigma_{\tilde{\xi}_j}}{\sqrt{2\pi}} \exp(-\frac{[\tilde{\boldsymbol{v}}_j^T \tilde{\boldsymbol{P}}\boldsymbol{A}\boldsymbol{b}]^2}{2\sigma^2_{\tilde{\xi}_j}}) \right\} \\ &= \tilde{\boldsymbol{v}}_i^T \tilde{\boldsymbol{P}} \tilde{\boldsymbol{r}}_j \quad i, j = 1, \ldots, \tilde{K}, \end{aligned} \tag{5.25}$$

where we use $\tilde{\boldsymbol{P}}\tilde{\boldsymbol{I}}_{\mathbf{n}} = \tilde{\boldsymbol{P}}_{\mathbf{n}}$ with $\tilde{\boldsymbol{I}}_{\mathbf{n}}$ a $(2K-1) \times \tilde{K}$ matrix, wherein the rows corresponding to the eliminated rows are all zeros and $\tilde{\boldsymbol{r}}_j$ is the term inside the curly brackets in the above equation.

The above equation can be written in a matrix form as:

$$E\{\tilde{\boldsymbol{z}} \mathrm{sgn}(\tilde{\boldsymbol{z}}^T)\} = \tilde{\boldsymbol{V}} \tilde{\boldsymbol{P}} \tilde{\boldsymbol{R}}, \tag{5.26}$$

where $\tilde{\boldsymbol{R}}$ is $(2K-1) \times \tilde{K}$ matrix whose columns are $\tilde{\boldsymbol{r}}_j$ with $j = 1, \ldots, \tilde{K}$. When the bootstrap algorithm converges, the left-hand side of Eq. (5.26) is a diagonal matrix with all positive terms, having full rank. Therefore $\tilde{\boldsymbol{R}}$ must have a full rank, $\tilde{K}$, resulting in a unique solution for $\tilde{\boldsymbol{V}}$.

5.2.3 BER Performance Analysis

The ith output of the bootstrap separator can be written as

$$\begin{aligned}
\tilde{z}_i &= \tilde{\boldsymbol{v}}_i^T \tilde{\boldsymbol{x}} \\
\tilde{z}_i &= \sqrt{a_i} b_i + \underline{\boldsymbol{\rho}}_i^T \underline{\boldsymbol{A}}_i \underline{\boldsymbol{b}}_i + \tilde{n}_i - \underline{\tilde{\boldsymbol{w}}}_i^T \underline{\tilde{\boldsymbol{x}}}_i \\
&= \sqrt{a_i} b_i + \underline{\boldsymbol{\rho}}_i^T \underline{\boldsymbol{A}}_i \underline{\boldsymbol{b}}_i + \tilde{n}_i - \underline{\tilde{\boldsymbol{w}}}_i^T (\underline{\tilde{\boldsymbol{P}}}_i \underline{\boldsymbol{A}}_i \underline{\boldsymbol{b}}_i + \underline{\tilde{\boldsymbol{p}}}_i \sqrt{a_i} b_i + \underline{\tilde{\boldsymbol{n}}}_i) \\
&= \sqrt{a_i}(1 - \underline{\tilde{\boldsymbol{w}}}_i^T \underline{\tilde{\boldsymbol{p}}}_i) b_i + (\underline{\boldsymbol{\rho}}_i^T - \underline{\tilde{\boldsymbol{w}}}_i^T \underline{\tilde{\boldsymbol{P}}}_i) \underline{\boldsymbol{A}}_i \underline{\boldsymbol{b}}_i + \boldsymbol{v}_i^T \boldsymbol{n}, \qquad (5.27)
\end{aligned}$$

where, in the above equation, the underlined vector is the vector without its ith element and the underlined matrix is the matrix without its ith row and ith column.

The BER for the ith user is

$$\mathrm{BER}_i = 2^{-(2K-2)} \sum_{\underline{\boldsymbol{b}}_i \in \{\cdot\}} Q\left(\frac{\sqrt{a_i}(1 - \underline{\tilde{\boldsymbol{w}}}_i^T \underline{\tilde{\boldsymbol{p}}}_i) + (\underline{\boldsymbol{\rho}}_i^T - \underline{\tilde{\boldsymbol{w}}}_i^T \underline{\tilde{\boldsymbol{P}}}_i) \underline{\boldsymbol{A}}_i \underline{\boldsymbol{b}}_i}{\sigma_{\tilde{\xi}_j}}\right), \qquad (5.28)$$

where the set $\{\cdot\}$ contains all 2^{2K-2} different combinations of $\underline{\boldsymbol{b}}_i$.

5.2.4 Simulation Results

Using length-seven Gold codes, a desired user (first user) and two interfering users are simulated with asynchronous CDMA communication. The interfering user signals are delayed with respect to the desired user so that the left half of their codes are equal. That is, the second and fourth one-shot signature sequences are dependent. The corresponding cross correlation matrix at the output of one-shot matched filters is

$$\boldsymbol{P} = \begin{bmatrix} 1.0 & 0 & -0.169031 & 0 & -0.169031 \\ 0 & 1.0 & 0 & 1.0 & 0 \\ -0.169031 & 0 & 1.0 & 0 & 0.2 \\ 0 & 1.0 & 0 & 1.0 & 0 \\ -0.169031 & 0 & 0.2 & 0 & 1.0 \end{bmatrix}. \qquad (5.29)$$

The BER performance of the adaptive bootstrap separator and its conventional (using pseudoinverse matrix) counterpart is depicted in Figure 5.2, for various desired and varying interfering users' SNRs. This figure shows similar behaviour to that with non-singular cross correlation matrix; that is, for low interference, the

BER performance of the bootstrap separator is better than the performance for the conventional decorrelator, whereas for high interference it is the same. Of special interest is the curves with $\mathrm{SNR}_1 = \mathrm{SNR}_i$ as it reflects the performance with power control.

Figure 5.3 repeats the results of the Figure 5.2, except that the singular cross correlation matrix obtained for the non-equal delay case,

$$\boldsymbol{P} = \begin{bmatrix} 1.0 & -0.534522 & -0.507093 & 0 & 0.654653 \\ -0.534522 & 1.0 & 0 & -0.707107 & 0 \\ -0.507093 & 0 & 1.0 & 0.447214 & -0.258199 \\ 0 & -0.707107 & 0.447214 & 1.0 & 0 \\ 0.654653 & 0 & -0.258199 & 0 & 1.0 \end{bmatrix}. \tag{5.30}$$

We finally conclude that the bootstrap algorithm with the adaptive rank test and update, can still be used for asynchronous CDMA communication, with any cross correlation matrix; singular or non-singular.

The resulting algorithm depicts the BER performance better or equal to what can be expected for the decorrelating detector. We emphasize that although the bootstrap approach require some more complexity, its ability to adapt to changing conditions of the wireless communication environment is desirable.

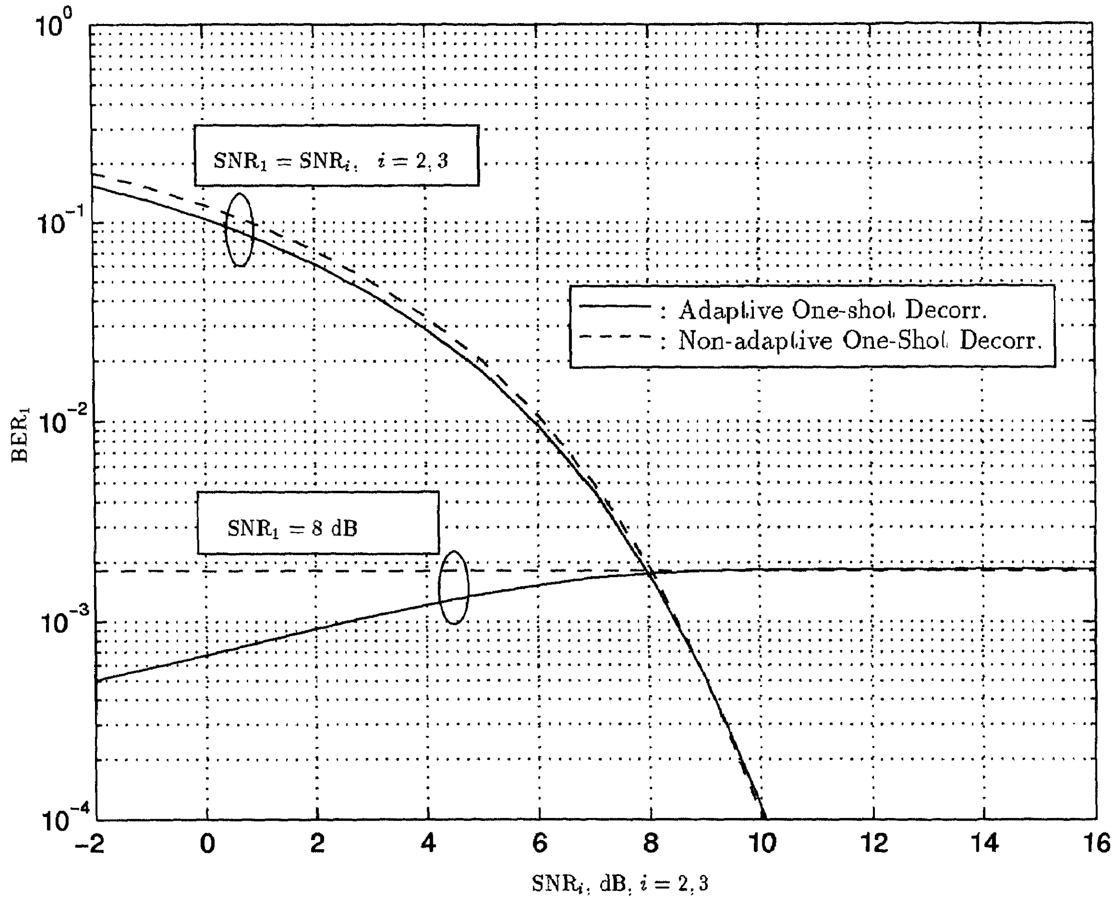

Figure 5.2 BER performance of three asynchronous users using the adaptive and non-adaptive decorrelating detectors.

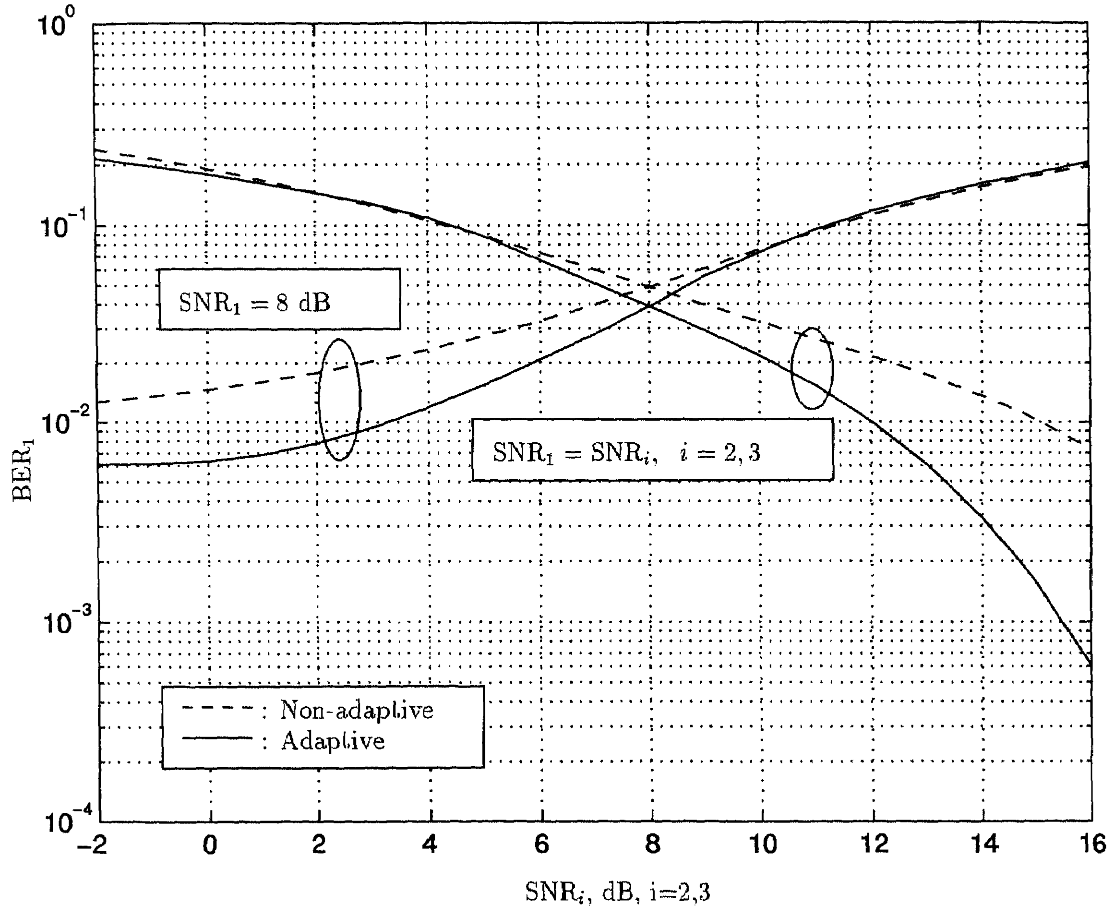

Figure 5.3 BER performance of three asynchronous users using the adaptive and non-adaptive decorrelating detectors.

5.3 Proposed Solution II

The second proposed method for avoiding the non-convergence of the bootstrap algorithm takes advantage of using a soft limiter for the weight updating scheme. It is shown analytically that using a soft limiter rather than a hard limiter for the weight adaptation scheme does not introduce the problem of convergence. This idea is supported with simulations of several asynchronous CDMA users when the one-shot cross correlation matrix of their signature sequence is singular.

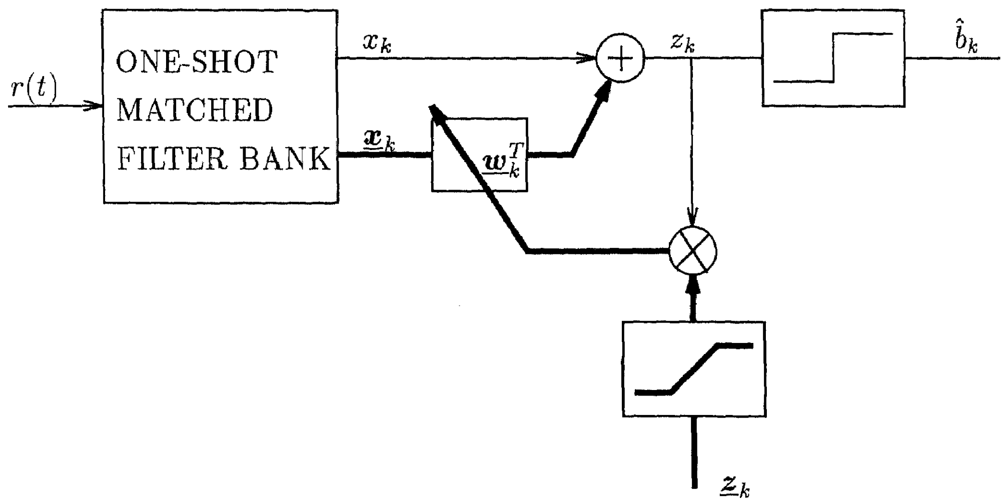

Figure 5.4 Modified bootstrap decorrelating detector for the users with dependent signature sequences.

5.3.1 Convergence Analysis

When the algorithm converges,

$$E\{z_i f(z_j)\} = 0, \quad i, j = 1, \ldots, 2K-1; \quad i \neq j, \tag{5.31}$$

where

$$\begin{aligned} z_i &= \boldsymbol{v}_i^T \boldsymbol{x} \\ &= \boldsymbol{v}_i \boldsymbol{P} \boldsymbol{A} \boldsymbol{b} + \xi_i, \end{aligned} \tag{5.32}$$

$\boldsymbol{v}_i^T = \begin{bmatrix} v_{i1} & \cdots & v_{i,2K-1} \end{bmatrix}$ and $\xi_i = \boldsymbol{v}_i^T \boldsymbol{n}$.

In Section 5.1, it was shown that when $f(\cdot) = \mathrm{sgn}(\cdot)$ (i.e. hard decision function), the adaptive weights do not converge if the PCCM is singular.

In order to resolve this problem, we propose the discrimination function:

$$f(z_j) = \begin{cases} 1 & \text{if } z_j > t \\ z_j/t & \text{if } -t \le z_j \le t \\ -1 & \text{if } z_j < -t, \end{cases} \tag{5.33}$$

where t is a real number called the threshold. Then

$$\begin{aligned} E\{z_i f(z_j)\} &= E\{(\boldsymbol{v}_i^T \boldsymbol{P}\boldsymbol{A}\boldsymbol{b} + \xi_i) f(\boldsymbol{v}_j^T \boldsymbol{P}\boldsymbol{A}\boldsymbol{b} + \xi_j)\} \\ &= E\{\boldsymbol{v}_i^T \boldsymbol{P}\boldsymbol{A}\boldsymbol{b} f(\boldsymbol{v}_j^T \boldsymbol{P}\boldsymbol{A}\boldsymbol{b} + \xi_j)\} + E\{\xi_i f(\boldsymbol{v}_j^T \boldsymbol{P}\boldsymbol{A}\boldsymbol{b} + \xi_j)\}. \end{aligned} \tag{5.34}$$

Both terms in the right hand side of the above equation are derived in Appendix B. Then

$$\begin{aligned} E\{z_i f(z_j)\} = 2^{-(2K-1)} \sum_{\boldsymbol{b} \in \{\cdot\}} \Bigg\{ & c_i [1 - Q(\frac{c_j - t}{\sigma_{\xi_j}}) - Q(\frac{c_j + t}{\sigma_{\xi_j}})] \\ & + \frac{c_i c_j}{t} [Q(\frac{c_j - t}{\sigma_{\xi_j}}) - Q(\frac{c_j + t}{\sigma_{\xi_j}})] + \frac{c_i \sigma_{\xi_j}}{t\sqrt{2\pi}} [\exp(-\frac{[c_j + t]^2}{2\sigma_{\xi_j}^2}) - \exp(-\frac{[c_j - t]^2}{2\sigma_{\xi_j}^2})] \\ & + \frac{\boldsymbol{v}_i^T \boldsymbol{P} \boldsymbol{v}_j}{\boldsymbol{v}_j^T \boldsymbol{P} \boldsymbol{v}_j} \frac{\sigma_{\xi_j}^2}{t} [Q(\frac{c_j - t}{\sigma_{\xi_j}}) - Q(\frac{c_j + t}{\sigma_{\xi_j}})] \Bigg\}, \end{aligned} \tag{5.35}$$

where $c_i = \boldsymbol{v}_i^T \boldsymbol{P}\boldsymbol{A}\boldsymbol{b}$ and $c_j = \boldsymbol{v}_j^T \boldsymbol{P}\boldsymbol{A}\boldsymbol{b}$, $\quad i, j = 1, \ldots, 2K-1$.

In the limit when $t \to 0$, using L'Hospital's rule, we can show that the second term in Eq. (5.35) cancels out the third term with the result in Eq. (5.5). Note that $\boldsymbol{P}$ is positive semidefinite; then, for $E\{z_i f(z_j)\} = 0$, $\boldsymbol{v}_j$ cannot be an eigenvector of $\boldsymbol{P}$ since then $\boldsymbol{v}_j^T \boldsymbol{P} \boldsymbol{v}_j = 0$, and the equation cannot be satisfied.

For a quite small t the sum of the second and third terms of Eq. (5.35) is almost zero, leaving

$$\begin{aligned} E\{z_i f(z_j)\} &= 2^{-(2K-1)} \sum_{\boldsymbol{b} \in \{\cdot\}} \Bigg\{ c_i [1 - Q(\frac{c_j - t}{\sigma_{\xi_j}}) - Q(\frac{c_j + t}{\sigma_{\xi_j}})] \\ &\qquad + \frac{\boldsymbol{v}_i^T \boldsymbol{P} \boldsymbol{v}_j}{\boldsymbol{v}_j^T \boldsymbol{P} \boldsymbol{v}_j} \frac{\sigma_{\xi_j}^2}{t} [Q(\frac{c_j - t}{\sigma_{\xi_j}}) - Q(\frac{c_j + t}{\sigma_{\xi_j}})] \Bigg\} \end{aligned}$$

$$
\begin{aligned}
&= \boldsymbol{v}_i^T \boldsymbol{P} \left\{ 2^{-(2K-1)} \sum_{\boldsymbol{b}\in\{\cdot\}} \boldsymbol{A}\boldsymbol{b}\alpha_{1j}(t) + \frac{2^{-(2K-1)}\boldsymbol{v}_j}{\|\boldsymbol{v}_j\|^2_{\boldsymbol{P}}} \sum_{\boldsymbol{b}\in\{\cdot\}} \alpha_{2j}(t) \right\} \\
&= 0, \quad i,j = 1,\ldots,2K-1; \quad i \neq j, \qquad (5.36)
\end{aligned}
$$

where

$$
\begin{aligned}
\alpha_{1j}(t) &= 1 - Q(\frac{c_j - t}{\sigma_{\xi_j}}) - Q(\frac{c_j + t}{\sigma_{\xi_j}}) \\
\alpha_{2j}(t) &= \frac{\sigma^2_{\xi_j}}{t}[Q(\frac{c_j - t}{\sigma_{\xi_j}}) - Q(\frac{c_j + t}{\sigma_{\xi_j}})] \\
\|\boldsymbol{v}_j\|^2_{\boldsymbol{P}} &= \boldsymbol{v}_j^T \boldsymbol{P} \boldsymbol{v}_j > 0. \qquad (5.37)
\end{aligned}
$$

Note that $\alpha_{1j}(t) > 0$ for $t > 0$ and any c_j, and $\alpha_{2j}(t) > 0$ for any t and any c_j.

From Eq. (5.36) we get:

$$
\boldsymbol{v}_i^T \boldsymbol{P}\boldsymbol{A} \sum_{\boldsymbol{b}\in\{\cdot\}} \boldsymbol{b}\alpha_{1j}(t) = -\frac{\boldsymbol{v}_i^T \boldsymbol{P} \boldsymbol{v}_j}{\|\boldsymbol{v}_j\|^2_{\boldsymbol{P}}} \sum_{\boldsymbol{b}\in\{\cdot\}} \alpha_{2j}(t), \quad i,j = 1,\ldots,2K-1; \quad i \neq j. \qquad (5.38)
$$

We may also write Eq. (5.36) in the form of

$$
E\{z_i f(z_j)\} = \boldsymbol{v}_i^T \boldsymbol{P} \boldsymbol{r}_j \qquad (5.39)
$$

where $\boldsymbol{r}_j$ is the term inside the curly brackets. Then

$$
\begin{aligned}
E\{\boldsymbol{z} f(\boldsymbol{z}^T)\} &= \begin{bmatrix} E\{z_1 f(z_1)\} & 0 & \cdots & 0 \\ 0 & E\{z_1 f(z_2)\} & \cdots & 0 \\ \vdots & \vdots & \ddots & \vdots \\ 0 & 0 & \cdots & E\{z_{2K-1} f(z_{2K-1})\} \end{bmatrix} \\
&= \boldsymbol{VPR}. \qquad (5.40)
\end{aligned}
$$

From Eq. (5.36), when $\boldsymbol{P}$ is singular $E\{z_i f(z_i)\}$ must be equal to zero for as many i as the nullity of $\boldsymbol{P}$. Therefore, from Eq. (5.36),

$$
\begin{aligned}
E\{z_i f(z_i)\} &= 2^{-(2K-1)} \boldsymbol{v}_i^T \boldsymbol{P}\boldsymbol{A} \sum_{\boldsymbol{b}\in\{\cdot\}} \boldsymbol{b}\alpha_{1i}(t) + \sum_{\boldsymbol{b}\in\{\cdot\}} \alpha_{2i}(t), \\
\boldsymbol{v}_i^T \boldsymbol{P}\boldsymbol{A} \sum_{\boldsymbol{b}\in\{\cdot\}} \boldsymbol{b}\alpha_{1i}(t) &= -\sum_{\boldsymbol{b}\in\{\cdot\}} \alpha_{2i}(t) \quad \text{for these } i\text{'s} \qquad (5.41) \\
\text{and } \boldsymbol{v}_i^T \boldsymbol{P}\boldsymbol{A} \sum_{\boldsymbol{b}\in\{\cdot\}} \boldsymbol{b}\alpha_{1i}(t) &\neq -\sum_{\boldsymbol{b}\in\{\cdot\}} \alpha_{2i}(t) \quad \text{for the other } i\text{'s}; \qquad (5.42)
\end{aligned}
$$

where $i = 1,\ldots,2K-1$. Considering Eqs. (5.38), (5.41) and (5.42) we conclude that steady state weights exist.

5.3.2 BER Performance Analysis

The adaptive weights for the K asynchronous users can be found using Eq. (5.36). The ith output of bootstrap separator can be written as,

$$\begin{aligned} z_i &= \sqrt{a_i} b_i + \underline{\boldsymbol{\rho}}_i^T \underline{\boldsymbol{A}}_i \underline{\boldsymbol{b}}_i + n_i - \underline{\boldsymbol{w}}_i^T \underline{\boldsymbol{x}}_i \\ &= \sqrt{a_i} b_i + \underline{\boldsymbol{\rho}}_i^T \underline{\boldsymbol{A}}_i \underline{\boldsymbol{b}}_i + n_i - \underline{\boldsymbol{w}}_i^T (\underline{\boldsymbol{P}}_i \underline{\boldsymbol{A}}_i \underline{\boldsymbol{b}}_i + \underline{\boldsymbol{p}}_i \sqrt{a_i} b_i + \underline{\boldsymbol{n}}_i) \\ &= (1 - \underline{\boldsymbol{w}}_i^T \underline{\boldsymbol{p}}_i) \sqrt{a_i} b_i + (\underline{\boldsymbol{\rho}}_i^T - \underline{\boldsymbol{w}}_i^T \underline{\boldsymbol{P}}_i) \underline{\boldsymbol{A}}_i \underline{\boldsymbol{b}}_i + n_i - \underline{\boldsymbol{w}}_i^T \underline{\boldsymbol{n}}_i, \end{aligned} \tag{5.43}$$

where, in the above equation, the underlined vector is the vector without its ith element and the underlined matrix is the matrix without its ith row and ith column.

The BER for the ith user is

$$\mathrm{BER}_i = 2^{-(2K-2)} \sum_{\underline{\boldsymbol{b}}_i \in \{\cdot\}} Q\left(\frac{(1 - \underline{\boldsymbol{w}}_i^T \underline{\boldsymbol{p}}_i)\sqrt{a_i} + (\underline{\boldsymbol{\rho}}_i^T - \underline{\boldsymbol{w}}_i^T \underline{\boldsymbol{P}}_i) \underline{\boldsymbol{A}}_i \underline{\boldsymbol{b}}_i}{\sigma_{\xi_j}}\right), \tag{5.44}$$

where the set $\{\cdot\}$ contains all 2^{2K-2} different combinations of $\underline{\boldsymbol{b}}_i$.

5.3.3 Simulation Results

Three asynchronous users with the same code sequences as in Section 5.2 are simulated using the proposed scheme.

In order to observe the effect of the threshold setting on the adaptive weight convergence, the threshold of the soft limiter is changed from 10^{-5} to about 10^5 for desired and interfering user's SNR equal to 8 dB. The bootstrap separator's weights converge for a wide range of threshold settings. The results are depicted in Figure 5.5.

With a threshold of 2.0, the adaptive bootstrap separator is simulated for various desired and interfering user SNRs. The separator weights converged for all the cases.

The BER performance of the adaptive bootstrap separator and its non-adaptive counterpart is depicted in Figure 5.6 and Figure 5.7 for various desired user and interfering users' SNRs. From these figures it can be observed that, for low interference, the BER performance of the bootstrap separator is better than the performance for the non-adaptive decorrelating detector, whereas for high interference it is the same.

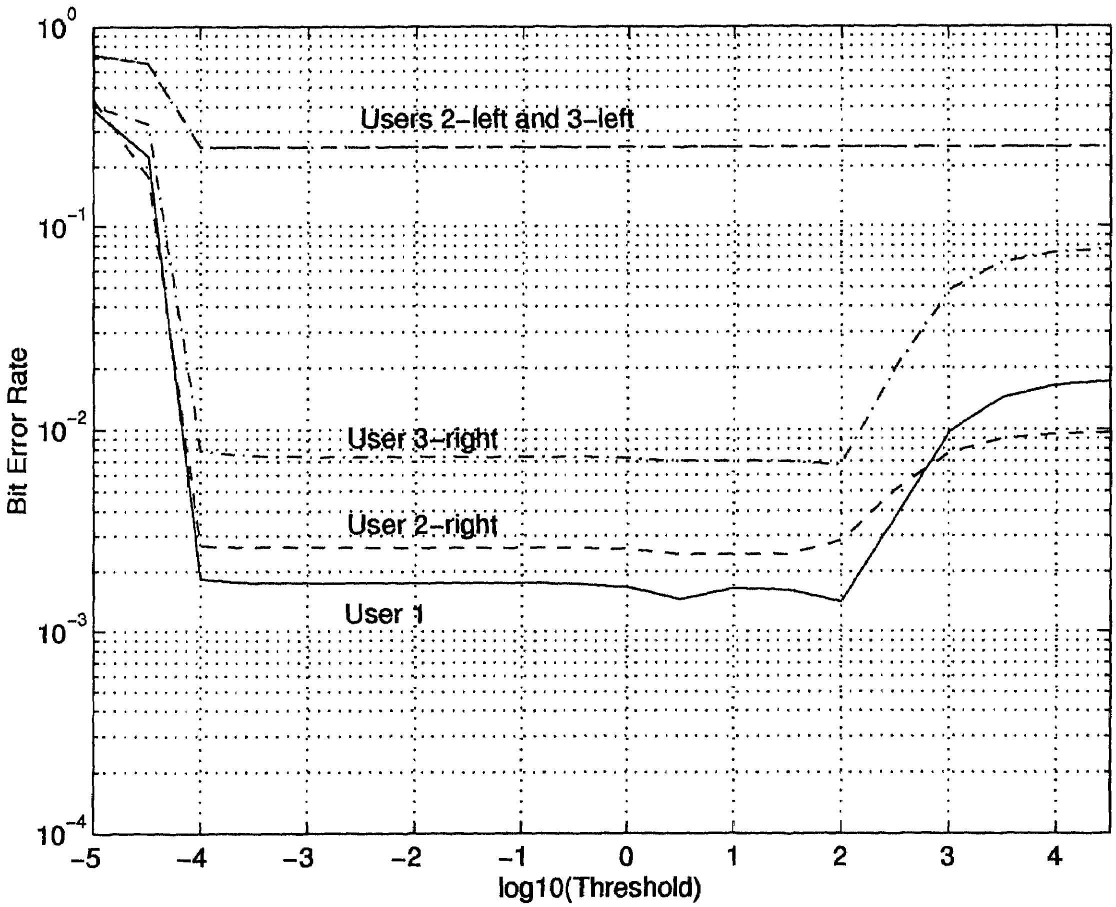

Figure 5.5 The effect of threshold setting on the convergence of adaptive decorrelating detector.

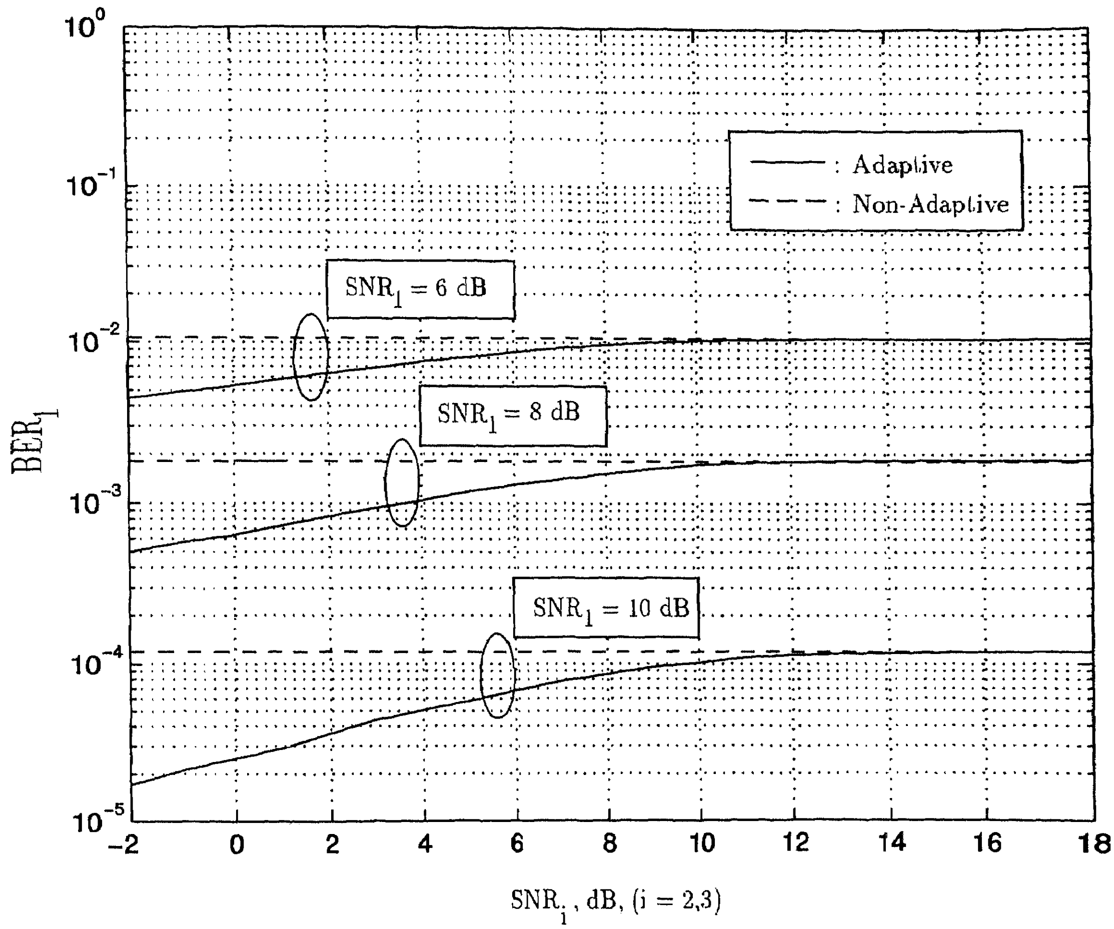

Figure 5.6 BER performance of one-shot adaptive and non-adaptive decorrelating detectors for three asynchronous CDMA users with dependent codes.

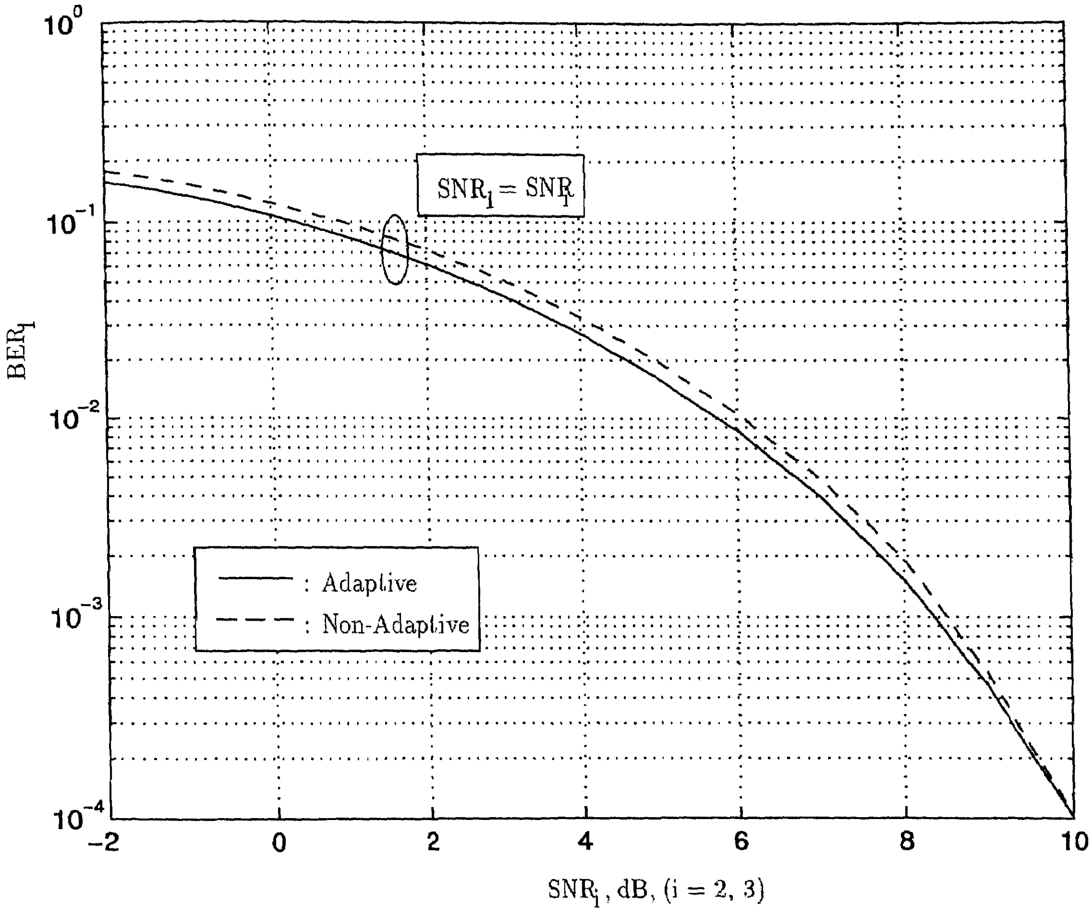

Figure 5.7 BER performance of one-shot adaptive and non-adaptive decorrelating detectors for three asynchronous CDMA users with dependent codes.

5.4 Summary

In this chapter we analysed the non-convergence problem of the adaptive bootstrap separator, which occurs whenever the cross correlation matrix of the user codes is singular. The singularity of the cross correlation matrix is a common phenomenon for the one-shot detection of asynchronous CDMA users. We proposed two different schemes as a solution to the convergence problem. The first scheme was based on obtaining a full rank cross correlation matrix by eliminating the dependent rows of the cross correlation matrix in a sequential manner. For this procedure, an adaptive power minimization algorithm was used. The second scheme takes advantage of using soft limiter as the discriminator function for the weight update rather than the hard limiter. BER performances of both methods were obtained by simulating three asynchronous CDMA users. The performance results of both proposed adaptive schemes are better than the performance of the non-adaptive decorrelating detector.

CHAPTER 6
CONCLUSION

We began this dissertation by addressing the need for an increase in the capacity for mobile radio communication. The capacities of the multiple access schemes currently in commercial use such as FDMA and TDMA are well below the required demand for the future generation of mobile radio communication. The CDMA multiple access scheme emerges as a possible solution to the growing demand for mobile communications. The capacity of CDMA is limited by the multiuser interference from the other users. The cancellation of multiuser interference for CDMA communications is one of the active research areas in the recent years.

Since the characteristics of the mobile communication environment are time varying, it is desirable for the detector to adapt itself to the changing conditions of the communication environment. Throughout this dissertation, the focus was on the adaptive schemes, for the cancellation of multiuser interference.

In Chapter 3, the advantage of using the adaptive decorrelating detector rather than the non-adaptive decorrelating detector is demonstrated by comparing their BER performance in an asynchronous CDMA environment with erroneous code delay estimation. It is observed that the non-adaptive decorrelating detector is very sensitive to the delay estimation errors, whereas the adaptive decorrelating detector is very robust. This adaptive decorrelating detector can be used as a first stage in the multi-stage CDMA detector.

In Chapter 4, an adaptive two-stage CDMA detector is proposed with an adaptive threshold setting algorithm. This algorithm finds the optimum threshold values by minimizing the energy at the output of the canceller stage with respect to the interfering signals. It is observed that minimizing the output energy is not the same as minimizing the BER of the desired user. However, the difference between the minimum BER and the BER corresponding to the minimum energy for the desired user is almost negligible. Therefore, the optimum threshold is found according to the adaptive energy minimization algorithm. Selecting the adaptive decorrelating detector studied in the Chapter 3, for this two-stage detector, makes the whole structure totally adaptive.

Finally in Chapter 5, the problem of non-convergence for the adaptive decorrelating detector is studied. It is analytically proven that the adaptive decorrelating detector weights do not converge when partial signature sequences which occur in one-shot asynchronous CDMA detection are dependent. Two different solution are then proposed and analysed using adaptive schemes. It is observed that both of the proposed schemes have better BER performance compared to the non-adaptive decorrelating detector.

APPENDIX A

DERIVATIONS FOR CHAPTER 4

A.1 Derivation of $E\{b_l f(\eta_{kl})\}$

It is easy to show that $E\{b_l f(\eta_{kl})|b_l = 1\} = E\{b_l f(\eta_{kl})|b_l = -1\}$. Therefore,

$$E\{b_l f(\eta_{kl})\} = \frac{1}{\sqrt{2\pi}\sigma_{\eta_{kl}}} \int_{-\infty}^{+\infty} f(\eta_{ki}) \exp\left(-\frac{(\eta_{kl} - \overline{\eta_{kl}})^2}{2\sigma_{\eta_{kl}}^2}\right) d\eta_{kl} \tag{A.1}$$

where $\overline{\eta_{kl}}$ and $\sigma_{\eta_{kl}}^2$ are the mean and the variance of the Gauissan random variable η_{kl}.

With $b_l = 1$ and therefore $\eta_{kl} = \lambda_{kl} z_l = \lambda_{kl}(\sqrt{a_l} + \xi_l)$ and $\overline{\eta_{kl}} = \lambda_{kl}\sqrt{a_l}$. Then evaluating the integral over its three regions, $(-\infty, -1]$, $[-1, 1]$ and $[1, \infty)$, with change of a variable, $x = (\eta_{kl} - \overline{\eta_{kl}})/\sigma_{\eta_{kl}}$, we get

$$\begin{aligned}
E\{b_l f(\eta_{kl})\} &= \frac{1}{\sqrt{2\pi}} \left[\int_{-\infty}^{-\alpha_2} e^{x^2/2} dx + \int_{-\alpha_2}^{\alpha_1} (\sigma_{\eta_{kl}} x + \lambda_{kl}\sqrt{a_l}) e^{-x^2/2} dx\right] \qquad \text{(A.2)} \\
&= \frac{\sigma_{\eta_{kl}}}{\sqrt{2\pi}} \left(e^{-\alpha_2^2/2} - e^{-\alpha_1^2/2}\right) + \lambda_{kl}\sqrt{a_l}\,[1 - Q(\alpha_1) - Q(\alpha_2)] + Q(\alpha_1) - Q(\alpha_2)
\end{aligned}$$

where $\alpha_1 = (1 - \lambda_{kl}\sqrt{a_l})/\sigma_{\eta_{kl}}$ and $\alpha_2 = (1 + \lambda_{kl}\sqrt{a_l})/\sigma_{\eta_{kl}}$.

A.2 Derivation of $E\{f^2(\eta_{kl})\}$

The $E\{f^2(\eta_{kl})\}$ can be written as

$$E\{f^2(\eta_{kl})\} = \frac{1}{2} E\{f^2(\eta_{kl})|b_l = 1\} + \frac{1}{2} E\{f^2(\eta_{kl})|b_l = -1\} \tag{A.3}$$

It is easy to show that conditioned on $b_l = 1$ and $b_l = -1$, both terms in the right hand side of the above equation are equal. Therefore,

$$\begin{aligned}
E\{f^2(\eta_{kl})\} &= E\{f^2(\eta_{kl})|b_l = 1\} \\
&= \frac{1}{\sqrt{2\pi}\sigma_{\eta_{kl}}} \int_{-\infty}^{+\infty} f^2(\eta_{kl}) \exp\left(-\frac{(\eta_{kl} - \lambda_{kl}\sqrt{a_l})^2}{2\sigma_{\eta_{kl}}^2}\right) d\eta_{kl} \\
&= \frac{1}{\sqrt{2\pi}\sigma_{\eta_{kl}}} \int_{0}^{\infty} f^2(\eta_{kl}) \exp\left(-\frac{(\eta_{kl} - \lambda_{kl}\sqrt{a_l})^2}{2\sigma_{\eta_{kl}}^2}\right) d\eta_{kl} \\
&\quad + \frac{1}{\sqrt{2\pi}\sigma_{\eta_{kl}}} \int_{0}^{\infty} f^2(\eta_{kl}) \exp\left(-\frac{(\eta_{kl} + \lambda_{kl}\sqrt{a_l})^2}{2\sigma_{\eta_{kl}}^2}\right) d\eta_{kl}. \qquad \text{(A.4)}
\end{aligned}$$

Substituting $x_1 = (\eta_{kl} - \lambda_{kl}\sqrt{a_l})/\sigma_{\eta_{kl}}$ in the first integral, $x_2 = (\eta_{kl} + \sqrt{a_l})/\sigma_{\eta_{kl}}$ in the second integral in the above equation and performing the integration we get

$$\begin{aligned} E\{f^2(\eta_{kl})\} &= \frac{\sigma^2_{\eta_{kl}}}{\sqrt{2\pi}}\left[(2\alpha_0 - \alpha_2)e^{-\alpha_2^2/2} - (2\alpha_0 + \alpha_1)e^{-\alpha_1^2/2}\right] \\ &\quad + \sigma^2_{\eta_{kl}}(1+\alpha_0^2)\left[1 - Q(\alpha_1) - Q(\alpha_2)\right] + Q(\alpha_1) + Q(\alpha_2), \quad (A.5) \end{aligned}$$

where $\alpha_0 = \lambda_{kl}\sqrt{a_l}/\sigma_{\eta_{kl}}$, $\alpha_1 = (1 - \lambda_{kl}\sqrt{a_l})/\sigma_{\eta_{kl}}$ and $\alpha_2 = (1 + \lambda_{kl}\sqrt{a_l})/\sigma_{\eta_{kl}}$.

A.3 Derivation of $E\{b_l df(\eta_{kl})/d\lambda_{kl}\}$

It is easy to show that $E\{b_l df(\eta_{kl})/d\lambda_{kl}\} = E\{b_l z_l df(\eta_{kl})/d\eta_{kl}\}$ and $E\{b_l z_l df(\eta_{kl})/d\eta_{kl}|b_l = -1\} = E\{b_l z_l df(\eta_{kl})/d\eta_{kl}|b_l = 1\}$. Therefore,

$$\begin{aligned} E\left\{b_l z_l \frac{df(\eta_{kl})}{d\eta_{kl}}\right\} &= E\left\{b_l z_l \frac{df(\eta_{kl})}{d\eta_{kl}}|b_l = 1\right\} \\ &= \frac{1}{\sqrt{2\pi}\sigma_{\eta_{kl}}}\int_{-1}^{1}\frac{\eta_{kl}}{\lambda_{kl}}\exp\left(-\frac{(\eta_{kl} - \lambda_{kl}\sqrt{a_l})^2}{2\sigma^2_{\eta_{kl}}}\right)d\eta_{kl} \qquad (A.6) \end{aligned}$$

Changing variable, $x = (\eta_{kl} - \lambda_{kl}\sqrt{a_l})/\sigma_{\eta_{kl}}$, in the above equation and performing the integration we get,

$$E\left\{b_l \frac{df(\eta_{kl})}{d\lambda_{kl}}\right\} = \frac{1}{\lambda_{kl}}\left\{\frac{\sigma_{\eta_{kl}}}{\sqrt{2\pi}}(e^{-\alpha_2^2/2} - e^{-\alpha_1^2/2}) + \lambda_{kl}\sqrt{a_l}\left[1 - Q(\alpha_2) - Q(\alpha_2)\right]\right\}, \qquad (A.7)$$

where α_1 and α_2 are defined in (A.5).

A.4 Derivation of $E\{f(\eta_{kl})df(\eta_{kl})/d\lambda_{kl}\}$

$$E\left\{f(\eta_{kl})\frac{df(\eta_{kl})}{d\lambda_{kl}}\right\} = \frac{1}{2}E\left\{f(\eta_{kl})\frac{df(\eta_{kl})}{d\lambda_{kl}}|b_l = -1\right\} + \frac{1}{2}E\left\{f(\eta_{kl})\frac{df(\eta_{kl})}{d\lambda_{kl}}|b_l = 1\right\} \qquad (A.8)$$

It is easy to show that, both terms in the right hand side of the above equation are equal. Therefore,

$$\begin{aligned} E\left\{f(\eta_{kl})\frac{df(\eta_{kl})}{d\lambda_{kl}}\right\} &= E\left\{f(\eta_{kl})z_l\frac{df(\eta_{kl})}{d\eta_{kl}}\right\} = E\left\{f(\eta_{kl})z_l\frac{df(\eta_{kl})}{d\eta_{kl}}|b_l = 1\right\} \\ &= \frac{1}{\sqrt{2\pi}\sigma_{\eta_{kl}}}\int_{-1}^{1}\frac{\eta_{kl}}{\lambda_{kl}}\exp\left(-\frac{(\eta_{kl} - \lambda_{kl}\sqrt{a_l})^2}{2\sigma^2_{\eta_{kl}}}\right)d\eta_{kl}. \qquad (A.9) \end{aligned}$$

Changing variable $x = (\eta_{kl} - \lambda_{kl}\sqrt{a_l})/\sigma_{\eta_{kl}}$ and performing the integration gives

$$E\left\{f(\eta_{kl})\frac{df(\eta_{kl})}{d\lambda_{kl}}\right\} = \frac{1}{\lambda_{kl}}\left\{\frac{\sigma^2_{\eta_{kl}}}{\sqrt{2\pi}}[(2\alpha_0 - \alpha_2)e^{-\alpha_2^2/2} - (2\alpha_0 + \alpha_1)e^{-\alpha_1^2/2}] + \sigma^2_{\eta_{kl}}(1+\alpha_0^2)[1 - Q(\alpha_1) - Q(\alpha_2)]\right\}. \quad \text{(A.10)}$$

A.5 Derivation of P_{e_1}

$$P_{e_1} = \frac{1}{2}[Pr(n_1 < u_{12}(\lambda_{12})f(\eta_{12}) - \rho\sqrt{a_2}b_2 - \sqrt{a_1}) + Pr(n_1 > u_{12}(\lambda_{12})f(\eta_{12}) - \rho\sqrt{a_2}b_2 + \sqrt{a_1})]. \quad \text{(A.11)}$$

By using the fact that $Pr(\eta_{12} < -1, b_2) = Pr(\eta_{12} > 1, -b_2)$ we can write,

$$\begin{aligned} P_{e_1} = {} & [Pr(n_1 < u_{12}(\lambda_{12}) - \rho\sqrt{a_2}b_2 - \sqrt{a_1}) \\ & + Pr(n_1 > u_{12}(\lambda_{12}) - \rho\sqrt{a_2}b_2 + \sqrt{a_1})]Pr(\eta_2 > 1|b_2) \\ & + \frac{1}{2}[Pr(n_1 < u_{12}(\lambda_{12})\eta_{12} - \rho\sqrt{a_2}b_2 - \sqrt{a_1},\ \eta_{12} < |1|) \\ & + Pr(n_1 > u_{12}(\lambda_{12})\eta_{12} - \rho\sqrt{a_2}b_2 + \sqrt{a_1},\ \eta_{12} < |1|)]. \end{aligned} \quad \text{(A.12)}$$

By letting

$$\begin{aligned} \delta_1 = \rho\sqrt{a_2}(c-1), \quad & \delta_2 = \rho\sqrt{a_2}(c+1), \\ \gamma_1 = \rho\sqrt{a_2}(c\eta_{12}-1), \quad & \gamma_2 = \rho\sqrt{a_2}(c\eta_{12}+1), \end{aligned} \quad \text{(A.13)}$$

where $c = u_{12}(\lambda_{12})/\rho\sqrt{a_2}$, we get

$$\begin{aligned} P_{e_1} = {} & \frac{1}{2}[Pr(n_1 < \delta_1 - \sqrt{a_1}) + Pr(n_1 > \delta_1 + \sqrt{a_1})]Pr(\eta_{12} > 1|b_2 = 1) \\ & + \frac{1}{2}[Pr(n_1 < \delta_2 - \sqrt{a_1}) + Pr(n_1 > \delta_2 + \sqrt{a_1})]Pr(\eta_{12} > 1|b_2 = 1) \\ & + \frac{1}{4}[Pr(n_1 < \gamma_1 - \sqrt{a_1},\ -1 < \eta_{12} < 1|b_2 = 1) \\ & + Pr(n_1 > \gamma_1 + \sqrt{a_1},\ -1 < \eta_{12} < 1|b_2 = 1)] \\ & + \frac{1}{4}[Pr(n_1 < \gamma_2 - \sqrt{a_1},\ -1 < \eta_{12} < 1|b_2 = -1) \end{aligned}$$

$$
\begin{aligned}
& + Pr(n_1 > \gamma_2 + \sqrt{a_1},\ -1 < \eta_{12} < 1 | b_2 = -1)] \\
= \ & \frac{1}{2}[1 - Q(\frac{\delta_1 - \sqrt{a_1}}{\sigma}) + Q(\frac{\delta_1 + \sqrt{a_1}}{\sigma})]Q(\alpha_1) \\
& + \frac{1}{2}[1 - Q(\frac{\delta_2 - \sqrt{a_1}}{\sigma}) + Q(\frac{\delta_2 + \sqrt{a_1}}{\sigma})]Q(\alpha_2) + \frac{1}{2}[1 - Q(\alpha_1) - Q(\alpha_2)] \\
& + \frac{1}{4}\left\{\frac{1}{\sqrt{2\pi}\sigma_{\eta_{12}}} \int_{-1}^{1} [Q(\frac{\gamma_1 + \sqrt{a_1}}{\sigma}) - Q(\frac{\gamma_1 - \sqrt{a_1}}{\sigma})] \exp(-\frac{(\eta_{12} - \lambda_{12}\sqrt{a_2})^2}{2\sigma_{\eta_{12}}^2}) d\eta_{12}\right\} \\
& + \frac{1}{4}\left\{\frac{1}{\sqrt{2\pi}\sigma_{\eta_{12}}} \int_{-1}^{1} [Q(\frac{\gamma_2 + \sqrt{a_1}}{\sigma}) - Q(\frac{\gamma_2 - \sqrt{a_1}}{\sigma})] \exp(-\frac{(\eta_{12} + \lambda_{12}\sqrt{a_2})^2}{2\sigma_{\eta_{12}}^2}) d\eta_{12}\right\}.
\end{aligned}
\tag{A.14}
$$

APPENDIX B

DERIVATIONS FOR CHAPTER 5

B.1 Derivation of $E\{\xi_i \mathrm{sgn}(\boldsymbol{v}_j^T \boldsymbol{P}\boldsymbol{A}\boldsymbol{b} + \xi_j)\}$

In order to calculate the second term in Eq. (5.2), we use a linear transformation such that,

$$\begin{bmatrix} \xi_i \\ \xi_j \end{bmatrix} = \begin{bmatrix} F & G \\ 0 & 1 \end{bmatrix} \begin{bmatrix} \lambda_i \\ \lambda_j \end{bmatrix}, \tag{B.1}$$

where

$$F = \frac{\sqrt{E\{\xi_i^2\}E\{\xi_j^2\} - E^2\{\xi_i\xi_j\}}}{E\{\xi_j^2\}} \tag{B.2}$$

and

$$G = \frac{E\{\xi_i\xi_j\}}{E\{\xi_j^2\}} = \frac{E\{\boldsymbol{v}_i^T \boldsymbol{n}\boldsymbol{n}^T \boldsymbol{v}_j\}}{E\{\boldsymbol{v}_j^T \boldsymbol{n}\boldsymbol{n}^T \boldsymbol{v}_j\}} = \frac{\sigma^2 \boldsymbol{v}_i^T \boldsymbol{P}\boldsymbol{v}_j}{\sigma^2 \boldsymbol{v}_j^T \boldsymbol{P}\boldsymbol{v}_j}. \tag{B.3}$$

Note that $\lambda_i = (\xi_j - G\xi_i)/F$, $\lambda_j = \xi_j$ and $E\{\lambda_i\lambda_j\} = 0$. From Eq. (5.2) we can write,

$$\begin{aligned} E\{\xi_i \mathrm{sgn}(\boldsymbol{v}_j^T \boldsymbol{P}\boldsymbol{A}\boldsymbol{b} + \xi_j)\} &= E\{(F\lambda_i + G\lambda_j)\mathrm{sgn}(\boldsymbol{v}_j^T \boldsymbol{P}\boldsymbol{A}\boldsymbol{b} + \lambda_j)\} \\ &= GE\{\xi_j \mathrm{sgn}(\boldsymbol{v}_j^T \boldsymbol{P}\boldsymbol{A}\boldsymbol{b} + \xi_j)\}, \end{aligned} \tag{B.4}$$

since λ_i and λ_j are uncorrelated. From the above equation,

$$\begin{aligned} E\{\xi_j \mathrm{sgn}(\boldsymbol{v}_j^T \boldsymbol{P}\boldsymbol{A}\boldsymbol{b} + \xi_j)\} &= E_{\boldsymbol{b}}\{\xi_j \mathrm{sgn}(\boldsymbol{v}_j^T \boldsymbol{P}\boldsymbol{A}\boldsymbol{b} + \xi_j), \boldsymbol{v}_j^T \boldsymbol{P}\boldsymbol{A}\boldsymbol{b} + \xi_j > 0\} \\ &\quad + E_{\boldsymbol{b}}\{\xi_j \mathrm{sgn}(\boldsymbol{v}_j^T \boldsymbol{P}\boldsymbol{A}\boldsymbol{b} + \xi_j), \boldsymbol{v}_j^T \boldsymbol{P}\boldsymbol{A}\boldsymbol{b} + \xi_j < 0\} \\ &= 2^{-(2K-1)} \sum_{\boldsymbol{b}\in\{\cdot\}} \left[\int_{-\boldsymbol{v}_j^T \boldsymbol{P}\boldsymbol{A}\boldsymbol{b}}^{\infty} \xi_j p_{\xi_j}(\xi_j) d\xi_j - \int_{-\infty}^{-\boldsymbol{v}_j^T \boldsymbol{P}\boldsymbol{A}\boldsymbol{b}} \xi_j p_{\xi_j}(\xi_j) d\xi_j \right] \\ &= 2^{-(2K-1)} \sum_{\boldsymbol{b}\in\{\cdot\}} \left[\int_{-\boldsymbol{v}_j^T \boldsymbol{P}\boldsymbol{A}\boldsymbol{b}}^{\infty} \xi_j p_{\xi_j}(\xi_j) d\xi_j + \int_{\boldsymbol{v}_j^T \boldsymbol{P}\boldsymbol{A}\boldsymbol{b}}^{\infty} \xi_j p_{\xi_j}(\xi_j) d\xi_j \right] \\ &= 2^{-(2K-1)} \sum_{\boldsymbol{b}\in\{\cdot\}} \frac{\sigma_{\xi_j}}{\sqrt{2\pi}} \left[\int_{-\boldsymbol{v}_j^T \boldsymbol{P}\boldsymbol{A}\boldsymbol{b}}^{\infty} \xi_j \exp(-\frac{\xi_j^2}{2\sigma_{\xi_j}^2}) d\xi_j + \int_{\boldsymbol{v}_j^T \boldsymbol{P}\boldsymbol{A}\boldsymbol{b}}^{\infty} \xi_j \exp(-\frac{\xi_j^2}{2\sigma_{\xi_j}^2}) d\xi_j \right] \\ &= 2^{-(2K-1)} \sum_{\boldsymbol{b}\in\{\cdot\}} \frac{\sigma_{\xi_j}}{\sqrt{2\pi}} \left[\exp(-\frac{[\boldsymbol{v}_j^T \boldsymbol{P}\boldsymbol{A}\boldsymbol{b}]^2}{2\sigma_{\xi_j}^2}) + \exp(-\frac{[\boldsymbol{v}_j^T \boldsymbol{P}\boldsymbol{A}\boldsymbol{b}]^2}{2\sigma_{\xi_j}^2}) \right]. \end{aligned} \tag{B.5}$$

Substituting into Eq. (B.4) results in Eq. (5.4).

B.2 Derivation of $E\{z_i f(z_j)\}$

The first term in Eq. (5.34) can be calculated as follows:

$$
\begin{aligned}
E\{\boldsymbol{v}_i^T\boldsymbol{PAb}f(\boldsymbol{v}_j^T\boldsymbol{PAb}+\xi_j)\} &= E_{\boldsymbol{b}}\{\boldsymbol{v}_i^T\boldsymbol{PAb}f(\boldsymbol{v}_j^T\boldsymbol{PAb}+\xi_j), \boldsymbol{v}_j^T\boldsymbol{PAb}+\xi_j>t\} \\
&+ E_{\boldsymbol{b}}\{\boldsymbol{v}_i^T\boldsymbol{PAb}f(\boldsymbol{v}_j^T\boldsymbol{PAb}+\xi_j), \boldsymbol{v}_j^T\boldsymbol{PAb}+\xi_j<-t\} \\
&+ E_{\boldsymbol{b}}\{\boldsymbol{v}_i^T\boldsymbol{PAb}f(\boldsymbol{v}_j^T\boldsymbol{PAb}+\xi_j), \boldsymbol{v}_j^T\boldsymbol{PAb}+\xi_j\le|t|\} \\
&= 2^{-(2K-1)}\sum_{\boldsymbol{b}\in\{\cdot\}}\boldsymbol{v}_i^T\boldsymbol{PAb}Pr\Big[\{\xi_j>t-\boldsymbol{v}_j^T\boldsymbol{PAb}\}-Pr\{\xi_j<-t-\boldsymbol{v}_j^T\boldsymbol{PAb}\} \\
&+\int_{-t-\boldsymbol{v}_j^T\boldsymbol{PAb}}^{t-\boldsymbol{v}_j^T\boldsymbol{PAb}}(\boldsymbol{v}_j^T\boldsymbol{PAb}+\xi_j)p_{\xi_j}(\xi_j)d\xi_j\Big] \\
&= 2^{-(2K-1)}\boldsymbol{v}_i^T\boldsymbol{PA}\sum_{\boldsymbol{b}\in\{\cdot\}}\boldsymbol{b}\Big\{[1-Q(\frac{\boldsymbol{v}_j^T\boldsymbol{PAb}-t}{\sigma_{\xi_j}})-Q(\frac{\boldsymbol{v}_j^T\boldsymbol{PAb}+t}{\sigma_{\xi_j}})] \\
&+\frac{\boldsymbol{v}_j^T\boldsymbol{PAb}}{t}[Q(\frac{\boldsymbol{v}_j^T\boldsymbol{PAb}-t}{\sigma_{\xi_j}})-Q(\frac{\boldsymbol{v}_j^T\boldsymbol{PAb}+t}{\sigma_{\xi_j}})] \\
&+\frac{\sigma_{\xi_j}}{t\sqrt{2\pi}}[\exp(-\frac{[\boldsymbol{v}_j^T\boldsymbol{PAb}+t]^2}{2\sigma_{\xi_j}^2})-\exp(-\frac{[\boldsymbol{v}_j^T\boldsymbol{PAb}-t]^2}{2\sigma_{\xi_j}^2})]\Big\}, \qquad \text{(B.6)}
\end{aligned}
$$

where $p_{\xi_j}(\xi_j)=(1/\sqrt{2\pi}\sigma_{\xi_j})\exp(-\xi_j^2/2\sigma_{\xi_j}^2)$ and $Q(x)=(1/\sqrt{2\pi})\int_x^\infty\exp(-y^2/2)dy$.

In order to calculate the second term in Eq. (5.34), we use the linear transformation given in Eq. (B.1). Hence the second term in Eq. (5.34) can be written as

$$
\begin{aligned}
E\{\xi_i f(\boldsymbol{v}_j^T\boldsymbol{PAb}+\xi_j)\} &= E\{(F\lambda_i+G\lambda_j)f(\boldsymbol{v}_j^T\boldsymbol{PAb}+\lambda_j)\} \\
&= GE\{\xi_j f(\boldsymbol{v}_j^T\boldsymbol{PAb}+\xi_j)\}, \qquad \text{(B.7)}
\end{aligned}
$$

where

$$
\begin{aligned}
E\{\xi_j f(\boldsymbol{v}_j^T\boldsymbol{PAb}+\xi_j)\} &= E_{\boldsymbol{b}}\{\xi_j f(\boldsymbol{v}_j^T\boldsymbol{PAb}+\xi_j), \boldsymbol{v}_j^T\boldsymbol{PAb}+\xi_j>t\} \\
&+ E_{\boldsymbol{b}}\{\xi_j f(\boldsymbol{v}_j^T\boldsymbol{PAb}+\xi_j), \boldsymbol{v}_j^T\boldsymbol{PAb}+\xi_j<-t\} \\
&+ E_{\boldsymbol{b}}\{\xi_j f(\boldsymbol{v}_j^T\boldsymbol{PAb}+\xi_j), \boldsymbol{v}_j^T\boldsymbol{PAb}+\xi_j\le|t|\} \\
&= 2^{-(2K-1)}\sum_{\boldsymbol{b}\in\{\cdot\}}\Big[\int_{t-\boldsymbol{v}_j^T\boldsymbol{PAb}}^{\infty}\xi_j p_{\xi_j}(\xi_j)d\xi_j-\int_{-\infty}^{-t-\boldsymbol{v}_j^T\boldsymbol{PAb}}\xi_j p_{\xi_j}(\xi_j)d\xi_j
\end{aligned}
$$

$$
\begin{aligned}
&+\frac{1}{t}\int_{-t-\boldsymbol{v}_j^T\boldsymbol{PAb}}^{t-\boldsymbol{v}_j^T\boldsymbol{PAb}} \xi_j(\boldsymbol{v}_j^T\boldsymbol{PAb}+\xi_j)p_{\xi_j}(\xi_j)d\xi_j\Bigg] \\
= \;& 2^{-(2K-1)}\sum_{\boldsymbol{b}\in\{\cdot\}}\frac{\sigma_{\xi_j}}{\sqrt{2\pi}}[\exp(-\frac{[\boldsymbol{v}_j^T\boldsymbol{PAb}+t]^2}{2\sigma_{\xi_j}^2})+\exp(-\frac{[\boldsymbol{v}_j^T\boldsymbol{PAb}-t]^2}{2\sigma_{\xi_j}^2})] \\
&+\frac{2^{-(2K-1)}}{t}\sum_{\boldsymbol{b}\in\{\cdot\}}\Bigg\{\boldsymbol{v}_j^T\boldsymbol{PAb}\frac{\sigma_{\xi_j}}{\sqrt{2\pi}}[\exp(-\frac{[\boldsymbol{v}_j^T\boldsymbol{PAb}+t]^2}{2\sigma_{\xi_j}^2})-\exp(-\frac{[\boldsymbol{v}_j^T\boldsymbol{PAb}-t]^2}{2\sigma_{\xi_j}^2})] \\
&+\frac{\sigma_{\xi_j}}{\sqrt{2\pi}}[(\boldsymbol{v}_j^T\boldsymbol{PAb}-t)\exp(-\frac{[\boldsymbol{v}_j^T\boldsymbol{PAb}-t]^2}{2\sigma_{\xi_j}^2})-(\boldsymbol{v}_j^T\boldsymbol{PAb}+t)\exp(-\frac{[\boldsymbol{v}_j^T\boldsymbol{PAb}+t]^2}{2\sigma_{\xi_j}^2})] \\
&+\sigma_{\xi_j}^2[Q(\frac{\boldsymbol{v}_j^T\boldsymbol{PAb}-t}{\sigma_{\xi_j}})-Q(\frac{\boldsymbol{v}_j^T\boldsymbol{PAb}+t}{\sigma_{\xi_j}})]\Bigg\}. \qquad \text{(B.8)}
\end{aligned}
$$

It is easy to notice that the first and second terms in the above equation are cancelled by the third, and substituting it into Eq. (B.7) we get

$$
E\{\xi_i f(\boldsymbol{v}_j^T\boldsymbol{PAb}+\xi_j)\} = 2^{-(2K-1)}\frac{\boldsymbol{v}_i^T\boldsymbol{Pv}_j}{\boldsymbol{v}_j^T\boldsymbol{Pv}_j}\frac{\sigma_{\xi_j}^2}{t}\sum_{\boldsymbol{b}\in\{\cdot\}}[Q(\frac{\boldsymbol{v}_j^T\boldsymbol{PAb}-t}{\sigma_{\xi_j}})-Q(\frac{\boldsymbol{v}_j^T\boldsymbol{PAb}+t}{\sigma_{\xi_j}})]. \qquad \text{(B.9)}
$$

REFERENCES

1. Y. Bar-Ness and J. Rokach, "Cross-coupled Bootstrapped Interference Canceller," in *Int'l Conf. on Antenna and Propogation*, Los Angeles, CA, pp. 292–295, June 1981.

2. Y. Bar-Ness, J. W. Carlin, and M. L. Steinbergerr, "Bootstraping Adaptive Cross Pol Cancellers for Satellite Communications," in *Proceedings of Int'l Conf. on Communications*, Philadelphia, PA, June 1982.

3. Y. Bar-Ness and A. Dinc, "Performance Comparison of LMS, Diagonalizer and Bootstrapped Adaptive Cross-Pol. Canceller over Non-dispersive Channel," in *MILCOM'90*, 1990.

4. Y. Bar-Ness, D. W. Chen, and Z. Siveski, "Adaptive Multiuser Bootstrapped Decorrelating CDMA Detector in Asynchronous Unknown Channels," in *Int'l Symph. on Personal, Indoor and Mobile Radio Comm.*, Delft, The Netherlands, Sept. 1994.

5. Y. Bar-Ness and J. B. Punt, "Adaptive Bootstrap Multiuser CDMA Detector," in *Special Issue on Signal Seperation and Interference Cancellation for Personal, Indoor and Mobile Radio Communications*, An International Journal, Kluwer Academic Publishers.

6. Y. Bar-Ness and N. Sezgin, "Adaptive Multiuser Bootstrapped Decorrelating CDMA Detector for One-shot Asynchronous Unknown Channels," in *Proceedings of the 1995 IEEE International Conference on Acoustics, Speech, and Signal Processing (ICASSP-95)*, Detroit, MI, pp. 1733–1736, May 1995.

7. Y. Bar-Ness and N. Sezgin, "Adaptive Threshold Setting for Multiuser CDMA Signal Seperators with Soft Tentative Decision," in *Proceedings of the Twenty-ninth Annual Conference on Information Sciences and Systems*, Baltimore, MD, pp. 174–179, March 1995.

8. Y. Bar-Ness and N. Sezgin, "Maximum Signal-to-Noise Ratio Data Combining for One-shot Asynchronous Multiuser CDMA Detector," in *Proceedings of The Sixth IEEE International Symposium on Personal, Indoor and Mobile Radio Communications (PIMRC-95)*, Toronto, Canada, Sept. 1995.

9. Y. Bar-Ness, Z. Siveski, and D. W. Chen, "Bootstrapped Decorrelating Algorithm for Adaptive Interference Cancellation in Synchronous CDMA Communication Systems," in *IEEE Int'l Symph. on Spread Spectrum Techniques and Applications*, Oulu, Finland, July 1994.

10. Y. Bar-Ness, Z. Siveski, R. E. Kamel, and D. W. Chen, "Adaptive Algorithms for Interference Cancellation in Multiuser Communication Systems," in *1st Symph. on Comm. and Vehicular Tech.*, Delft, The Netherlands, Sept. 1993.

11. D. W. Chen, Z. Siveski, and Y. Bar-Ness, "Synchronous Multiuser Detector with Soft Decision Adaptive Canceller," in *28th Annual Conf. on Info. Sci. and Sys.*, Princeton, NJ, March 1994.

12. P. Comon, C. Jutten, and J. Herault, "Blind Seperation of Sources, Part II: Problems Statement," *Signal Processing, Elsevier Science Publishers*, vol. 24, pp. 11–20, 1991.

13. A. Dinc and Y. Bar-Ness, "Bootstrap: A Fast Adaptive Signal Seperator," in *ICASSP'92*, 1992.

14. A. Dinc and Y. Bar-Ness, "Convergence and Performance Comparison of Three Different Structures of Bootstrap Blind adaptive Algorithm for Multisignal Co-channel Seperation," in *Proceedings of Conf. on Military Comm.*, San Diego, CA, pp. 913–918, Oct. 1992.

15. Z. C. Fluhr and P. T. Porter, "Advanced Mobile Phone Service: Control Architecture," *The Bell System Technical Journal*, vol. 58, pp. 43–69, Jan. 1979.

16. K. Gilhousen, I. M. Jacobs, R. Padovani, A. J. Viterbi, L. A. Weaver Jr. and C. E. Wheatley, "On the Capacity of Cellular CDMA System," *IEEE Trans. on Vehicular Technology*, vol. 40, pp. 303–312, May 1991.

17. H. Hashemi, "The Indoor Propagation Channel," *Proceedings of the IEEE*, vol. 81, no. 7, pp. 943–967, July 1993.

18. C. Jutten and J. Herault, "Blind Seperation of Sources, Part I: An Adaptive Algorithm Based on Neuromimetic Architecture," *Signal Processing, Elsevier Science Publishers*, vol. 24, pp. 1–10, 1991.

19. R. Lupas and S. Verdú, "Linear Multiuser Detector for Synchronous Code Division Multiple Access Channels," *IEEE Trans. on Info. Theory*, vol. IT-35, pp. 123–136, Jan. 1989.

20. R. Lupas and S. Verdú, "Near-far Resistance of Multiuser Detectors in Asynchronous Channels," *IEEE Trans. on Communications*, vol. 38, pp. 496–508, April 1990.

21. H. Messer and Y. Bar-Ness, "Bootstrapped Spatial Seperation of Wideband Superimposed Signals," in *EUSIPCO'92*, 1992.

22. R. Pickholtz, D. L. Schilling, and L. B. Milstein, "Theory of Spread Spectrum Communications: A Tutorial," *IEEE Trans. on Comm.*, vol. COM-30, pp. 855–884, May 1982.

23. N. Sezgin and Y. Bar-Ness, "Adaptive Soft Limiter Bootstrap Seperator for One-shot Asynchronous CDMA Channel with Singular Partial Cross correlation Matrix," in *ICC'96.*

24. Z. Siveski, Y. Bar-Ness, and D. W. Chen, " Error Performance of Synchronous Multiuser Code Division Multiple Access Detector with Multidimensional Adaptive Canceller ," *European Trans. on Telecommunications and Related Technologies*, 1994.

25. Z. Siveski, Y. Bar-Ness, and D. W. Chen, "Adaptive Multiuser Detector for Synchronous Code Division Multiple Access Applications," in *1994 Int'l Zurich Seminar on Digital Comm.*, Zurich, Switzerland, March 1994.

26. Z. Siveski, L. Zhong, and Y. Bar-Ness, "Adaptive Multiuser CDMA Detector for Asynchronous AWGN Channels," in *IEEE Int'l Symph. on Personal, Indoor and Mobile Radio Comm.*, 1994.

27. E. Sorouchyari, "Blind Seperation of Sources, Part III: Stability Analysis," *Signal Processing, Elsevier Science Publishers*, vol. 24, pp. 21–29, 1991.

28. S. Stein, " Fading Channel Issues in System Engineering," *IEEE Journal on Selected Areas in Communications*, vol. SAC-5, no. 2, pp. 68–89, Feb. 1987.

29. G. Strang, *Linear Algebra and its Applications*, Harcourt Brace Jovanovich, Inc., San Diego, 1988.

30. G. L. Turin, "Introduction to Spread-Spectrum Antimultipath Techniques and Their Applications to Urban Digital Radio," *Proccedings of IEEE*, vol. 68, pp. 328–353, March 1980.

31. M. K. Varanasi and B. Aazhang, "Multistage detection in asynchronous Code Division Multiple Access communications," *IEEE Trans. on Comm.*, vol. 38, pp. 509–519, April 1990.

32. M. K. Varanasi and B. Aazhang, " Near Optimum Detector with Synchronous Code Division Multiple Access System," *IEEE Trans. on Comm.*, vol. 39, pp. 725–736, May 1991.

33. S. Verdú, *Advances in Communication and Signal Processing*, Springer-Verlag, Berlin, 1989.

34. S. Verdú, "Minimum Probability of Error for Asynchronous Gaussian Multiple Access Channels," *IEEE Trans. on Info. Theory*, vol. IT-32, pp. 85–96, Jan. 1986.

35. F. Viehofer, Z. Siveski, and Y. Bar-Ness, "Soft Decision Adaptive Multiuser CDMA Detector for Asynchronous AWGN Channel," in *The 32nd Annual Allerton Conference on Communication, Computing and Control*, Urbana-Champaign, IL, Sept. 1994.

36. D. P. Whipple, "The CDMA Standard," *Applied Microwave and wireless*, pp. 24–37, 1995.

37. X. Zhang and D. Brady, "Soft-Decision Multistage Detection for Asynchronous AWGN Channels," in *The 31st Annual Allerton Conference on Communication, Computing and Control*, Monticello, IL, Sept. 1993.